Comparative evaporation measurements above commercial forestry and sugarcane canopies in the KwaZulu-Natal Midlands

Caren Burger

B.Sc.Agric.Hons. (Agrometeorology)

University of the Orange Free State

Submitted in partial fulfilment of the requirements for the degree of

MASTER OF SCIENCE IN AGRICULTURE

in the

School of Applied Environmental Sciences

Faculty of Science and Agriculture

University of Natal

Pietermaritzburg

South Africa

January 1999

ABSTRACT

An understanding of the water use of different crops commonly grown in an area is essential for the implementation of integrated catchment management in South Africa. With increasing pressure on water resources, mainly due to the recent changes in the Water Act, it has become important to determine the actual water demands of agricultural and other crops. Policy makers require knowledge of whether forestry canopies use more water than grassland and other agricultural crops.

The Bowen ratio and Penman-Monteith methods were used in a comparative study of the evaporation from *Saccharum, Acacia* and *Eucalyptus*. All of the research was conducted at marginal sites located in the KwaZulu-Natal Midlands of South Africa over a period of two years.

The Bowen ratio energy balance (BREB) technique combines the Bowen ratio (β) (the ratio between the sensible, H and latent heat flux density, λE), with the net irradiance (R_n) and soil heat flux densities (G) to calculate evaporation. A comparative study of the site-specific energy balance components (R_n, G, H and λE), general climatic conditions (rainfall, solar irradiance and air temperature) and other site-specific parameters (leaf area index and average canopy height) was conducted on *Saccharum* and young commercial forests consisting of *Acacia* and *Eucalyptus*. The energy balance highlighted important differences in the energy balance components between the different canopies. The differences between the reflection coefficients at the three sites contributed mainly to the differences in the evaporation rates. The low reflection coefficients of the forest canopies (*Acacia* and *Eucalyptus*) (0.1 and 0.08 respectively) were smaller than of the sugarcane canopy (0.2). This resulted in more energy available ($\approx$ 6 %) for partitioning between the sensible and latent heat flux densities and higher evaporation rates for the forestry canopies. Where low leaf area indices existed (*Acacia* and *Eucalyptus* sites) (LAI < 2), the soil heat flux density contributed up to 40 % of the net irradiance ($G = 0.4\ R_n$).

The evaporation rates for *Saccharum, Acacia* and *Eucalyptus* averaged 2 mm day^{-1} in winter and 5 mm day^{-1} in summer. The slightly higher summer evaporation rate for *Eucalyptus* (5.6 mm day^{-1}), compared to *Acacia* (4.9 mm day^{-1}), resulted from the lower reflection coefficients and canopy resistance (r_c) for *Eucalyptus* ($\alpha_s = 0.08$, $r_c = 35$ s m^{-1}) compared to *Acacia* ($\alpha_s = 0.1$, $r_c = 45$ s m^{-1}).

Automatic weather station data (solar irradiance, air temperature, water vapour pressure and windspeed) were applied to site-specific Penman-Monteith equations to predict evaporation for all three sites. Statistically significant relationships (slope, m $\approx$ 1, $r^2 > 0.8$) were found between the measured (Bowen ratio) and simulated (site-specific Penman-Monteith) evaporation estimates. The current study has demonstrated the effectiveness of applying the Penman-Monteith equation to forest and sugarcane canopies to predict evaporation, provided accurate net irradiance, soil heat flux densities and canopy resistances are used.

Declaration

I hereby certify that the research work reported in this dissertation is the result of my own original investigation except where acknowledged.

Signed ___CBurger___

Date ___8·4·1999___

Caren Burger

ACKNOWLEDMENTS

I wish to record my sincere gratitude to:

Prof. M.J. Savage for guidance, time and valuable scientific inputs

Dr. C.S. Everson for valuable scientific inputs and encouragement

Dr. P.J. Dye for you valuable scientific inputs

Mr. J.N. Bosch and Mr. M.B. Gush for encouragement

Phillip Vilakazi and Robert Ndlela for help while conducting field work

Mondi Forests specially mentioning Mr. P. Gardner, Mr. D. Chard and Mr. J. Nortje for help on the Canema-Mistley estate while conducting the experiment

The Department of Water Affairs and Forestry for funding the comparative evaporation project

My friends for encouragement, love and prayers

To my Heavenly Father for his love and grace

Pa, Ma vir besondere ondersteuning, liefde en gebede; Antoinette, Gert en Pieter, vir julle liefde.

"We are all born ignorant, but one must work hard to remain stupid."

Benjamin Franklin

"Experience is a hard teacher, because she gives the test first, the lesson afterwards."

Vernon Sanders Law

"Ambition is a poor excuse for not having sense enough to be lazy."

Charlie McCarthy

"The real winners in life are the people who look at every situation with an expectation that they can make it work or make it better."

Barbara Pletcher

"It is extraordinary how extraordinary the ordinary person is."

George Will

"What lies behind us and what lies before us
are tiny matters
compared to what lies within us."

Oliver Wendell Holmes

TABLE OF CONTENTS

NOTATION LIST

Lower case

c	Specific heat capacity of the soil	J kg^{-1} K^{-1}
c_p	Specific heat capacity of air at constant pressure	J kg^{-1} K^{-1}
c_s	Specific heat capacity of dry soil	J kg^{-1} K^{-1}
c_w	Specific heat capacity of water	J kg^{-1} K^{-1}
d	Solar declination angle	Degrees
d	Zero plane displacement	m
de	True profile water vapour pressure difference	kPa
dT	True profile temperature difference	°C or K
dθ	True profile equivalent temperature difference	°C or K
e_1	Water vapour pressure at z_1	kPa
e_2	Water vapour pressure at z_2	kPa
e_a	Atmospheric water vapour pressure	kPa
e_s	Saturated water vapour pressure	kPa
j	Day of year	Unitless
k_v	Diffusivity coefficient for latent heat transfer	m^2 s^{-1}
k_h	Diffusivity coefficient for sensible heat transfer	m^2 s^{-1}
l	Latitude at a site	Degrees
r_a	Aerodynamic resistance	s m^{-1}
r_c	Canopy resistance	s m^{-1}
r_v	Combined canopy and aerodynamic resistance to water vapour	s m^{-1}
t	Clock time	h
t	Equation of time	day
t_o	Time of solar noon	h
t_{out}	Output interval	s
u	Windspeed	m s^{-1}

u_{zu}	Windspeed at height z_u	m s^{-1}
z_1	Height of measurement at level 1	m
z_2	Height of measurement at level 2	m
z_{oh}	Roughness length for heat and water vapour transferm	
z_{om}	Roughness length for momentum transfer	m
z_t	Height of air temperature and humidity measurement	m
z_u	Height of windspeed measurement	m

Upper case

A	Altitude	m
E(T)	Resolution limit for temperature sensor	°C
E(e)	Resolution limit for water vapour pressure sensor	kPa
E(θ)	Resolution limit in terms of the equivalent temperature	K
E_a	Evaporation in Penman equation	mm
ET	Actual evaporation	mm
ET_o	Potential or reference Penman-Monteith evaporation	mm
ET_p	Potential Priestley-Taylor evaporation	mm
ET_q	Equilibrium evaporation	mm
ET_{avg}	Daily average site specific Penman-Monteith evaporation	mm
ET_{tot}	Total accumulated site specific Penman-Monteith evaporation	mm
λE	Latent heat flux density	W m^{-2}
F	Soil heat flux density at 80 mm	W m^{-2}
G	Soil heat flux density	W m^{-2}
G_s	Simulated soil heat flux density	W m^{-2}
H	Sensible heat flux density	W m^{-2}
L	Longitude of site	Degrees
L_c	Longitude correction	Degrees

L_{ni}	Atmospheric radiant emittance minus the crop emittance at air temperature		W m^{-2}
L_{nic}	Atmospheric radiant emittance minus the crop emittance at air temperature under clear skies		W m^{-2}
L_s	Longitude of the standard meridian		Degrees
M_d	Molecular mass of dry air		kg mol^{-1}
M_w	Molecular mass of water	0.018	kg mol^{-1}
P	Atmospheric pressure		kPa
P_o	Sea level pressure		kPa
R	Universal gas constant	8.3143×10^{-3}	kJ mol^{-1} K^{-1}
R_n	Net irradiance		W m^{-2}
R_{ns}	Simulated net irradiance		W m^{-2}
R_o	Potential net irradiance		W m^{-2}
R_s	Solar irradiance		W m^{-2}
S	Average heat flux density stored in the soil		W m^{-2}
T_1	Air temperature at z_1		°C or K
T_2	Air temperature at z_2		°C or K
T_a	Air temperature		°C or K
T_o	Surface air temperature		°C or K

Other

α	Potential evaporation coefficient	Unitless
α_s	Crop reflection coefficient (albedo)	Unitless
β	Bowen ratio	Unitless
δ	Equilibrium layer thickness	m
δ (x)	Probable error in x	Unitless
δe	Measured water vapour pressure profile difference	kPa
δT	Measured air temperature profile difference	°C or K
$\delta\theta$	Measured profile equivalent temperature	°C or K

δz	Measured separation difference		m
Δ	Slope of the saturation water vapour pressure *vs.* air temperature		Pa °C^{-1}
Δe	Water vapour pressure difference		kPa
ΔT	Temperature difference		°C or K
Δz	Difference in height		m
ε	Ratio of the molecular mass of water to that of dry air		Unitless
γ	Thermodynamic psychrometer constant		kPa K^{-1}
γ^*	Apparent psychrometer constant		kPa K^{-1}
φ	Elevation angle of the sun		Degrees
λ	Specific latent heat of vaporization	2450	kJ kg^{-1}
λET_B	Bowen ratio total evaporation		mm
θ	Kelvin temperature	293	K
θ_g	Gravimetric soil water content		kg kg^{-1}
θ_v	Volumetric soil water content		m^3 m^{-3}
ρ	Density of air		kg m^{-3}
ρ_s	Bulk density of soil		kg m^{-3}

Chapter 1

INTRODUCTION

An understanding of the characteristic water use of various crops is essential for the implementation of integrated catchment management in South Africa. With increasing pressure on water resources, it has become increasingly important to determine the actual water demands of agricultural and other crops. The need to conserve South Africa's limited water resources is placing policy makers in direct conflict with land managers. Rational decisions can only be made if based on sound and timely scientific data.

Considerable research has been concerned with the question: do forests use more water than grassland and agricultural crops? Evaporation comparisons between forest and other crops were often motivated from a need to know the effect of afforestation on streamflow. In high rainfall areas where water is more abundant, it appears that the evaporation from forests exceeds the evaporation from nearby areas with lower plant covers by 10 to 20 percent (Rutter, 1972). This may result from greater precipitation interception efficiency and subsequent rapid evaporation due to the lower radiation reflection coefficient and aerodynamic resistance of forests. In drier areas, the biggest difference in the water use of forests and agricultural crops results from the ability of the deep-rooted trees to tap water supplies not readily available to agricultural crops and grasses (Rutter, 1972).

This study extends evaporation measurements previously made in the Winterton area on wheat, maize, grassland and *Eucalyptus* spp. In the present trial, total evaporation is measured simultaneously above commercial forestry (*Acacia* and *Eucalyptus*) and sugarcane (*Saccharum*) canopies at a marginal KwaZulu-Natal Midlands forestry site.

Blad and Rosenberg (1974) suggested the use of micrometeorological methods (*e.g.* Bowen ratio energy balance technique) to provide direct evaporation measurements where lysimeters are unavailable. The Bowen ratio energy balance technique (BREB) was therefore chosen.

The Bowen ratio energy balance technique became popular due to its relative simplicity, reliability and the additional valuable information gained on the distribution of energy at a surface (Tanner, 1960; Denmead and McIllroy, 1970; Campbell, 1973; Blad and Rosenberg, 1974; Revfeim and Jordan, 1976; Angus and Watts, 1984; Nie *et al.*, 1992; Cellier and Olioso, 1993; Malek, 1993; Ibanez *et al.*, 1998).

In 1926, Bowen introduced a ratio between the sensible and latent heat flux densities (β) and further showed how this Bowen ratio (β) coupled with net irradiance (R_n) and soil heat flux density (G) could be used to calculate evaporation and aid our understanding of crop water use.

The elucidation of the accuracy of the Bowen ratio energy balance technique for forest studies is more important than for application above other agricultural crops. Air temperature and water vapour pressure gradients (used in the calculation of the Bowen ratio) above forests (tree canopies) are small compared to gradients over agricultural crops due to the height of the crop (Black and McNaughton, 1971). Spittlehouse and Black (1980), Everson (1995) and Beringer and Tapper (1996) found the Bowen ratio energy balance technique to be suitable for forest evaporation measurements.

The Bowen ratio technique fails to perform during periods when the Bowen ratio approaches -1 (as occurs in the early morning and late afternoon) and the sensible and latent heat flux densities are similar in magnitude but opposite in direction. Practical and theoretical limitations therefore result in data rejection. Periodic unreliable data sets and data exclusion may therefore leave gaps in the energy balance and evaporation data sets.

Alternative means of evaporation estimation need to be investigated to complete the Bowen ratio evaporation data sets, whether by means of other techniques (*e.g.* the Heat Pulse Velocity technique) or through modelling. As a result of readily available real-time automatic weather station data, site-specific Penman-Monteith equations were employed to patch incomplete Bowen ratio energy balance data sets (Campbell, undated).

Chapter 2
MOTIVATION

Water is a limited resource in many areas of South Africa. The need to conserve water results in changing legislation, placing policy makers in direct conflict with land managers. Rational decisions can best be made if supported by sound scientific data. Accurate water use measurements from different crops and land uses, are therefore becoming increasingly important for water management. Policy makers require knowledge of whether forestry canopies use more water than grassland and agricultural crops.

This project is extending the evaporation measurements previously made (Everson, 1995) in the marginal Winterton area on *Eucalyptus*, wheat, maize and grassland at good sites (i.e. deep soils and high rainfalls) in the KwaZulu-Natal Midlands. In the present trial, simultaneous, direct comparisons of evaporation are being carried out on *Saccharum*, *Acacia* and *Eucalyptus* using the Bowen ratio energy balance (BREB) technique.

The trial has been established in recently planted areas of the three selected species so that even aged stands can be compared and followed to maturity. This implies that the trial will continue for a number of years.

Chapter 3

AIMS

This project aims to quantify the water use of *Saccharum*, *Acacia* and *Eucalyptus*. *Acacia* (black wattle) is considered to be a conservative water user although currently there is little evidence to substantiate this claim. *Eucalyptus* and *Saccharum* are considered to both have high water requirements. The transpiration differences between *Saccharum* and *Eucalyptus* trees have not been compared in South Africa using actual evaporation measurements. The results of this project will contribute valuable scientific data on three key species planted extensively in the KwaZulu-Natal Midlands.

More specific objectives addressed in this study were:

- the collection of reliable, accurate and long term Bowen ratio energy balance (BREB) data;
- comparative BREB total evaporation measurements over three different vegetation types;
- seasonal BREB total actual evaporation measurement; and
- BREB total evaporation comparison with site specific Penman-Monteith evaporation estimates.

Specific aims discussed were:

- examine the energy balance differences;
- examine the evaporation differences;
- simulate evaporation using site-specific Penman-Monteith equations; and
- evaluate the Bowen ratio energy balance technique as a practical method for measuring evaporation above forest and sugarcane.

Chapter 4
EVAPORATION THEORY

4.1 Definitions

Evaporation is the "*physical process by which a liquid or solid is transferred to the gaseous state*" (Huschke, 1959), whereas transpiration can be defined as evaporation of water that has passed through the plant. Evaporation from the soil and the plant (total evaporation) occurs simultaneously and involves different processes, therefore the term evapotranspiration can be defined as the total process of water movement into the atmosphere (Rosenberg et al., 1983). Advection is defined as "the process of transport of an atmospheric property solely through the mass motion of the atmosphere" (Huschke, 1959).

4.2 Introduction to evaporation theory

Crop water use or total evaporation (evapotranspiration) can be determined by different methods (Rosenberg *et al.*, 1983; Savage *et al.*, 1993; Spittlehouse and Black, 1980a; Stull, 1988). Rosenberg *et al.* (1983) specifies three dominant groups; *viz.*:

- the hydrological or water balance method,
- climatological methods, and
- micrometeorological methods.

Climatological methods include *air temperature based formulas* (Thornthwaite method, Blaney-Criddle method, Hargreaves method, Linacre method), *solar radiation formulas* (regression methods, Makkink method, Jensen-Haise method, Solar thermal unit method), *solar and thermal radiation methods* and *combination formulas* (Penman method, Penman-Monteith method, Slatyer and McIlroy method, Priestley-Taylor model) (Rosenberg *et al.*, 1983).

Micrometeorological methods include *mass transport methods*, the *aerodynamic method*, the *Bowen ratio energy balance method*, *resistance methods* and *eddy correlation methods* (Rosenberg *et al.*, 1983).

In the present study the total evaporation measured by the Bowen ratio energy balance method was compared to the Penman-Monteith and equilibrium evaporation estimates.

4.2.1 *Description of the Bowen ratio energy balance (BREB) technique*

The shortened (*Section 4.2.1.1.1*) canopy surface energy balance equation

$$R_n - G - \lambda E - H = 0 \qquad 4.1$$

consists of the net irradiance (R_n) (incoming irradiance minus outgoing irradiance of all wave lengths), the soil heat flux density (G), the latent heat flux density (λE) and the sensible heat flux density (H) (Monteith and Unsworth, 1990; Oke, 1978; Rosenberg *et al.*, 1983). The sign convention used is R_n positive when directed towards the surface and G, λE and H positive when directed away from the surface.

Finite water vapour pressure and air profile temperature differences are measured over a vertical gradient in the atmosphere and an effective eddy diffusivity assumed, to calculate the latent (λE) and sensible heat flux densities (H)

$$\lambda E = (\lambda \rho \varepsilon K_v / P)[(\bar{e}_1 - \bar{e}_2) / (\bar{z}_1 - \bar{z}_2)] \qquad 4.2$$

$$H = \rho c_p K_h [(\bar{T}_1 - \bar{T}_2) / (\bar{z}_1 - \bar{z}_2)] \qquad 4.3$$

with the diffusivity coefficient for latent (K_v) and sensible heat transfer (K_h), the density of the air (ρ), the ratio of the molecular mass of water (M_w) to that of dry air (M_d) ($\varepsilon = M_w/M_d$), atmospheric pressure (P), the specific heat capacity of dry air at constant pressure (c_p) and the vapour pressure $((\bar{e}_1 - \bar{e}_2) / (\bar{z}_1 - \bar{z}_2))$ and air temperature gradient $((\bar{T}_1 - \bar{T}_2) / (\bar{z}_1 - \bar{z}_2))$.

When the diffusivity coefficients (K_v, K_h) are assumed equal, the Bowen ratio (β) is given by

$$\beta = H / \lambda E \qquad 4.4$$

$$\beta = P\, c_p / \lambda\, \varepsilon\, [(\bar{T}_1 - \bar{T}_2) / (\bar{e}_1 - \bar{e}_2)]$$

$$\beta = \gamma\ [(\bar{T}_1 - \bar{T}_2) / (\bar{e}_1 - \bar{e}_2)] \qquad 4.5$$

with the psychrometric constant (γ) (Anonymous, 1998).

Using the surface energy balance (*Eq. 4.1*) and the computed Bowen ratio (*Eq. 4.4*) Bowen (1926) showed the sensible (*Eq. 4.6*) and latent heat flux densities (*Eq. 4.7*) to be

$$H = \beta\, (R_n - G) / (\beta + 1) \qquad 4.6$$

and

$$\lambda E = (R_n - G) / (\beta + 1) \qquad 4.7$$

where $\beta \neq -1$ (Sinclair *et al.*, 1975; Spittlehouse and Black, 1980a; Ohmura, 1982).

The Bowen ratio total evaporation (λET_B) is solved as

$$\lambda ET_B = (R_n - G) / (\beta + 1) \qquad 4.8$$

where λ is the latent heat of vaporization (Angus and Watts, 1984).

4.2.1.1 Assumptions of the Bowen ratio energy balance technique

The Bowen ratio energy balance technique assumes a shortened energy balance, finite air temperature and water vapour pressure differences and similarity of the transfer coefficients.

4.2.1.1.1 *Assumption of a shortened energy balance*

The Bowen ratio energy balance technique utilizes a shortened energy balance equation (*Eq. 4.1*), which neglects advection and physically and photosynthetically stored energy in the canopy, as they are considered negligible (Thom, 1975; Savage *et al.*, 1997).

4.2.1.1.2 *Assumption of finite differences to measure the entity gradients*

The Bowen ratio energy balance technique assumes finite differences as being an adequate indication of gradients in air temperature ($\delta\overline{T}/\delta z$) and vapour pressure ($\delta\overline{e}/\delta z$)

$$[(\delta\overline{T}/\delta z)/(\delta\overline{e}/\delta z)] \approx \Delta\overline{T}/\Delta\overline{e}$$

with Δz for small values of δz ($\delta z \approx 1$ to 3m) (Savage *et al.*, 1997).

The Bowen ratio further assumes that the two levels at which the temperature and vapour pressure measurements are made, must be within the boundary layer of air flow (Angus and Watts, 1984; Nie *et al.*, 1992; Beringer and Tapper, 1996).

4.2.1.1.3 *Assumption of Similarity*

Under conditions of neutral stability, the exchange coefficients for momentum (K_m), sensible heat and water vapour are assumed to be the same ($K_m = K_h = K_v$) (Metelerkamp, 1993; Savage *et al.*, 1997).

The processes involved occur across the *same* interface and concerns the *same* set of vapours in the *same* atmospheric layer moving in the *same* direction. This however, is not always the case (Pieri and Fuchs, 1990; Metelerkamp, 1993; Savage *et al.*, 1997).

4.2.1.1.3.1 *Stability aspects of the Similarity assumption*

During unstable conditions K_h exceeds K_v because of the preferential upward transport of heat (Monteith, 1963; Metelerkamp, 1993). Therefore, under conditions of high evaporative flux levels (β small) and an assumption of $K_h = K_v$ (where K_h and K_v are not markedly different), no serious errors in the λE estimates will be measured. During dry conditions when λE is small (β large) and $K_h \neq K_v$, conditions can lead to errors of the same magnitude of λE (Denmead and McIllroy, 1970; Metelerkamp, 1993; Savage *et al.*, 1997).

4.2.1.1.3.2 *The effects of Advection on the Similarity assumption*

The application of the Bowen ratio energy balance technique in semi-arid conditions, leads to the inadequate performance of this technique (Angus and Watts, 1984; Metelerkamp, 1993; Unland *et al.*, 1998). Blad and Rosenberg (1974) questioned the use of the assumption of similarity under these advective conditions.

The erroneous assumption of similarity lead to underestimation of λE under advective conditions (Blad and Rosenberg, 1974; Metelerkamp, 1993).

4.2.1.2 Limitations of the Bowen ratio energy balance (BREB) technique

The application of the BREB technique is limited by theoretical, practical and boundary layer limitations. These limitations can invalidate the Bowen ratio energy balance technique (Barr *et al.*, 1994).

4.2.1.2.1 *Theoretical limitations of the BREB technique*

Examining the denominator $(1 + \beta)$ in the calculation of the latent heat flux density (*Eq. 4.7*) (which may not become zero), the calculation of λE tends to infinity as the Bowen ratio approaches -1. The Bowen ratio often tends to -1 during early morning and late afternoon periods when the available energy $(R_n - G)$ approaches zero. Rainfall events cause β to approach -1. The latent heat flux density during these periods is low and can be ignored. For Bowen ratio values ranging between -1.25 and -0.75, the latent heat flux densities are assumed to be negligible and are not calculated or included in evaporative totals (Ohmura, 1982; Savage, *et al.*, 1997; Anonymous, 1998).

4.2.1.2.2 *Practical limitations of the BREB technique*

4.2.1.2.2.1 Measurement limitations

Sustained operation of the Bowen ratio instrumentation for long periods is technically difficult (Pieri and Fuchs, 1990). Continuous and accurate measurement of water vapour pressure at two levels is a particular limitation (Lukangu, 1998). Accurate net irradiance and soil heat flux density measurements, could also be a major measurement limitation (Savage *et al.*, 1997).

4.2.1.2.2.2 Resolution limitations

A major difficulty associated with the Bowen ratio energy balance technique is the instrumentation. Instrumentation must detect temperature and vapour pressure differences of the same magnitude as the bias of the sensors (Pieri and Fuchs, 1990). The measured temperature and vapour pressure difference across a vertical distance must therefore be larger than the resolution of the individual sensors for meaningful results to be obtained (Savage *et al.*, 1997). If the air temperature and water vapour pressure differences approach the resolution limits of the different sensors, the measured differences tend to zero.

When resolution limits are approached, the sensor separation should be increased. This results in increased air temperature and water vapour pressure differences (Cellier and Olioso, 1993; Savage *et al.*, 1997).

4.2.1.2.2.3 Condensation limitations

Dew condensation on thermocouples, air intakes and net radiometer domes precludes any meaningful measurement of flux densities. Dew condensation occurs during periods when the Bowen ratio approaches -1 (early morning and late afternoon) and the evaporation rates are low. Data recorded under these conditions need to be rejected (Cellier and Olioso, 1993; Savage *et al.*, 1997).

4.2.1.2.3 *Boundary layer/fetch limitations of the BREB technique*

The BREB technique is theoretically restricted to ideal sites which require an infinite, homogenous canopy in flat terrain (Businger, 1986). Only when there is horizontal uniformity can the vertical fluxes be considered to be similar in form (Angus and Watts, 1984). In order to overcome heterogeneity caused by the horizontal distribution of foliage, the measurements must be made sufficiently high above the canopy layer (Brutsaert, 1982).

Fetch requirements relate to the boundary layer requirements (Heilman and Brittin, 1989). Ideally measurements should be made within the equilibrium sub-layer (Savage *et al.*, 1996). The internal equilibrium layer (δ) is the lower portion of the boundary layer, which has reached water vapour pressure, air temperature and momentum equilibrium with the surface. Brutsaert (1982) defined this layer as the region where the momentum flux density is within 10 % of the value at the surface. The thickness of the internal equilibrium layer is calculated using the Munro and Oke (1975) equation (*Eq. 4.9*) for stable conditions

$$\delta = x^{0.8} z_{om}{}^{0.2} \qquad 4.9$$

with x equal to the fetch and roughness length for momentum transfer (z_{om}) (Heilman and Brittin, 1989).

Practically fetch is often limited. The necessary fetch required to establish equilibrium conditions has often been assumed to be 100 times the maximum measurement height above the ground (Blad and Rosenberg, 1974; Angus and Watts, 1984). If the fetch is very large, the location of the sensors within the equilibrium sub-layer (while still maintaining detectable temperature and humidity differences between the two levels) is relatively easy (Stannard, 1997). Fetch-to-height ratios ranging from 10 : 1 to 200 : 1 have been recommended with 100 : 1 considered adequate for most measurements (Heilman and Brittin, 1989; Nie *et al.*, 1992). Practical limitations result in measured δT and δe values affected by an upwind surface and some measurements made above the equilibrium layer (Stannard, 1997).

Heilman and Brittin (1989) evaluated the effect of fetch and measurement height, on the Bowen ratio estimation of sensible and latent heat flux densities (Heilman and Brittin, 1989). The variability of the Bowen ratio tends to increase with measurement height because of the departure from the ideal site (Heilman and Brittin, 1989).
Yeh and Brutsaert (1971) indicated that the Bowen ratio method may be less sensitive to imperfect fetch conditions when β is small (Heilman and Brittin, 1989) and can be successfully used at fetch-to-height ratios as low as 20 : 1 (Heilman and Brittin, 1989). Hanks *et al.* (1971) found that under advective conditions changes, in air temperature and vapour pressure were still evident at fetch-to-height ratios of 105 : 1 (Hanks *et al.*, 1971). The Bowen ratio energy balance fetch can be reduced significantly by lowering the lower as well as the upper sensor (Stannard, 1997).

4.2.1.3 Rejection criteria of the Bowen ratio energy balance data

A rejection scheme is important to prevent the acceptance of physically inconsistent or extremely inaccurate flux values (Ohmura, 1982). Ohmura (1982) stresses the importance of judging whether the results are close to reality or not.

Various data rejection criteria exist which need to be used with discretion so as not to exclude data unnecessarily.

4.2.1.3.1 Derivation of the data rejection criteria equation

Following Ohmura (1982), objective Bowen ratio rejection criteria, for $\beta \rightarrow -1$ are derived. Savage *et al.* (1997) shows a much more elegant method of obtaining the rejection criteria in terms of the equivalent temperature (θ)

$$\theta = T + e/\gamma \qquad 4.10$$

Assuming δT and δe to be the measured profile air temperature and water vapour pressure differences, and $E(T)$ and $E(e)$ the resolution limits of the air temperature and hygrometer sensors, the true profile air temperature difference dT

$$\delta T - 2E(T) < dT < \delta T + 2E(T) \qquad 4.11$$

and the true water vapour pressure difference de

$$\delta e - 2E(e) < de < \delta e + 2E(e) \qquad 4.12$$

must fall between the two limits (Savage *et al.*, 1997).

Converting *Eq. 4.11* and *Eq. 4.31* yields

$$c_p[\delta T\text{-}2E(T)]+(\varepsilon L_v/P)[\delta e\text{-}2E(e)] < c_p dT+(\varepsilon L_v/P)de < c_p[\delta T+2E(T)]+(\varepsilon L_v/P)[\delta e+2E(e)] \quad 4.13$$

For

$$\beta = \gamma dT/de = (c_p P/\varepsilon L_v)dT/de = -1 \quad 4.14$$

$$c_p dT + (\varepsilon L_v/P)de = 0$$

Then,

$$(\varepsilon L_v / c_p P)[\delta e - 2E(e)] - 2E(T) < -\delta T < (\varepsilon L_v / c_p P)[\delta e + 2E(e)] + 2E(T)$$

$$\text{or } -2E(e)/\gamma - 2E(T) < \delta e/\gamma + \delta T < E(e)/\gamma + 2E(T) < 2E(e)/\gamma + 2E(T) \quad 4.15$$

$$\text{or } -2E(\theta) < \delta e/\gamma + \delta T < 2E(\theta) \quad 4.16$$

$$\text{where } \delta\theta = \delta e/\gamma + \delta T \quad 4.17$$

Another way of deriving the rejection criteria in terms of the resolution limits for the temperature and vapour pressure sensor assumes the difference between the measured profile-equivalent temperature difference ($\delta\theta$) and the true profile-equivalent temperature difference ($d\theta$) to be less than twice the resolution limit in equivalent temperature $E(\theta)$:

$$/\delta\theta - d\theta/ < 2E(\theta) \quad 4.18$$

$$\text{where } E(\theta) = E(T) + E(e)/\gamma \quad 4.19$$

If

$$\beta = \gamma dT/de = -1$$

then

$$d\theta = 0$$

which implies that the equivalent temperature is the same at both levels in the atmosphere. Substituting $d\theta = 0$ into *Eq. 4.18* and expanding *Eq. 4.18*

$$-2E(\theta) < \delta e/\gamma + \delta T < 2E(\theta) \quad 4.20$$

$$\text{or } -\delta e/\gamma - 2E(\theta) < \delta T < -\delta e/\gamma + 2E(\theta) \quad 4.21$$

(Ohmura, 1982; Savage *et al.*, 1997).

This rejection criterium was found to be too rigorous, leading to rejection of most of the Bowen ratio energy balance data sets.

4.2.1.3.2 Use of the data rejection criteria

The following rejection criteria were adopted in this study:

Condition 1

Where β approaches -1 (at sunrise and sunset), numerically meaningless fluxes are calculated and the data points should be excluded from further data analysis (Metelerkamp, 1993; Cellier and Olioso, 1993; Ortega-Farias, 1996). Frequently the equation

$$-1.25 < \beta < -0.75 \quad 4.22$$

has been employed to reject data.

Condition 2

Data suggesting periods where the water vapour pressure (e_1 or e_2) exceeds the saturation water vapour pressure (e_s), must be excluded from further data analysis (Metelerkamp, 1993; Savage *et al.*, 1997)

$$e_1 \text{ or } e_2 > (e_s + 0.01) \qquad 4.23$$

Condition 3

If the air temperature difference (δT) decreases below the thermocouple sensor resolution $E(T)$ (0.006 °C), the data should be rejected and considered unsuitable for processing (Savage *et al.*, 1997).

$$\delta T < \text{resolution limit of temperature sensor}$$
$$\delta T < 0.006\ ^{\circ}C$$

Condition 4

When the water vapour pressure difference (δe) decreases below the dewpoint hygrometer sensor resolution $E(e)$ (0.01 kPa), the data for that period are inconclusive and should be rejected (Savage *et al.*, 1997).

$$\delta e < \text{resolution limits of vapour pressure sensor (DEW-10 hygrometer)}$$
$$\delta e < 0.01\ kPa$$

It was decided to reject all data for periods when any of conditions 1 to 4 were met.

4.2.1.4 Accuracy of the Bowen ratio energy balance technique

The BREB technique has been thoroughly tested in the past and its validity as a reference evaporation measurement has been well established (Fritschen, 1966; Fuchs and Tanner, 1970; Sinclair *et al.*, 1975).

The BREB technique proved to be most appropriate on extensive homogenous surfaces (Malek, 1993). The majority of the studies utilizing the BREB method have been concerned with irrigated pastures and crops or other types of vegetation (*eg.* forests) (Angus and Watts, 1984). Malek indicated that the BREB technique provided accurate estimates of evaporation over any agricultural or non-agricultural ecosystem (Malek, 1993). Spittlehouse and Black (1980) indicated the application of BREB over forests to be more difficult although suitable.

4.2.1.5 Error considerations in the Bowen ratio energy balance technique

Ohmura (1982) stresses the importance of checking the Bowen ratio flux calculation to see whether it is close to reality or rather faulty due to measurement error or instrumentation resolution limits (Ohmura, 1982).

The BREB estimate of latent heat flux density (λE) is directly proportional to the available energy $(R_n - G)$ and inversely proportional to $1 + \beta$. If R_n or G are underestimated, λE will be underestimated. Accurate estimates of net irradiance are therefore critical for reliable λE estimates. Soil heat flux density measurements are less critical (in complete cover situations G is very small in comparison to R_n) (Blad and Rosenberg, 1974). The accuracy of the calibration of net radiometers is stated to be 2.5 % and for the soil heat flux plates, 5 %. If sampling problems and spatial variability of soil is included, a combined error of up to 20% for soil heat flux plates is possible (Angus and Watts, 1984). Errors in the latent and soil heat flux densities depend on the sign of the Bowen ratio. When β is positive and large, a large relative error in the evaporation rate exists (after Fuchs and Tanner, 1970). For $-0.6 < \beta < 2$, the error in the available energy $(R_n - G)$ is a major contributor to the error in the total evaporation rate. For conditions where β exceeds 2, the accuracy to which the water vapour pressure differences are measured, is important (Spittlehouse and Black, 1980).

From a modelling point of view, however, the absolute error in the latent heat flux density is usually more important than the relative error (Angus and Watts, 1984).

The accuracy of the computed latent heat flux density is strongly dependent on the accuracy of β (Angus and Watts, 1984). Where evaporation is close to potential rates ($-0.2 < \beta < 0.2$), relative errors of approximately 30 % in β produce errors of less than 5 % in the latent heat flux density (where R_n and G is included, the error in λE increases to 9 %). During periods of high evaporation rates, the relative accuracy of the computed latent heat flux density is increased even if the Bowen ratio is poorly measured (Angus, 1984). For $\beta \rightarrow -1$ (such as at sunrise and sunset), the relative error in λE becomes infinite (δT approaches 0 and $R_n - G \approx 0$) as it occurs over short periods and the error introduced into the daily evaporation totals is insignificant. For $\beta = -1$, finite latent heat flux density errors are calculated, provided that there is some available energy ($R_n - G \neq 0$).

The relative error in the latent heat flux density is increased, due to the errors in β when water becomes less available and the Bowen ratio increases (Angus and Watts, 1984).

4.2.2 *Description of the Penman-Monteith reference evaporation equation*

Penman (1948) derived a formula to account for the energy required to sustain evaporation and a mechanism to remove the vapour. The original Penman equation for reference evaporation (E_o) over a open water surface is given as

$$E_o = (\Delta R_n + \gamma E_a) / (\Delta + \gamma) \qquad 4.24$$

where Δ is the slope of the saturation water vapour pressure *vs* temperature curve at the surface temperature (T_o) and

$$E_a = f(u)\,(e_s - e_a) \qquad 4.25$$

where $(e_s - e_a)$ is the water vapour pressure deficit and ($f(u)$) the wind function given by

$$f(u) = 0.27\,(1 + u/100) \qquad 4.26$$

where u is the windspeed (Rosenberg, *et al.*, 1983). The Penman equation was later modified by Monteith (1963, 1964) to give the Penman-Monteith combination equation.

The Penman-Monteith equation combines a "radiative" and aerodynamic component to calculate the Penman-Monteith reference evaporation (ET_o) (Appendix 1)

$$ET_o = \Delta\,(R_{ns} - G_s) / [\lambda\,(\Delta + \gamma^*)] + \gamma^* M_w\,(e_a - e_d) / [R(T_a + 273.15) r_v\,(\Delta + \gamma^*)] \qquad 4.27$$

$$ET_o = \text{“radiative” component} + \text{aerodynamic component}$$

where γ^* is the apparent psychrometer constant, M_w the molar mass of water, R the universal gas constant, T_a the air temperature and r_v the combined aerodynamic and canopy resistance to water vapour

$$r_v = r_a + r_c \qquad 4.28$$

where r_a is the aerodynamic resistance for heat transfer and r_c the canopy resistance (Campbell; undated; Oke, 1978; Allen *et al.*, 1989; Monteith and Unsworth, 1990; Metelerkamp, 1993).

The net irradiance (R_{ns}) is simulated from the solar irradiance (R_s)

$$R_{ns} = (1 - \alpha_s)\,R_s + L_{ni} \qquad 4.29$$

where α_s is the reflection coefficient of the crop and L_{ni} the atmospheric radiant emittance minus the crop emittance at air temperature. The soil heat flux density (G_s) is calculated as a fraction of the simulated net irradiance (*Eq. 4.29*)

$$G_s = 0.1R_{ns} \qquad 4.30$$

A common procedure for estimating evapotranspiration (ET) from a well-watered crop, is to first estimate reference evapotranspiration (ET_o) (Allen *et al.*, 1989) from a standard surface and then apply an appropriate empirical crop coefficient (k_c) (Van Zyl and De Jager, 1992) such as presented by Doorenbos and Pruitt (1977) and Wright (1981,1982).

$$ET = k_c ET_o \qquad 4.31$$

The Penman-Monteith equation has been applied successfully over different surfaces (crops and forests) of optimal or limited water supply where the resistance required, are known (Campbell, undated; Rosenberg *et al.*, 1983).

4.2.2.1 *Application of the Penman-Monteith equation to site specific conditions*

In general, the Penman-Monteith evaporation equation is applied to calculate reference evaporation (*Section 4.2.2*). Van Dam *et al.* (1997), however, noted that the Penman-Monteith evaporation equation can be applied to calculate potential and actual evaporation.

In the evaporation experiment conducted at Sevenoaks, the Penman-Monteith equation (*Eq. 4.27*) has been applied to site-specific conditions, where actual total evaporation (ET) was calculated. Site specific reflection coefficients (α_s) were used in the simulation of the net irradiance (R_{ns}) (*Eq. 4.14*). The soil heat flux density (G_s) was calculated as a fraction of the simulated net irradiance. A combined resistance (r_v) was calculated from the aerodynamic resistance to vapour transfer (r_a) and the canopy resistance (r_c). The aerodynamic resistance was calculated as a function of the zero-plane displacement height (d), roughness length for momentum transfer (z_{om}) and roughness length for heat and vapour pressure transfer (z_{oh}). The aerodynamic resistance is a function of the height of the windspeed measurement (z_u), the average canopy height (h), the zero plane displacement (d), the roughness length for momentum (z_{om}) and heat and vapour transfer (z_{oh}), Von Karman's constant (k) and the windspeed at height z_u (u_{zu}) (Monteith and Unworth, 1990; Campbell, undated).

$$r_a = \ln[(z_u - d)/z_{om}]\ln[(z_t - d)/z_{om}]/k^2 u_{zu} \quad 4.32$$

$$d = 2/3h \quad 4.33$$

$$z_{om} = 0.13h \quad 4.34$$

$$z_{oh} = 0.1\, z_{om} \quad 4.35$$

The canopy resistance (r_c) was back-calculated (utilizing the Penman-Monteith equation and the actual Bowen ratio total evaporation), providing average 20 minute r_c estimates over the different seasons for the different canopies. The generalised canopy resistances were then used in the site-specific Penman-Monteith total evaporation calculation.

4.2.3 *Description of the Equilibrium equation*

The equilibrium evaporation (ET_q)

$$ET_q = [\Delta / (\Delta + \gamma)]\,(R_n - G) \quad 4.36$$

can be defined as the lowest possible evaporation rate from a wet surface. The equilibrium evaporation depends entirely on the available energy $(R_n - G)$ and the temperature (Rosenberg *et al.*, 1983).

4.2.4 *Description of the Priestley-Taylor equation*

The Priestley-Taylor potential evaporation (ET_p) (Priestley and Taylor, 1972), refers to the rate of evaporation over an extended short, green surface, which covers the soil completely, exerts little or no resistance to evaporation and is well supplied with water and nutrients at all times

$$ET_p = \alpha [\Delta / (\Delta + \gamma)] (R_n - G) \qquad 4.37$$

The potential evaporation (ET_p) represents an upper limit to evaporation from a wet surface.

The first term (α) represents a measure of the departure from the equilibrium evaporation rate (ET_q). Priestley and Taylor (1972) concluded that for a large saturated land, an accurate estimate of α *is* 1.26. Potential evaporation takes place if the available energy is the only limiting factor (Rosenberg *et al.*, 1983; Brutsaert and Stricker, 1979).

4.3 Application of the evaporation theory

The water use (total evaporation) from *Saccharum*, *Acacia* and *Eucalytpus* canopies was measured in an evaporation experiment conducted at Sevenoaks, using the Bowen ratio energy balance (BREB) technique. The measured net irradiance, soil heat flux, soil temperature and air temperature and water vapour pressure differences were used to complete the simplified energy balance (*Eq. 4.1*). The Bowen ratio total evaporation was subsequently calculated and compared to the equilibrium evaporation. Total evaporation was simulated using site specific Penman-Monteith equations and compared to the measured Bowen ratio evaporation estimates.

Chapter 5

MATERIALS AND METHODS

5.1 Site description and species studied

The experiment was conducted on Mistley-Canema Estate (Mondi Forests) (Fig. 5.1) in the Sevenoaks district, approximately 70 km from Pietermaritzburg. Total evaporation measurements were made above three different canopies: *Saccharum*, *Acacia* and *Eucalyptus* species.

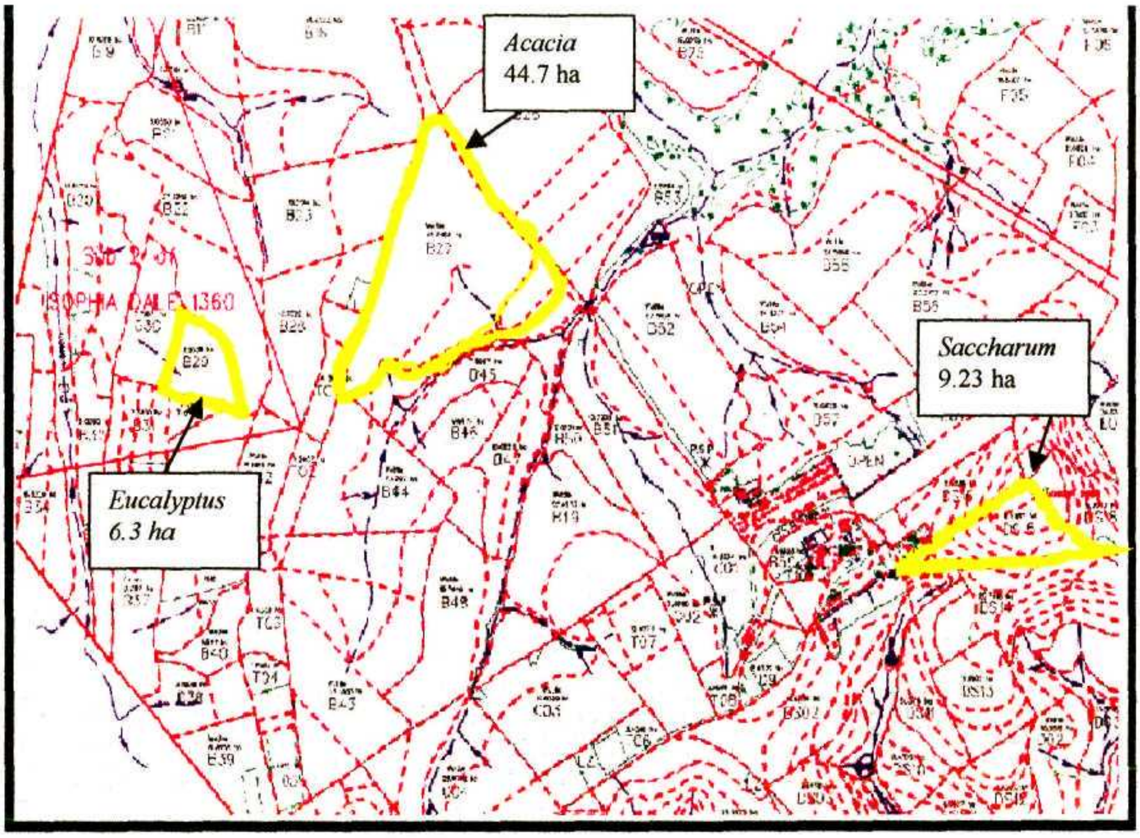

Figure 5.1 Location of the *Saccharum, Acacia* and *Eucalyptus* sites studied (Map Mondi Forests)

Security considerations influenced the layout of the project and electric fencing (5 m by 5 m) had to be installed at two sites (*Acacia* and *Eucalyptus*) to protect the equipment against vandalism. The *Saccharum* site, situated close to the fire lookout tower was considered safe and was only fenced with razor wire.

Scaffolding towers (2.5 m by 2.5 m), which permit free air flow were erected at the three sites, upon which to mount the Bowen ratio equipment and other sensors. The towers started off at a height of three metres, which permitted the Bowen ratio arms and net radiometers to be sufficiently elevated above the canopy. During the growing season, the towers at the *Acacia* and *Eucalyptus* sites had to be raised as the plant height increased.

5.1.1 *Saccharum site description*

The dryland *Saccharum* (sugarcane) site (Fig. 5.2), compartment DS15 (30.67 °S, 29.194 °E), covers an area of 9.23 ha and is situated at an altitude of approximately 1100 m a.m.s.l. The study area was planted with the N12 variety, with a row spacing of 1.1 m.

Figure 5.2 A uniform sugarcane canopy visible at the *Saccharum* site with the Fire tower in the background (Photo CS Everson)

The sugarcane canopy was uniform with a fetch distance greater than 100 m in all directions. The crop was planted during November 1989 and evaporation measurements commenced in August 1997, with the crop in third ratoon. The crop was harvested at the end of August 1998.

5.1.2 *Acacia site description*

Acacia mearnsii (black wattle) (Fig. 5.3) was planted in compartment B27 (30.647 °S, 29.183 °E to 30.644 °S, 29.191 °E) at an average altitude of 1000 to 1100 m a.m.s.l. and covers an area of 44.7 ha, with the shortest distance to the leading edge being greater than 500 m. The trees were planted in June 1996 with a plant spacing of 0.45 m. When total evaporation measurements commenced in August 1997, the average canopy height was 1.1 m.

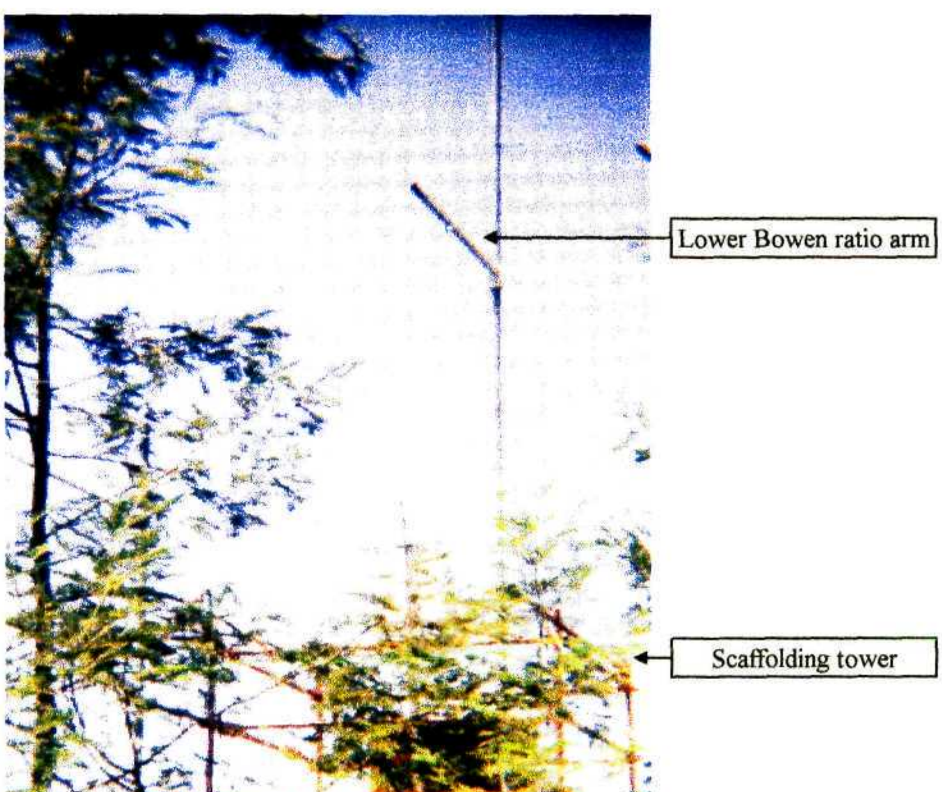

Figure 5.3 The lower Bowen ratio arm mounted onto the scaffolding tower, visible at the *Acacia* site (Upper Bowen ratio arm not visible) (CS Everson)

5.1.3 *Eucalyptus site description*

Eucalyptus dunii and *Eucalyptus macarthurii* (blue gum) (Fig. 5.4) were planted in compartment B29 (30.637 °S, 29.19 °E) during June 1996, covering an area of 6.3 ha with a slope of less than 11 %, at an average altitude of 1000 to 1100 m a.m.s.l. Evaporation measurements started in September 1997, with an average canopy height of 1.8 m. This site is gently sloping with a southern aspect and has a minimum fetch of more than 500 m.

Figure 5.4 Two Bowen ratio sampling arms mounted onto a scaffolding tower, visible at the *Eucalyptus* site (Photo CS Everson)

5.2 Bowen ratio system description

The Bowen ratio energy balance method requires measurements of net irradiance (R_n), soil heat flux density (G) and the mean air temperature and water vapour pressure differences over 20 minutes. The net irradiance and soil heat flux density are used to establish the available energy (R_n - G). The available energy is partitioned between the sensible (H) and latent heat flux densities (λE) (Monteith and Unsworth, 1990; Malek and Bingham, 1993).

5.2.1 *Net irradiance measurement*

The net irradiance (the difference between the total incoming and outgoing irradiance fluxes at all wavelengths) was measured every 10 seconds with Q-6 net radiometers and averaged over 20 minute periods.

5.2.2 *Soil heat flux density estimation for the BREB system*

Two soil heat flux plates, together with four averaging thermocouples were used to calculate the soil heat flux density (G) at the soil surface (*Eq. 5.1*).

$$G = F + S \tag{5.1}$$

The buried soil heat flux plates sense the soil heat flux density at 80 mm (F). This depth is chosen to exclude errors due to vapour transport of heat if the plates were placed near the surface.

The two pairs of averaging thermocouples, buried at 20 and 60 mm, are used to calculate the heat stored above the soil heat flux plates (*S*) (*Eq. 5.2*).

$$S = dT_s/[t_{out}D\ \rho_s\ (c_s + c_w\theta_g)] \qquad 5.2$$

for the soil temperature increase dT_s (for the 20 to 60 mm soil depth) from one 20 minute to the next (t_{out})

The heat stored in the soil is calculated from the change in soil temperature (averaged over a 20 minute period) and the specific heat capacity of the soil (*c*) (*Eq. 5.3*). The specific heat capacity of the soil is a function of the bulk density of the soil (ρ_s), the specific heat of dry soil (c_s), the specific heat of water (c_w) and the soil water content (θ_g) (Anonymous, 1991; Beringer and Tapper, 1996; Anonymous, 1998).

$$c = \rho_s\ (c_s + c_w\theta_g) \qquad 5.3$$

Initially, the soil water content (θ_g) was estimated gravimetrically. Subsequently, this method was replaced with a time domain reflectometry (TDR) method (Campbell Scientific CS615 probe). The TDR method (Anonymous, 1998) was used to estimate volumetric soil water content (θ_v) at 20 minute intervals.

Two soil heat flux plates and four averaging thermocouples were installed to represent the average soil conditions (Figs 5.5 and 5.6). As the ground cover did not vary considerably, it was not considered necessary to include additional sensors (Anonymous, 1991; Beringer and Tapper, 1996).

Figure 5.5 Field installation of soil heat flux plates and averaging soil thermocouples (Photo CS Everson)

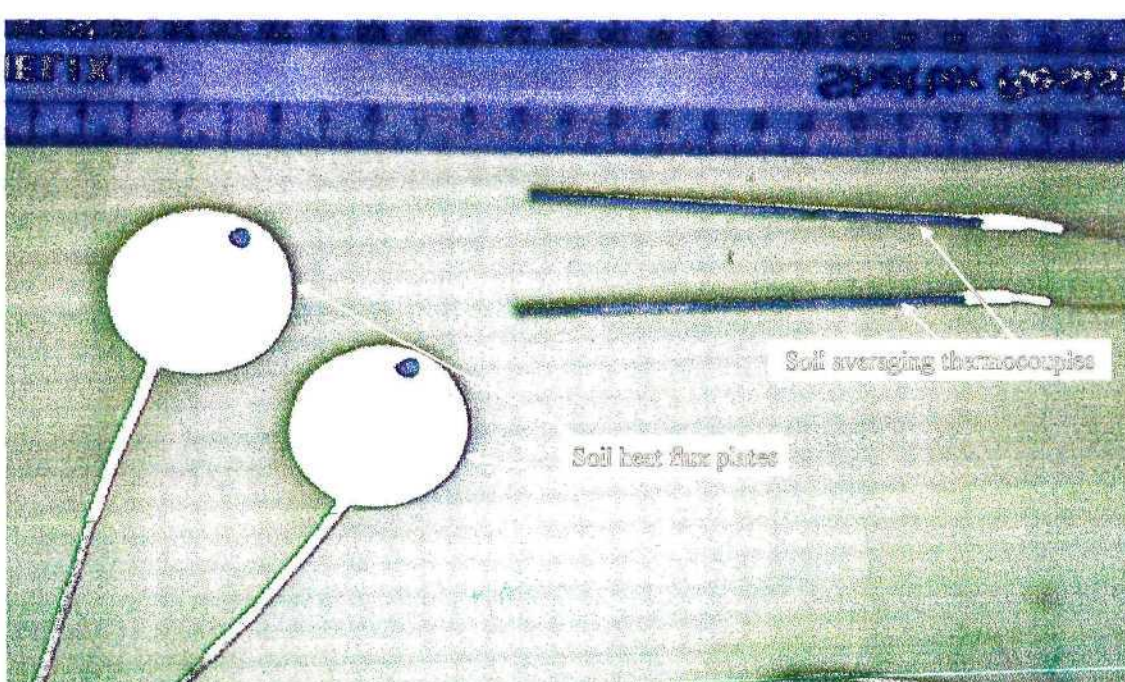

Figure 5.6 Soil heat flux plates and soil averaging thermocouples (Photo CS Everson)

5.2.3 *Air temperature measurement for the BREB system*

Lower and upper air temperatures (T_1, T_2) were measured at heights z_1 and z_2 utilising chromel-constantan thermocouples (type-E). The air temperatures were used in the Bowen ratio and sensible heat flux calculations. A differential voltage (mV) was measured due to a temperature difference between T_1 and T_2 and converted into a temperature difference by multiplying by 0.04 °C mV^{-1}. The resolution of the datalogger is 0.006 °C with a 0.1 µV rms noise.

Differences in the radiative heating of the two thermocouples cause errors in the gradient measurements, but since only the air temperature difference is required, the errors are minimized.

The Bowen ratio system uses two sets of thermocouples on each Bowen ratio system - one set of 25 µm (suffer less from irradiance) and one set of 76 µm diameter (less prone to breakage) (Fig. 5.7). The use of two parallel junctions at each height acts as a back up against breakage (Beringer and Tapper, 1996; Anonymous, 1998).

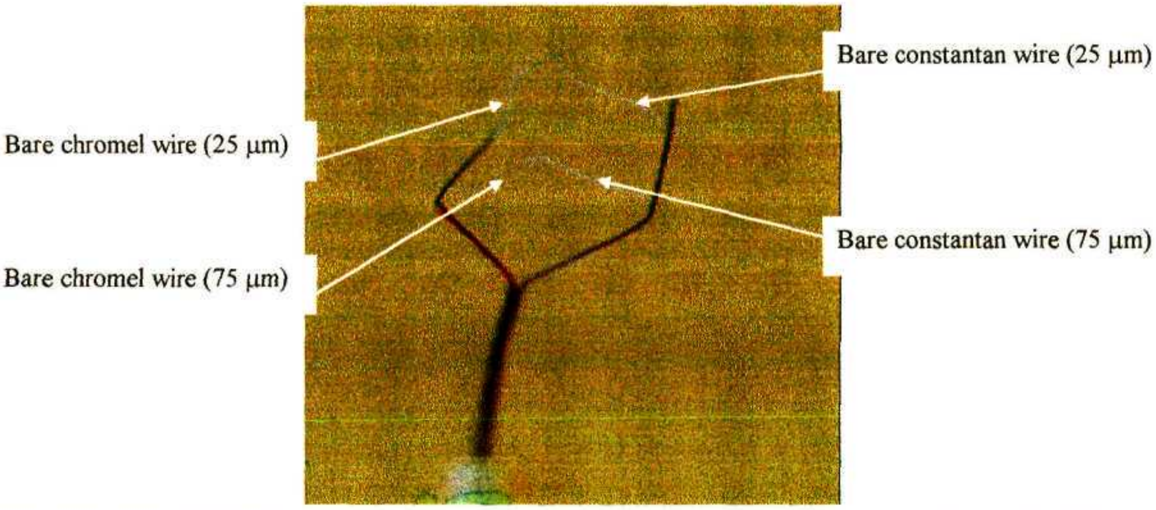

Figure 5.7 Thermocouple configuration. The parallel set of thermocouples ensures temperature averaging and continuation of measurement if one thermocouple is damaged (Photo CS Everson)

5.2.4 *Water vapour pressure measurement for the BREB system*

The Campbell Scientific Inc. (CSI) Bowen ratio system utilizes a single cooled-mirror dew point hygrometer to measure the water vapour pressure difference. Air samples are drawn into the system at two heights (z_1 and z_2) through 25 mm diameter filter containers attached to the arms. The attached containers are fitted with teflon filters with a 1 μm pore size. Air samples drawn into the system are routed through mixing bottles (2 ℓ) to the cooled mirror. The flow is switched between the two levels every two minutes, using a solenoid valve (Fig. 5.8). Forty seconds are allowed for the system to stabilise and 80 seconds for measurements during a two minute cycle. The water vapour pressure is averaged every 20 minutes for each height and is calculated from the measured dew point temperature. The dew point hygrometer yields a water vapour pressure resolution of ±0.01 kPa (Anonymous, 1991; Cellier and Olioso, 1993; Anonymous, 1998).

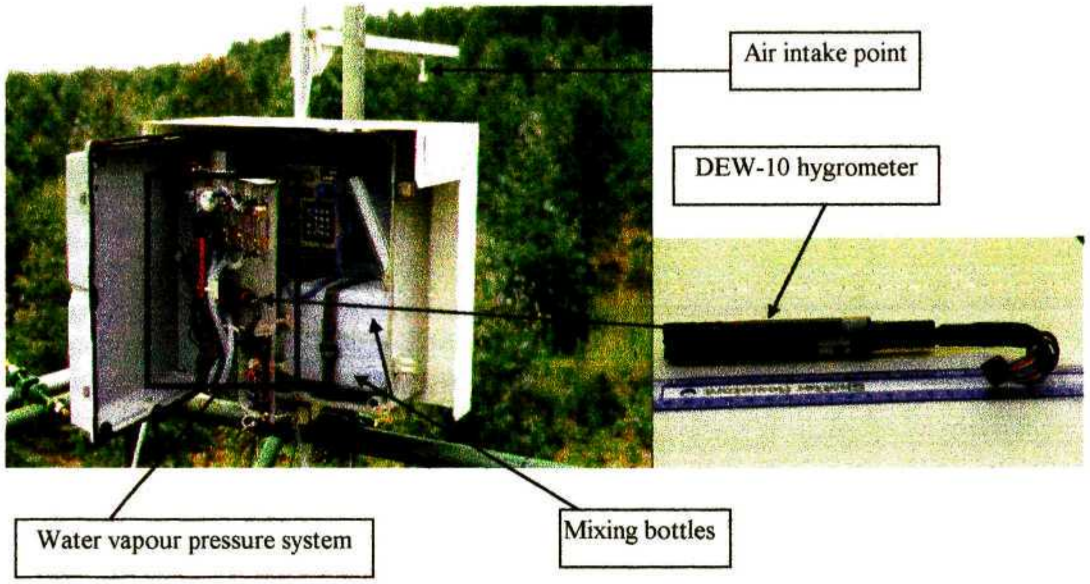

Figure 5.8 Water vapour pressure system with the air intake point, DEW-10 hygrometer and mixing bottles visible (Photo CS Everson)

5.2.5 *Installation of the Bowen ratio energy balance system*

The Bowen ratio system components were mounted onto the scaffolding towers (Appendix 2). The sampling arms of the Bowen ratio energy balance system were orientated due north to avoid partial shading of the thermocouples while the net radiometers were positioned to prevent sensor shading. The separation distance between the arms is influenced by several factors. The air sensed should be representative of the surfaces studied (Anonymous, 1991). A distance separation distance of 0.5 to 3 m between the Bowen ratio sampling arms is suggested in the CSI Bowen ratio instruction manual. With an increased distance between the arms, the water vapour pressure and air temperature differences are increased. The lower arm is installed low enough that the bulk crop surface environment is not sensed. The upper arm is installed low enough in order not to sense a different environment upwind. Garratt (1978) suggested that the lower arm be installed three to five times the roughness length (z_o) above the soil surface (Heilman and Brittin, 1989).

5.3 Additional instrumentation used in the Sevenoaks evaporation experiment

Additional to the Bowen ratio system, every site was equipped with a time domain reflectometer (TDR) probe (CS615). The TDR probe was used to measure real-time volumetric soil water content.

An automatic weather station (solarimeter, air temperature and relative humidity probe, windspeed and direction sensors and raingauge) (Appendix 3) was installed at the *Saccharum* site. A Kipp solarimeter (utilising a Moll thermopile) was used to measure total (direct and diffuse) solar irradiance every second above the canopy. The average solar irradiance was output at 20 minute intervals.

Air temperature and relative humidity, measured with a model 207 temperature and humidity sensor, were used to calculate the water vapour pressure. Windspeed and wind direction were measured with MC System sensors (MC177 and MC176 sensors respectively). Rainfall was measured every 10 seconds with a Rimco tipping bucket raingauge.

5.4 General information on the datalogger

Three Campbell Scientific Inc. 21X dataloggers together with SM192 storage modules were used to collect data at the three experimental sites.

Independent Bowen ratio systems were installed at the three different sites, with an additional automatic weather station at the *Saccharum* site. The programme for the 21X datalogger at the *Saccharum* site (Appendix 4) differs slightly from the basic Bowen ratio datalogger programme (Appendix 5).

A standard Bowen ratio programme consists of three programme tables as listed below.

- Table 1 - high execution rate - sensors were interrogated every second and include air temperature, relative humidity, dewpoint temperature and solar irradiance.
- Table 2 - low execution rate - sensors were interrogated every 10 seconds and included net irradiance, soil heat flux density and soil temperature measurements.
- Table 3 - subroutine for low battery voltage.

Many authors suggest averaging of measured air temperature and water vapour pressure differences over periods between 20 to 60 minutes during daylight hours (Jensen *et al.*, 1989; Spittlehouse and Black, 1980a; Monteith and Unsworth, 1990; Malek, 1993). In this experiment all sensors were sampled several times per minute and averaged over a 20 minute period. Massman (1992) recommended using data from daylight hours only.

The 21X dataloggers control the power to the cooled-mirror and pump and were programmed to turn the pump off between 19h00 and 05h00 to only include daylight values and save power. The 21X is programmed to shut the system off if the battery voltage is below a specified value (11.5 V).

5.4.1 *Wiring of the sensors*

The wiring connections for all the Bowen ratio and automatic weather station sensors to a 21X Campbell Scientific Inc. datalogger, are given in Appendix 6 (Anonymous, 1991).

5.4.2 *Power supply to the datalogger and sensors*

Fourty Watt solar panels and 70 A h batteries were used at the three experimental sites (*Saccharum Acacia* and *Eucalyptus*), which were capable of providing 300 to 350 mA, falling well within the component power requirements (Appendix 7).

5.5 Processing of the Bowen ratio energy balance data

The Campbell Scientific Inc. PC208W (version 2.1) software package consists of seven separate programmes, including a SPLIT parameter file programme. The SPLIT programme is a data reduction programme, which accesses data input files, performs specific operations on the data and outputs the data to an output file. The SPLIT programme is applied for data processing, file reformatting, data quality checking, time synchronization, table generation (with report and table headings) and data selection based on time or conditions (Anonymous, 1998). Writing parameter files for data processing is part of the calculation of the heat flux densities (Savage *et al.*, 1997).

5.5.1 *Description of split parameter files for processing of BREB data*

In the evaporation experiment, all sensors were sampled several times per minute, averaged over a 20 minute period and output by the datalogger into two arrays (one for each programme table) as comma separated ASCII data

5.5.1.1 Pass0 (Pass0a, Pass0b and Pass0c) parameter files

Pass0 collates two arrays (the output from programme table one and two) into a file consisting of a single array. *Pass0a* extracts the first array, identified with an array identifier '1' and *Pass0b* the second array identified with an array identifier '2'. *Pass0c* combines the extracted first and second arrays into a single array making use of time synchronisation. To avoid missing any data during data extraction, ranges of 100..199 and 200..299 are used in the 'COPY from' line of the parameter file. Output from programme table three only occurs when the battery voltage decrease below 11.75 V, reporting the date and time of the system shutdown, resulting in a third array.

5.5.1.2 Pass1 parameter file

Pass1 combines the raw Bowen ratio data developed in *Pass0* with the soil water content, utilizing the time synchronization capacity of SPLIT.

5.5.1.3 Pass2 parameter file

Pass2 is included for any corrections to the raw data. The order of the columns is changed to exclude duplication. The output of this step can replace the raw Bowen ratio data as no data has been lost, but overlaps have been eliminated and the soil water content has been included.

5.5.1.4 Pass3 parameter file

The *Pass2* output is imported into the *Pass3* split parameter file. This file is used to calculate the heat flux densities, the Bowen ratio and evaporation (Bowen ratio and equilibrium) (Metelerkamp, 1993; Savage *et al.*, 1997; Anonymous, 1998).

5.6 Reliability and maintenance of the Bowen ratio energy balance system

Cellier and Olioso (1993) stressed the importance of the reliability of the complete Bowen ratio system. Maintenance should take high priority (Cellier and Olioso, 1993). The BREB technique can be used with reliability for long term continuous measurement of total evaporation (Spittlehouse and Black, 1980; Blad and Rosenberg, 1974; Cellier and Olioso, 1993; Malek, 1993). The dew point hygrometer mirror cleanliness needs regular checking due to the permanent presence of liquid water on the mirror (Cellier and Olioso, 1993).

The Campbell Scientific Instruction (CSI) manual prescribes the following routine maintenance activities:

- Change air intake filter 1-2 weeks
- Clean mirror and adjust bias 1-2 weeks
- Clean thermocouples as needed
- Clean net radiometer domes as needed

(Anonymous, 1998).

Chapter 6
RESULTS AND DISCUSSION

6.1 Total evaporation comparison using the Bowen ratio energy balance technique

A typical day for each season (Winter 1997, Summer 1997, Winter 1998 and Summer 1998) has been chosen for comparison at the three sites. These four days are compared in terms of diurnal, site-specific differences in the energy balance components (R_n, G, H and λE), other measured variables (δe and δT) and the Bowen ratio and equilibrium evaporation estimates. In addition, the general climatic conditions (rainfall, air temperature and solar irradiance) and the general canopy characteristics (leaf area indices and average canopy heights) for the periods and canopies studied, are described.

6.1.1 *A description of the general climatic conditions at the study sites*

A description of the total annual rainfall, average air temperatures (daily and monthly) and daily and monthly average solar irradiance totals, are given to aid the interpretation of the changes in the energy balance components and evaporation estimates over the different seasons.

The total annual rainfall (1 August 1997 to 1 August 1998) was 615.3 mm, implying a marginal forestry site. With the exception of a few rainfall events, all the rainfall occurred during the spring/summer rainfall period (DOY 243 to DOY 60) (Fig. 6.1). The rainfall during August 1997 (21 mm) and September 1997 (49 mm), exceeded the rainfall during August 1998 (19 mm) and September 1998 (21 mm).

The average air temperature (daily and monthly) (Fig. 6.2) and solar radiant density totals (Fig. 6.3) followed similar patterns, with maximum air temperatures and solar irradiance totals reached during Summer 1997 (DOY 332 and 60). The average daily air temperatures measured during August 1998 (14.7 °C) and September 1998 (16.9 °C) were higher than those measured during the corresponding period in 1997 (14.3 and 15.5 °C respectively). This implies that 1998 was hotter and drier than 1997.

The daily solar radiant density totals reached during August 1997 (11.92 MJ m^{-2}) and September 1997 (11.95 MJ m^{-2}), exceeded the solar radiant density totals during August 1998 (10.11 MJ m^{-2}) and September 1998 (11.08 MJ m^{-2}). The decrease in the average daily solar radiant density totals, resulted in less energy being available.

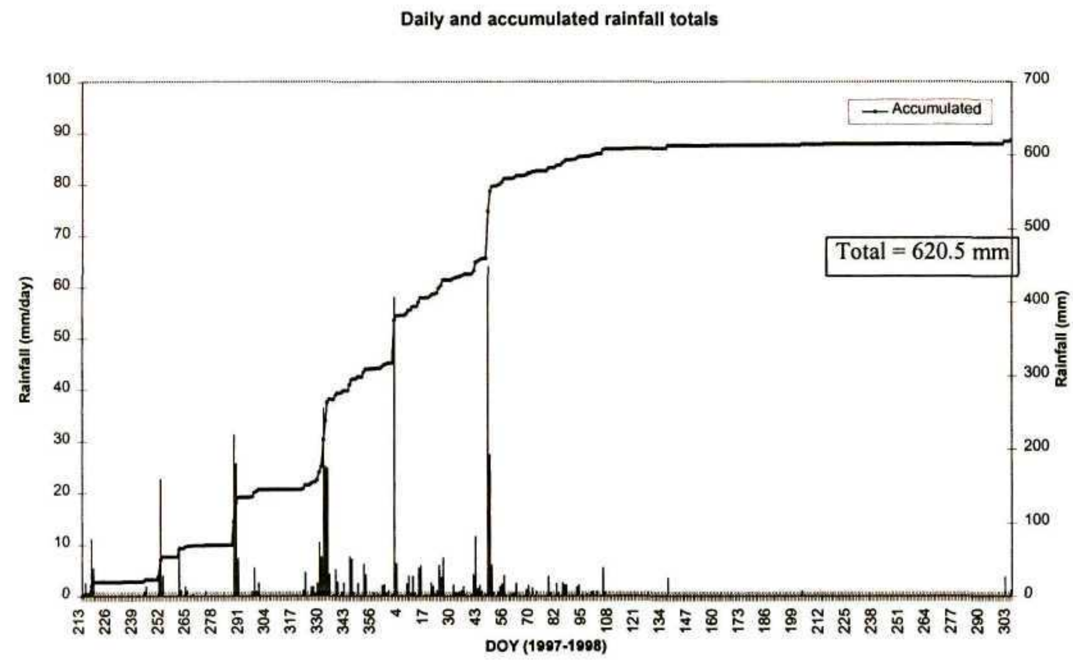

Figure 6.1 Daily and accumulated rainfall totals from 1 August 1997 to 31 October 1998 at the Sevenoaks evaporation experiment sites

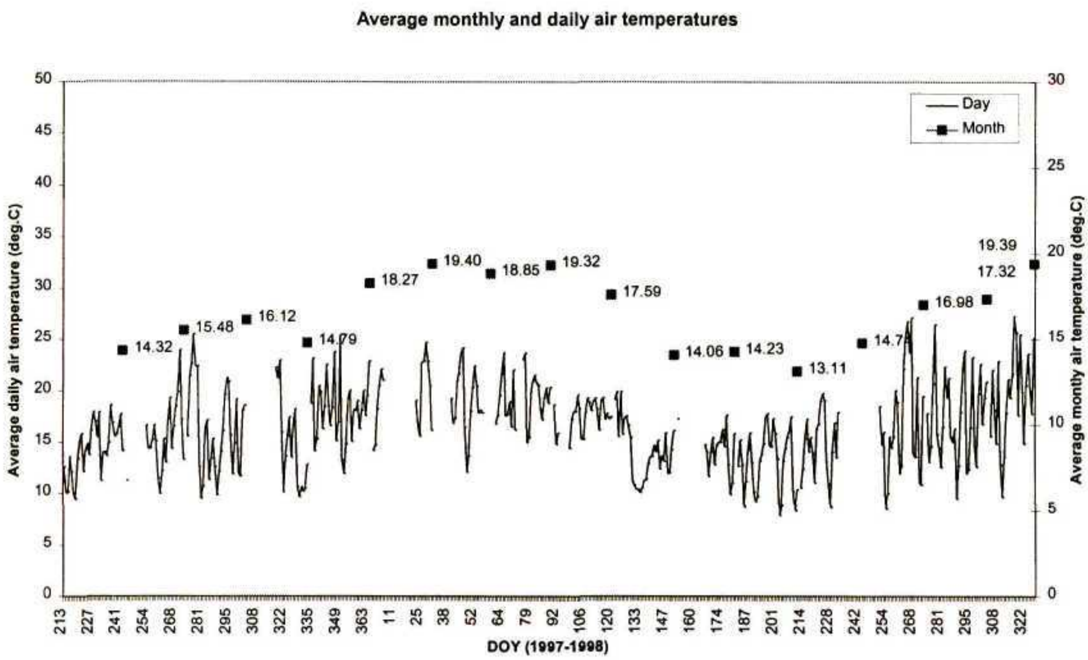

Figure 6.2 Daily and monthly average air temperatures measured at the sites studied

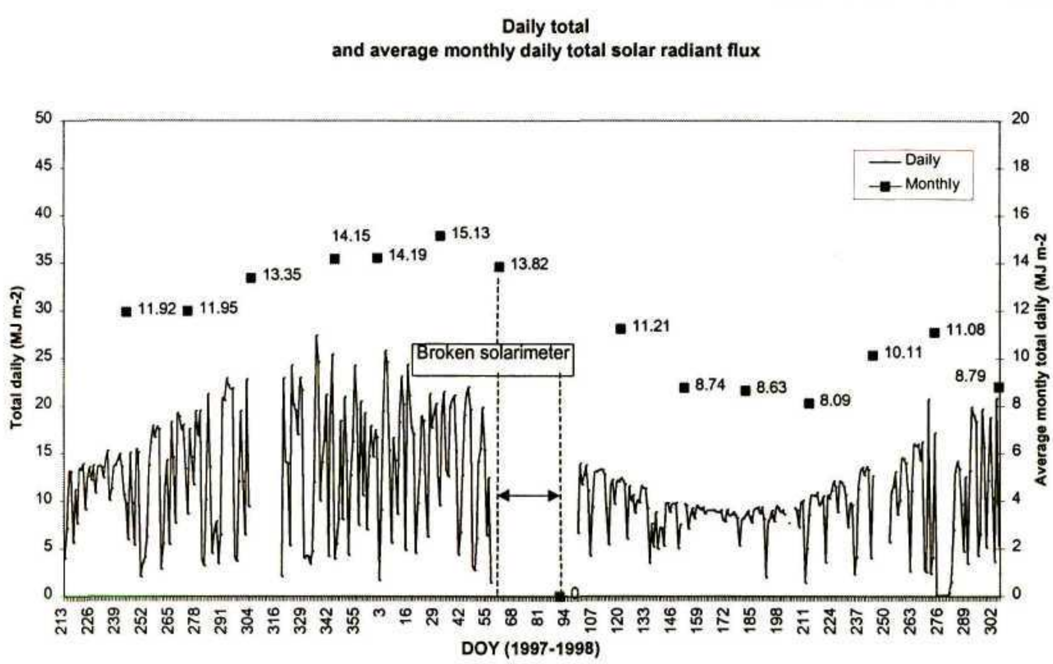

Figure 6.3 Daily and monthly average solar radiant flux measured at the sites studied

6.1.2 *A description of other site specific parameters studied*

The leaf area index (LAI) was measured every two to four weeks with a LI-COR LAI 2000 canopy analyzer. The average leaf area indices at the commencement of the evaporation experiment were approximately 6, 1.7 and 1.5 respectively at the *Saccharum, Acacia* and *Eucalyptus* sites (Fig. 6.4). The leaf area index at the *Saccharum* site increased from a value of 6 on DOY 243 (1997) to a maximum value of approximately 7.5 on DOY 243 (1998). The leaf area indices at the *Acacia* and *Eucalyptus* sites (1.7 and 1.5 respectively) Winter 1997, increased to values of approximately 2.5 and 3.5 respectively, towards the end of Summer 1997 (DOY 60). The leaf area indices decreased slightly during Winter 1998 (DOY 250 to 273) at both the *Acacia* and *Eucalyptus* sites, and an increase in the leaf area indices was visible at the beginning of Summer 1998 (DOY 280).

The average *Acacia* and *Eucalyptus* canopy heights were calculated from 20 tagged *Acacia* and *Eucalyptus* trees, of which the heights and stem diameters were measured every two to three weeks. The average *Saccharum* canopy height was calculated as the average of 20 randomly chosen sugarcane plants. The average canopy height at the *Saccharum, Acacia* and *Eucalyptus* sites, increased between DOY 213 (1997) and DOY 243 (1998) (Fig. 6.5). At the beginning of the evaporation experiment (DOY 213 1997), the average *Saccharum* canopy height was approximately 2.5 m. The average canopy height increased by approximately 3.9 mm day^{-1} during 1997 and 1998 and reached a height of approximately 3.5 m during Winter 1998. The small increase in the average *Saccharum* canopy height during this period (DOY 110 to 240), was attributed to a decreased growth rate (1.5 mm day^{-1}), as the crop reached maturity. During the period studied (DOY 213 1997 to DOY 300 1998), the average canopy heights at the *Acacia* and *Eucalyptus* sites followed the same increasing trend, with the average *Eucalyptus* canopy height constantly exceeding the average *Acacia* canopy height.

The average canopy height at both the *Acacia* and *Eucalyptus* sites increased from September 1997 (DOY 243) (1.5 m and 2 m respectively) to February 1998 (DOY 60) (5 m and 5.5 m respectively) with average growth rates of 19.2 mm day^{-1} and 18.7 mm day^{-1} respectively. The increased growth rates during this period were attributed to higher solar radiant densities (11.9 to 15.1 MJ m^{-2}), increased air temperatures (15.5 to 19.3 °C) and rainfall (550 mm).

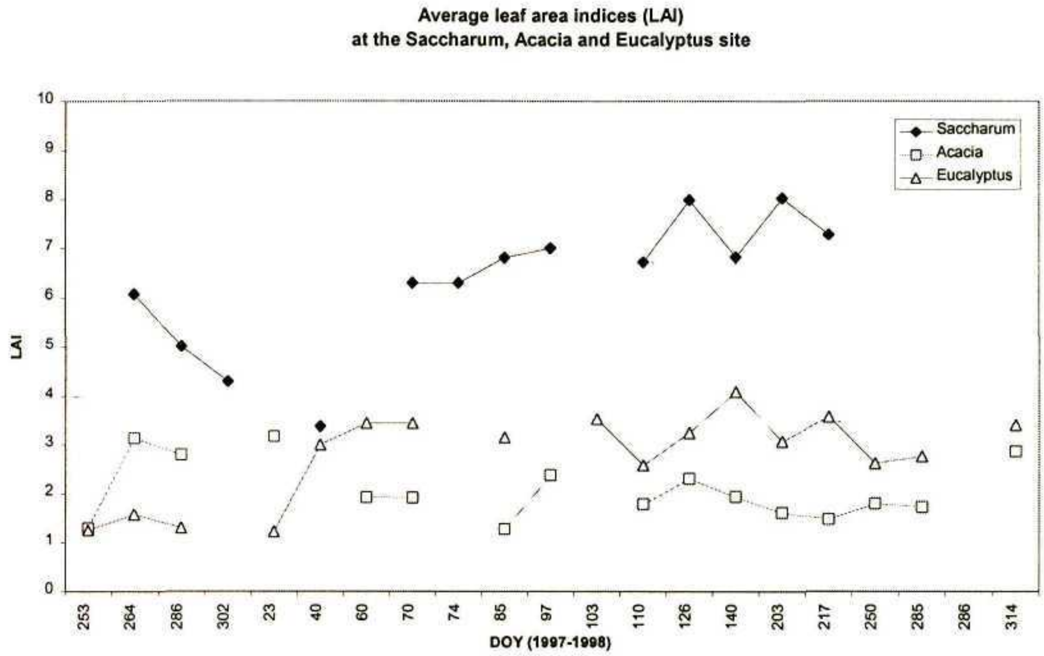

Figure 6.4 Average leaf area indices for *Saccharum, Acacia* and *Eucalyptus*

During the Winter 1998 period (DOY 60 to 243), the growth rate of the *Acacia* and *Eucalyptus* trees (4.9 mm day^{-1} and 6.8 mm day^{-1} respectively) declined as the climatic conditions became unfavourable. The growth rate at both the *Acacia* and *Eucalyptus* sites (11.5 mm day^{-1} and 14.6 mm day^{-1}), increased from September 1998 (DOY 243) with the onset of spring.

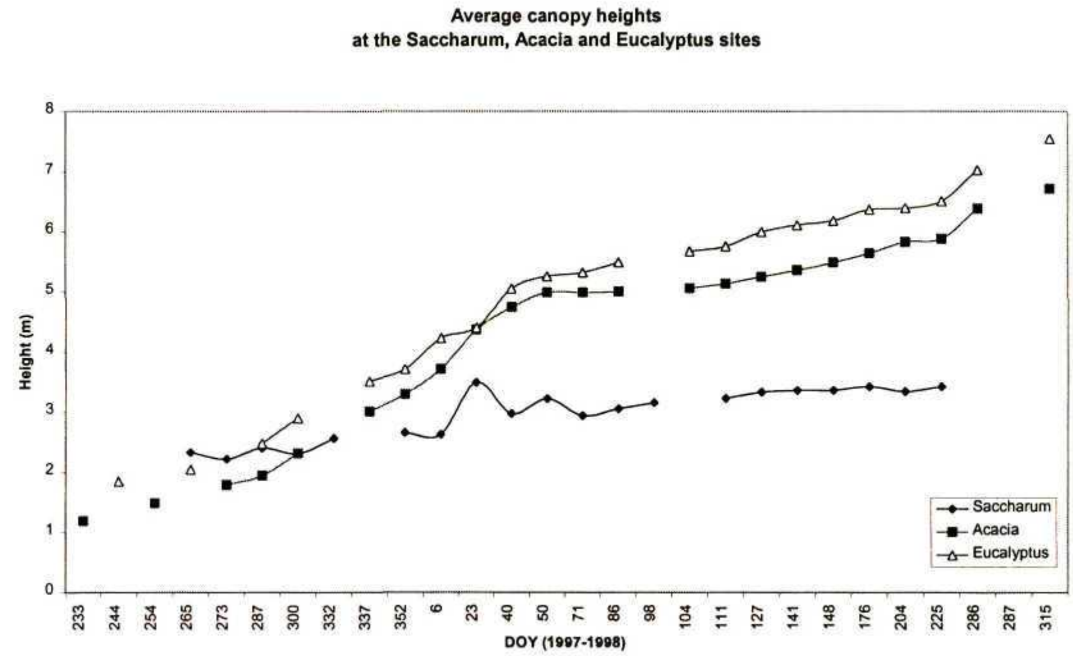

Figure 6.5 Average canopy heights for *Saccharum, Acacia* and *Eucalyptus* sites

6.1.3 *The Bowen ratio energy balance component comparison*

The Bowen ratio energy balance components (R_n, G, H and λE) and other measured variables (δT and δe) differed between the *Saccharum, Acacia* and *Eucalyptus* sites during the periods studied (Winter 1997, Summer 1997, Winter 1998 and Summer 1998).

6.1.3.1 Comparison of the net irradiance and soil heat flux density

The net irradiance at the *Eucalyptus* site constantly exceeded the net irradiance at both the *Acacia* and *Saccharum* sites for a given solar irradiance (R_s) (Winter 1997, Summer 1997, Winter 1998 and Summer 1998) (Figs 6.6 to 6.9). The differences in the net irradiance between the three sites, were at least partially explained by the differences in reflection coefficient (α_s). Similar differences were found by Oke (1978), who measured low reflection coefficients for forest canopies, by comparison with most other agricultural vegetation. Stanhill (1970) found that the reflection coefficient of tall vegetation (*e.g.* forest canopies) was less than that of short vegetation, partly explaining the relatively small reflection coefficients over the forest canopies found in this study. Average reflection coefficients for sugarcane and coniferous forest, are give in Table 6.1.

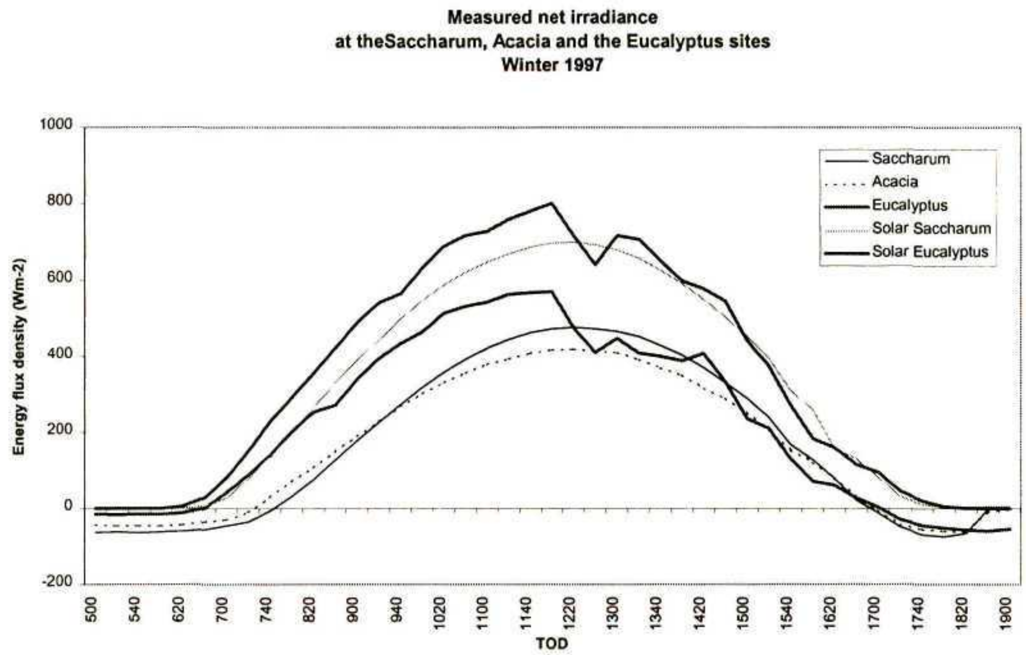

Figure 6.6 Net irradiance at the *Saccharum, Acacia* and *Eucalyptus* sites during Winter 1997 (DOY 229)

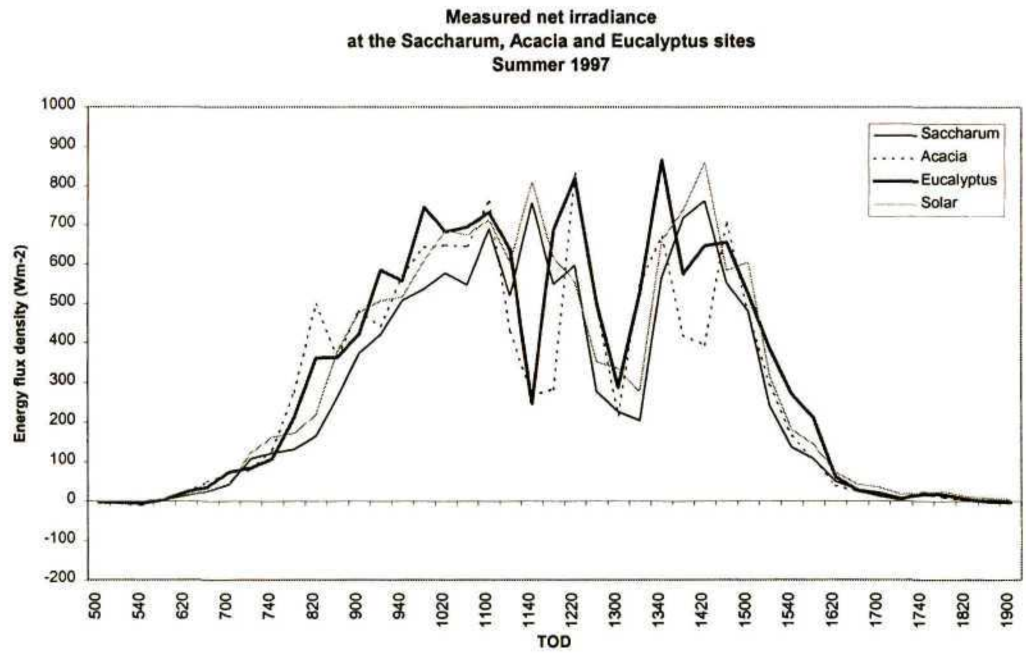

Figure 6.7 Net irradiance at the *Saccharum, Acacia* and *Eucalyptus* sites during Summer 1997 (DOY 34)

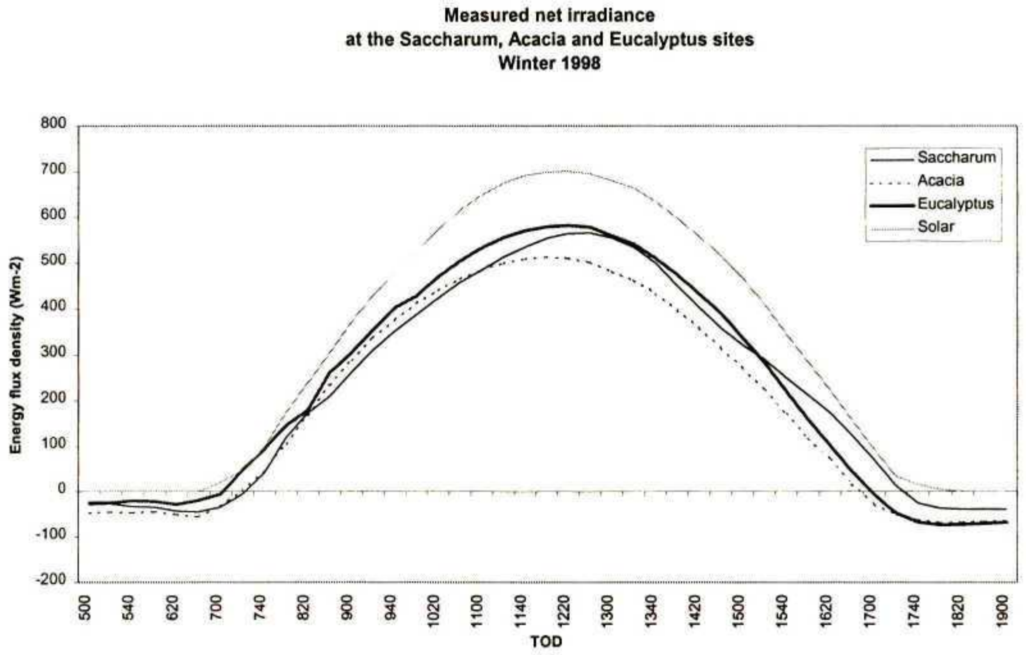

Figure 6.8 Net irradiance at the *Saccharum, Acacia* and *Eucalyptus* sites during Winter 1998 (DOY 227)

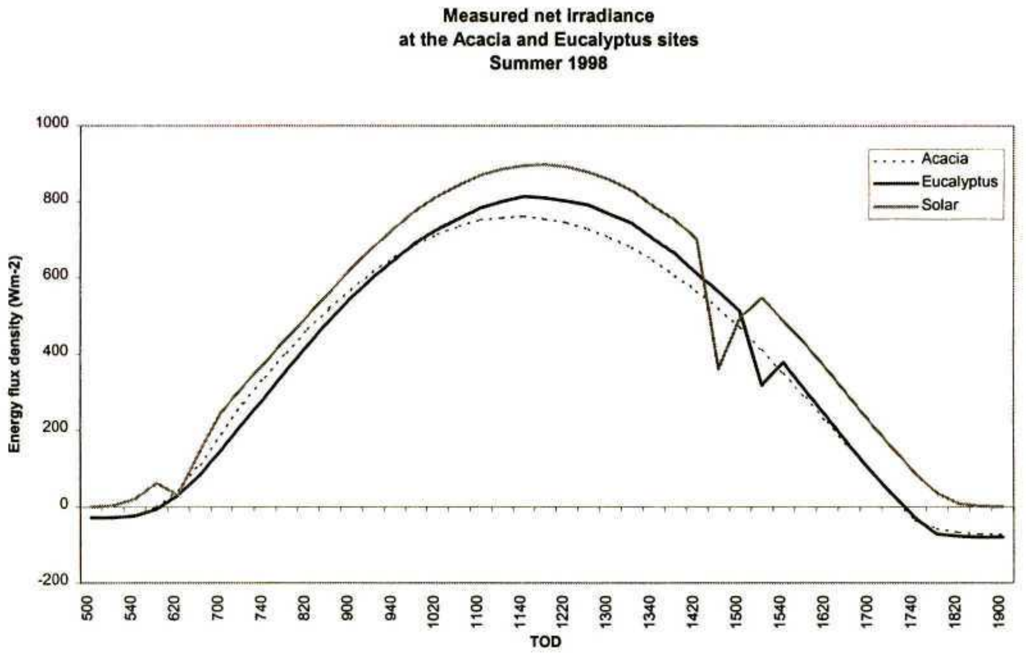

Figure 6.9 Net irradiance at the *Acacia* and *Eucalyptus* sites during Summer 1998 (DOY291)

Table 6.1 Reflection coefficients for sugarcane (*Saccharum*) and coniferous forest (*Acacia* and *Eucalyptus*)

Reflection coefficient	**Sugarcane**	**Coniferous forest**
α_s	0.228 (McGlinchey and Inman-Bamber, 1996)	0.11 to 0.15 (Rosenberg *et al.*, 1983; Monteith, 1976)

The linear relationship between the soil heat flux density (G) and the net irradiance (R_n) at the beginning of the evaporation experiment, showed the important contribution of the soil heat flux density to the energy balance (*Eq. 4.1*) at both the *Acacia* and *Eucalyptus* sites (Figs 6.10 and 6.11). During Winter 1997, the soil heat flux density accounted for more than 40 percent of the net irradiance at both the *Acacia* and *Eucalyptus* sites (slope relationship m = 0.44 and m = 0.42 respectively) (Figs 6.10 and 6.11). At the *Saccharum* site, the soil heat flux density accounted for approximately 10 percent (m = 0.11) of the net irradiance during Winter 1997, Summer 1997 and Winter 1998 (Figs 6.12 to 6.14). The differences in the soil heat flux densities were attributed to differences in the shade provided by the canopy as a result of differences in the leaf area indices. Monteith (1975) suggested that the soil heat flux density, ranging between 2 and 20 % of the net irradiance, varied in approximately inverse proportion to the direct shading of the soil surface by the vegetation. Under very dense canopies (*e.g. Saccharum*) and on overcast days in more open canopies, the soil heat flux density accounts for a small, almost negligible fraction of the net irradiance (less than 10 %) (Monteith, 1976). In more open canopies (*e.g. Acacia* and *Eucalyptus* during Winter 1997) on sunny days, the soil heat flux density is a significant fraction (more than 40 %) of the net irradiance.

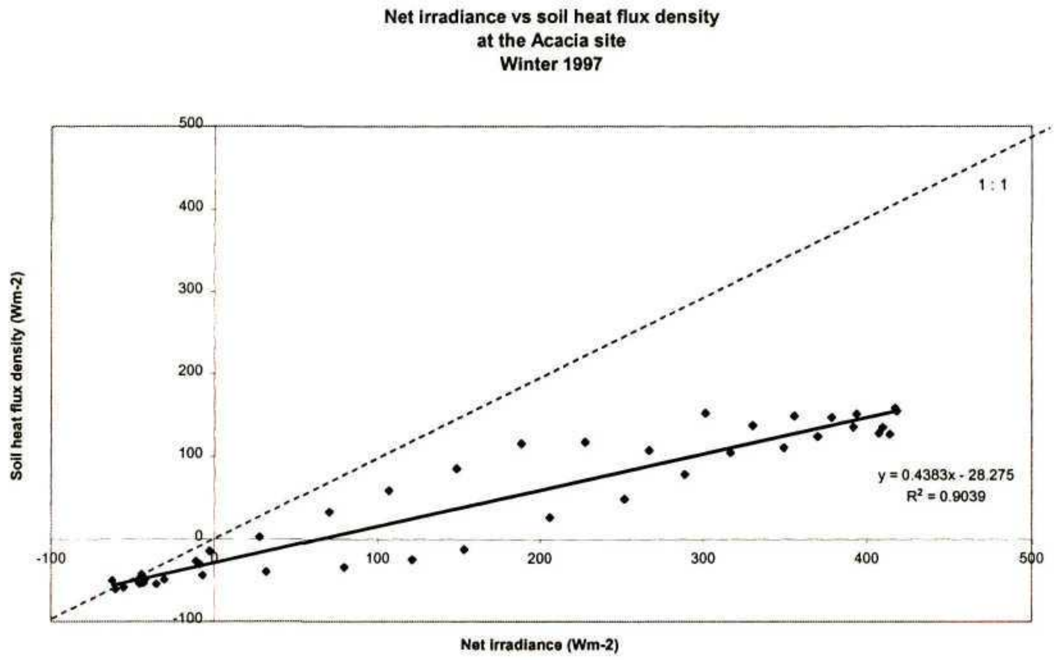

Figure 6.10 Measured net irradiance *vs* soil heat flux density at the *Acacia* site during Winter 1997 (DOY 229)

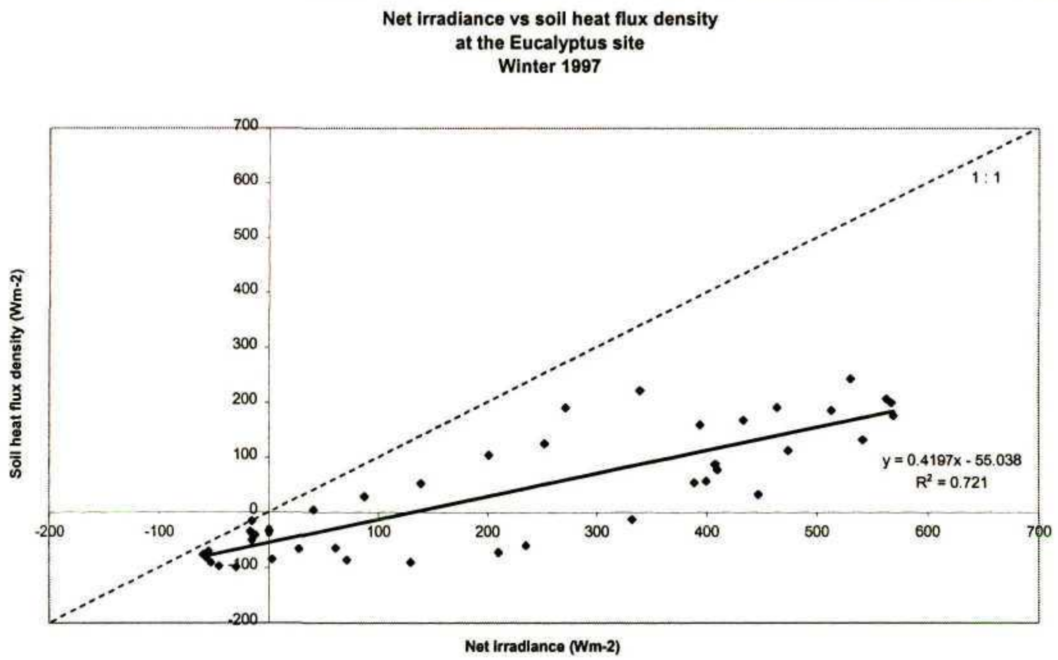

Figure 6.11 Measured net irradiance *vs* soil heat flux density at the *Eucalyptus* site during Winter 1997 (DOY 229)

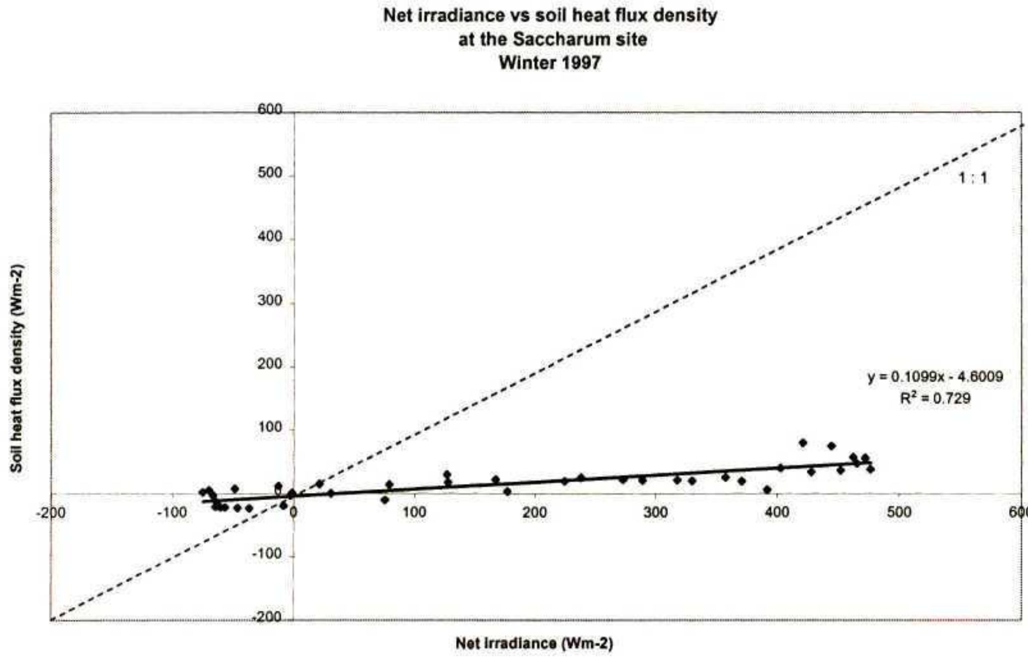

Figure 6.12 Measured net irradiance *vs* soil heat flux density at the *Saccharum* site during Winter 1997 (DOY 229)

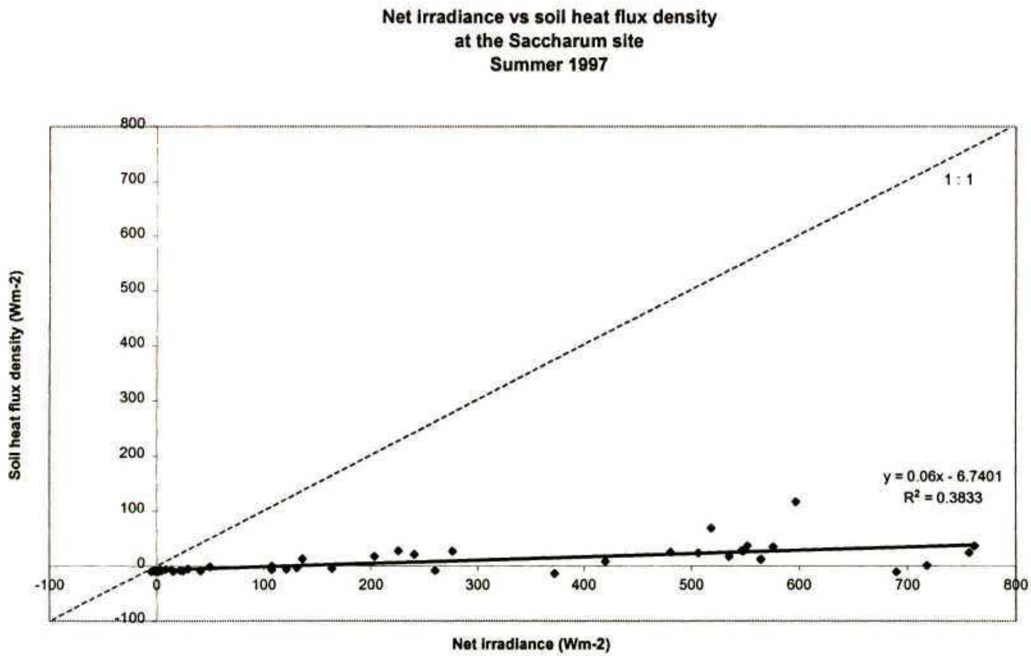

Figure 6.13 Measured net irradiance *vs* soil heat flux density at the *Saccharum* site during Summer 1997 (DOY 229)

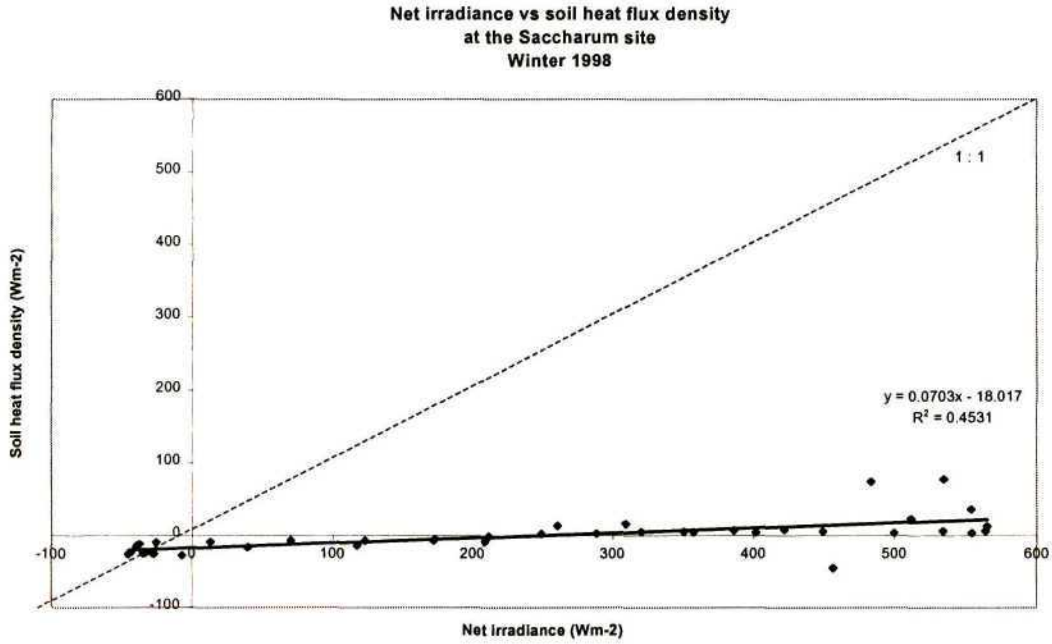

Figure 6.14 Measured net irradiance *vs* soil heat flux density at the *Saccharum* site during Winter 1998 (DOY 227)

The soil heat flux density, as a fraction of the net irradiance changed significantly from Winter 1997 to Summer 1998 at both the *Acacia* and *Eucalyptus* sites, as the canopy shading (*i.e.* LAI's) increased (Table 6.2). The soil heat flux density therefore accounted for approximately 10 percent of the net irradiance during Summer 1997, Winter 1998 and Summer 1998 at the three sites (Figs 6.15 to 6.20). Campbell (undated) used 10 % for his reference evaporation calculation.

Table 6.2 Average ratio of the soil heat flux density to the net irradiance (%) during the four seasons studied

Average ratio of G to R_n (%)	Winter 1997	Summer 1997	Winter 1998	Summer 1998
Saccharum	10.99	6.00	7.03	-
Acacia	43.83	9.24	10.71	13.24
Eucalyptus	41.97	12.19	13.24	9.44

6.1.3.2 Comparison of the latent heat flux density and Bowen ratio

The latent heat flux density (λE) at the *Saccharum* site exceeded the latent heat flux densities at both the *Eucalyptus* and *Acacia* sites during Winter 1997 (Fig. 6.17). Thus, the evaporation from the *Saccharum* site exceeded the evaporation from both the *Eucalyptus* and *Acacia* sites. During this winter period, most of the available energy was surprisingly enough partitioned into the latent heat flux density at the *Saccharum* and *Acacia* sites. This was surprising as this a period where the sensible heat flux density is expected to dominate the energy balance, because of very small water vapour pressure differences measured. Average Bowen ratios (β) of -0.46 and 0.34 were measured respectively (Fig. 6.18) (Table 6.3). Monteith (1976) noted the importance of the size of the Bowen ratio over forests on afforestation and watershed management. The Bowen ratio ranges from approximately -0.5 to +0.5 for irrigated agricultural crops and Bowen ratio values less than -1 occur when advected heat is important.

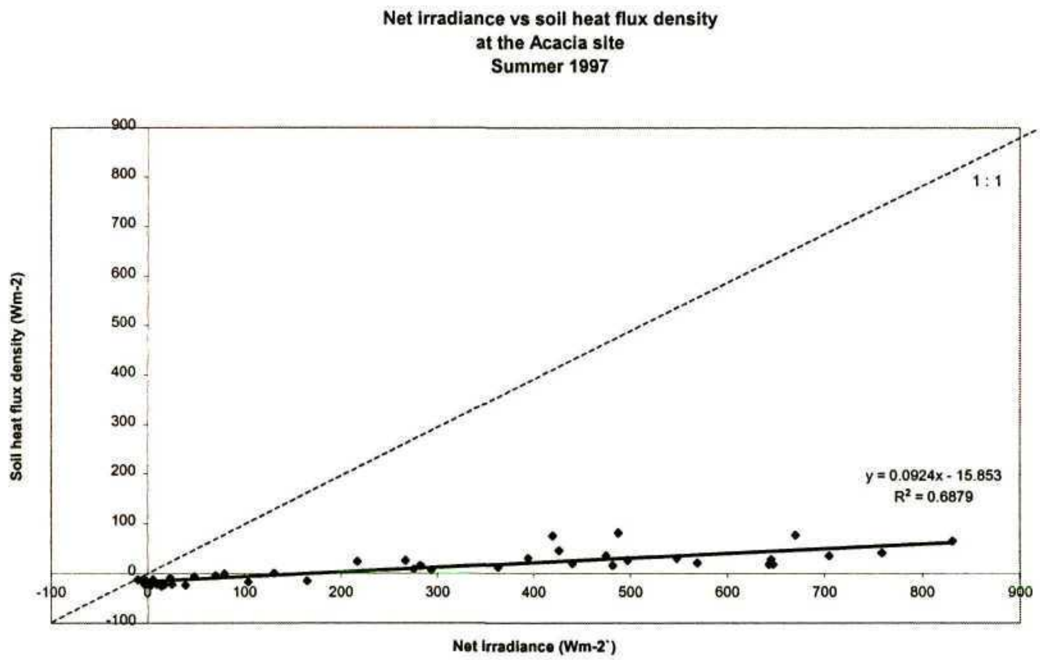

Figure 6.15 Measured net irradiance *vs* soil heat flux density at the *Acacia* site during Summer 1997 (DOY 34)

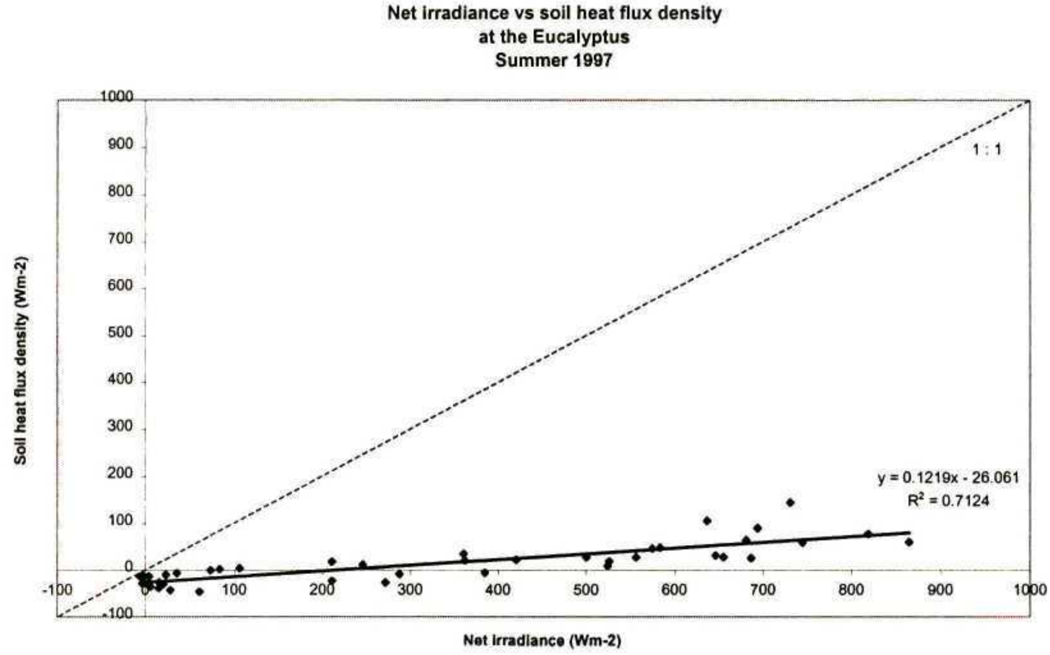

Figure 6.16 Measured net irradiance *vs* soil heat flux density at the *Eucalyptus* site during Summer 1997 (DOY 34)

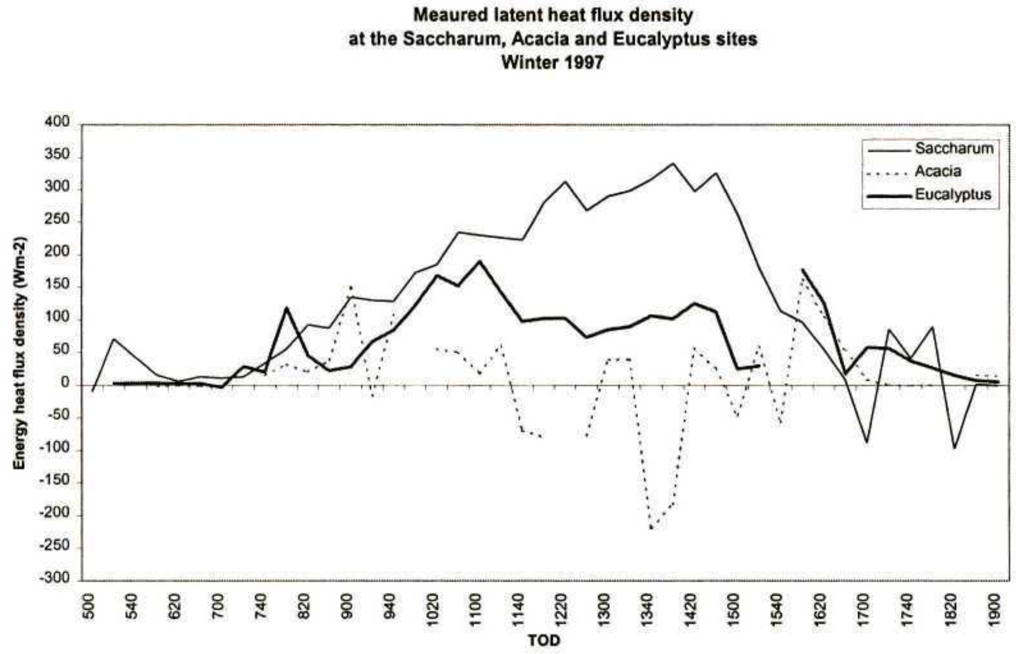

Figure 6.17 Latent heat flux densities at the *Saccharum, Acacia* and *Eucalyptus* site during Winter 1997 (DOY 229)

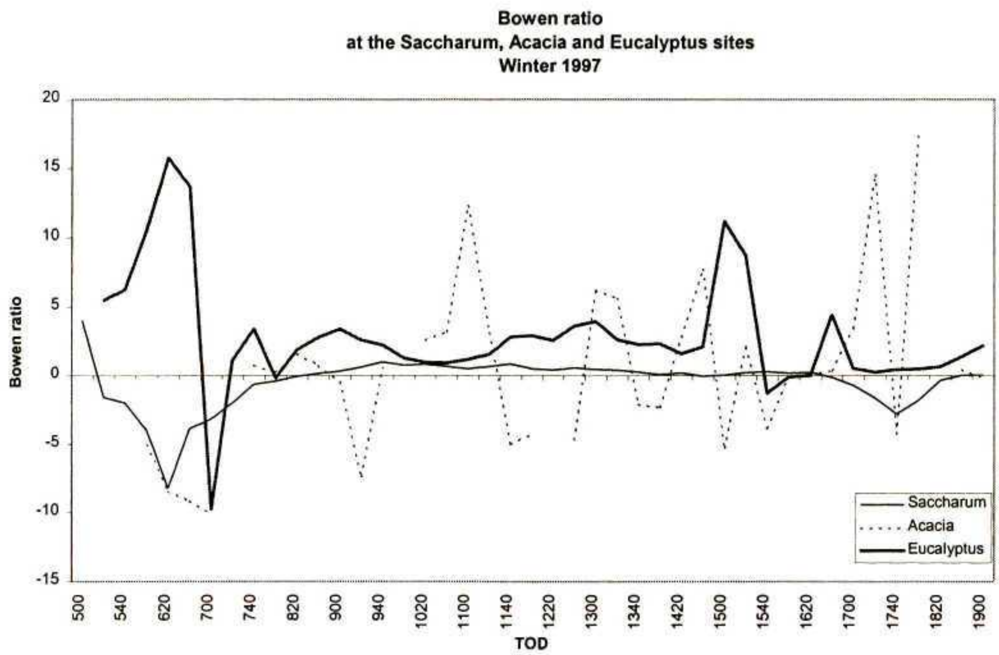

Figure 6.18 Bowen ratio at the *Saccharum, Acacia* and *Eucalyptus* sites during Winter 1997 (DOY 227)

The negative average Bowen ratio at the *Saccharum* site during Winter 1997 merely indicated that the two fluxes, the sensible and latent heat flux densities, have different signs. The evaporative flux is therefore directed away from the surface, whereas the sensible heat flux density is directed towards the surfaces. At the *Eucalyptus* site, the average Bowen ratio was 2.8 and most of the available energy was therefore partitioned into the sensible heat flux density. Bowen ratio measurements over forest fall into two groups (Monteith, 1976). When the canopy is wet with rain or dew, low Bowen ratio values varying between -0.7 and 0.4 were measured. Occasionally, however, much larger Bowen ratio values and low evaporation rates, were measured (up to 4) (Monteith, 1976).

Table 6.3 Average Bowen ratio values as measured at the *Saccharum, Acacia* and *Eucalyptus* sites

	Winter 1997	**Summer 1997**	**Winter 1998**	**Summer 1998**
Saccharum	-0.46	1.82	1.85	-
Acacia	0.34	0.78	-0.21	0.84
Eucalyptus	2.80	0.01	1.63	0.20

Monteith (1976) noted that the Bowen ratio (β) for forest exceed the Bowen ratio for field crops. A wide range of Bowen ratio values over forests occur, depending on the stomatal resistance as well as the general climatic and local weather conditions at a site. The Bowen ratio is approximately proportional to the canopy resistance. Large Bowen ratios result from stomatal closure resulting in increased canopy resistance or small water vapour pressure profile differences.

Bowen ratios of less than unity during Summer 1997 and Summer 1998 (Table 6.3) at both the *Acacia* (0.78 and 0.84 respectively) and *Eucalyptus* sites (0.01 and 0.27 respectively) showed that most available energy was partitioned into the latent heat flux density (Figs 6.19 and 6.20). High evaporation rates were therefore expected at both the *Acacia* and *Eucalyptus* sites. The Bowen ratio at the *Acacia* site exceeded the Bowen ratio at the *Eucalyptus* site during both Summer 1997 and Summer 1998.

The latent heat flux density at the *Eucalyptus* site, therefore exceeded the latent heat flux density at the *Acacia* site during Summer 1997 and Summer 1998 (Figs 6.21 and 6.22).

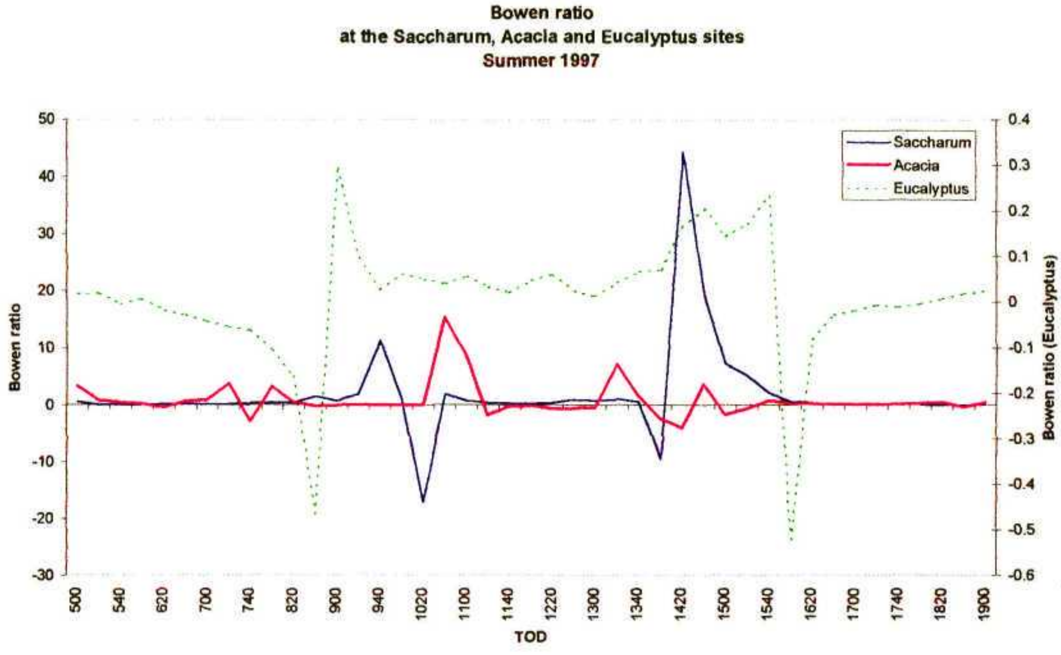

Figure 6.19 Bowen ratio at the *Saccharum, Acacia* and *Eucalyptus* sites during Summer 1997 (DOY 34)

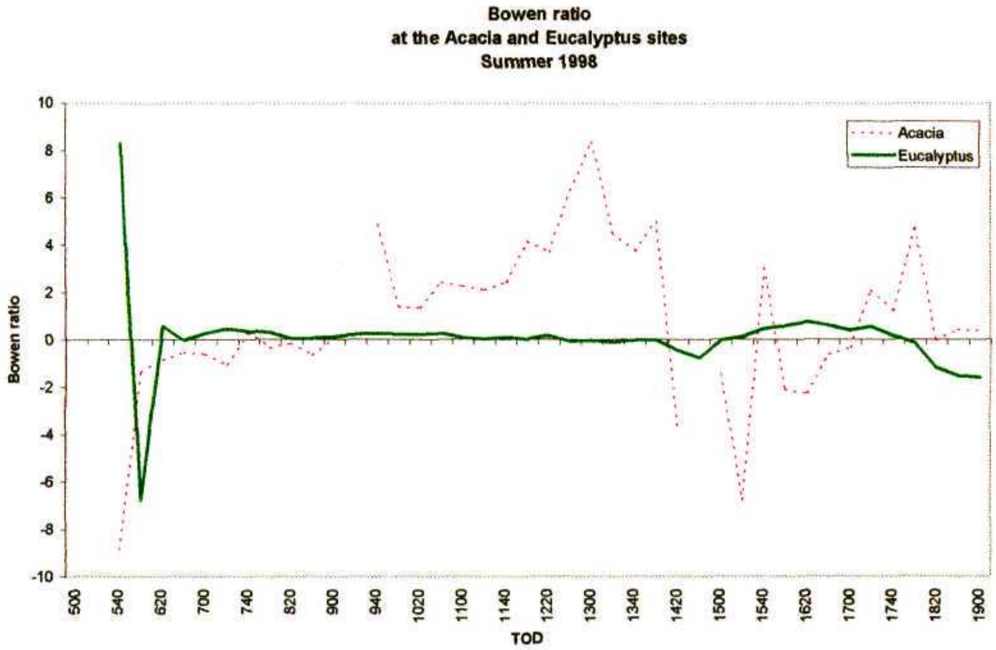

Figure 6.20 Bowen ratio at the *Acacia* and *Eucalyptus* sites during Summer 1998 (DOY 291)

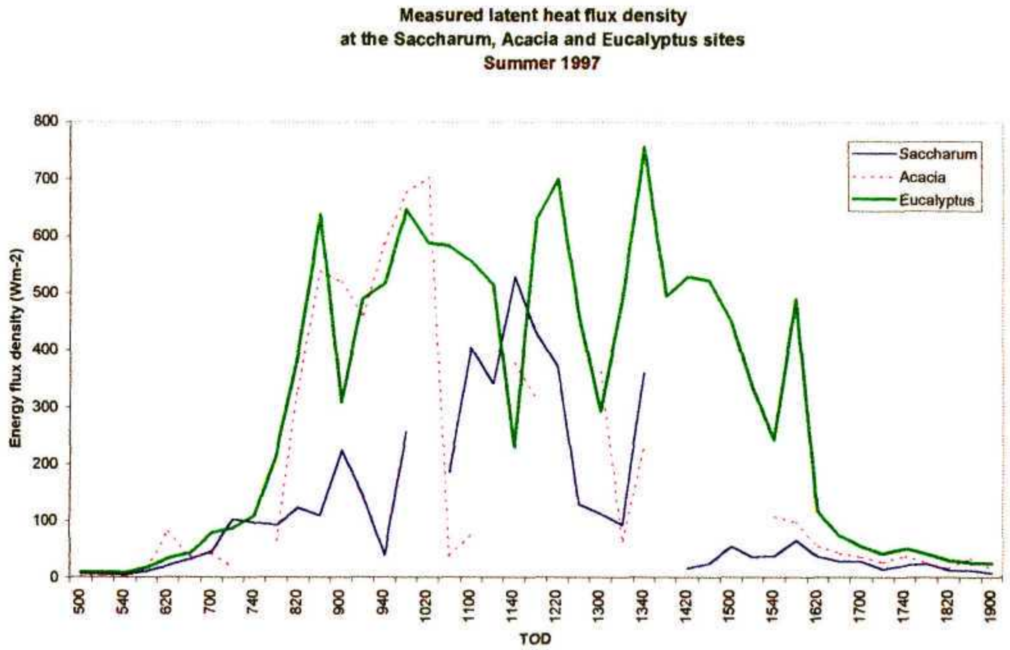

Figure 6.21 Latent heat flux densities at the *Saccharum*, *Acacia* and *Eucalyptus* site during Summer 1997 (DOY 34)

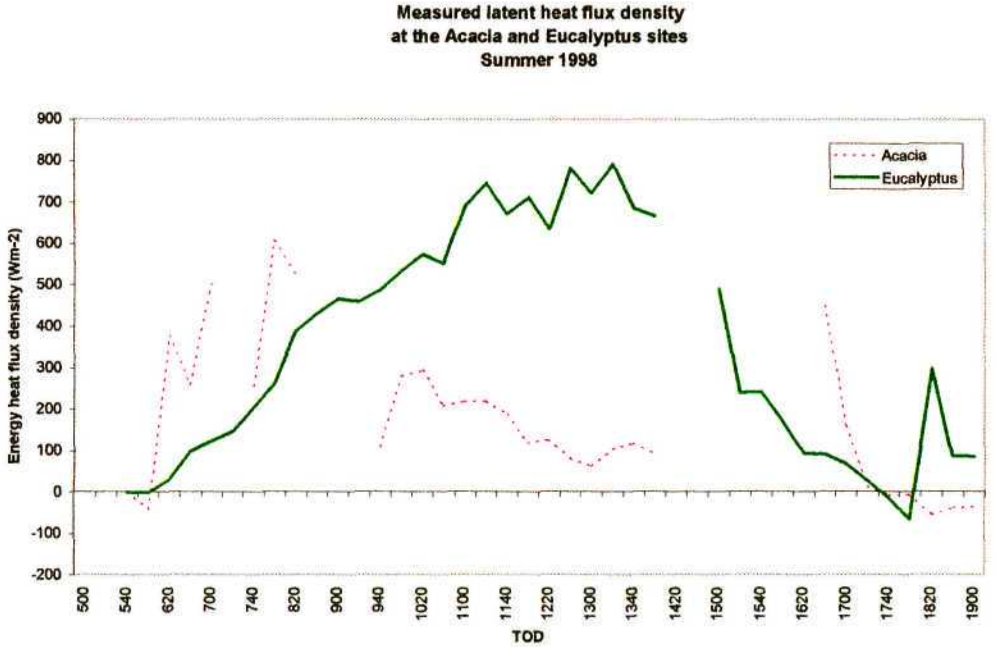

Figure 6.22 Latent heat flux densities at the *Acacia* and *Eucalyptus* site during Summer 1998 (DOY 291)

6.1.3.3 Comparison of the air temperature and water vapour pressure profile differences

The precision of the air temperature and water vapour pressure sensors enable accurate measurements of the small temperature and water vapour pressure differences above the forest canopy. The air temperature and water vapour pressure differences above forest canopies (*e.g. Acacia* and *Eucalyptus*) were periodically a limitation in the use of the Bowen ratio energy balance technique during winter. During these periods, however, the periodic rejection of the Bowen ratio data had little effect on the calculation of the evaporation totals since it corresponded with small negative Bowen ratios and small evaporation rates.

The measured air temperature difference above *Saccharum* (-0.191 to 0.439 °C with an average of -0.04 °C) was generally greater than that above *Acacia* (-0.498 to 0.136 °C with an average of -0.044 °C) and *Eucalyptus* (-0.564 to 0.212 °C with an average of -0.009 °C) during Winter 1998 (Fig. 6.23). Wicke and Bernhofer (1996) found the temperature differences above forests to be approximately an order of magnitude smaller than above a grass surface. Everson (1993) found the same trend, with air temperature differences above the grassland up to four times greater than those above forest canopies. The large air temperature differences above *Saccharum* were well within the resolution of the sensors (0.006 °C). In contrast, the air temperature differences above *Acacia* were small (average of 0.009 °C). Insufficient sampling height, however contributed to the small air temperature differences above the *Acacia* site (Fig. 6.24). The air temperature differences were periodically rejected at the three sites, where the Bowen ratios approached -1 (07h00 to 08h00 and 17h00 to 17h30) and evaporation rates were low.

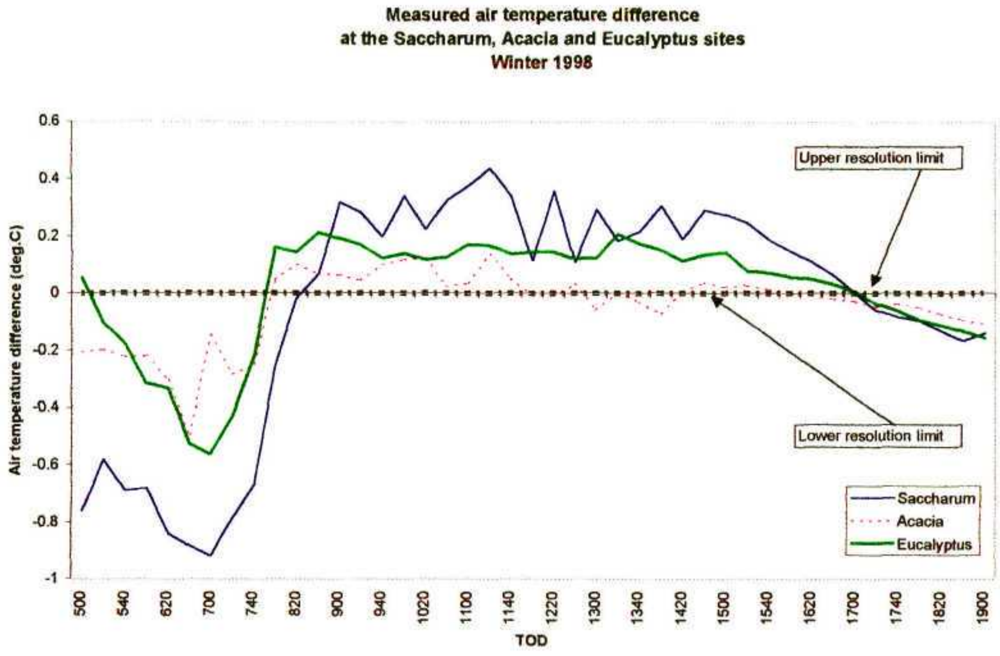

Figure 6.23 Air temperature differences at the *Saccharum, Acacia* and *Eucalyptus* sites during Winter 1998 (DOY 227)

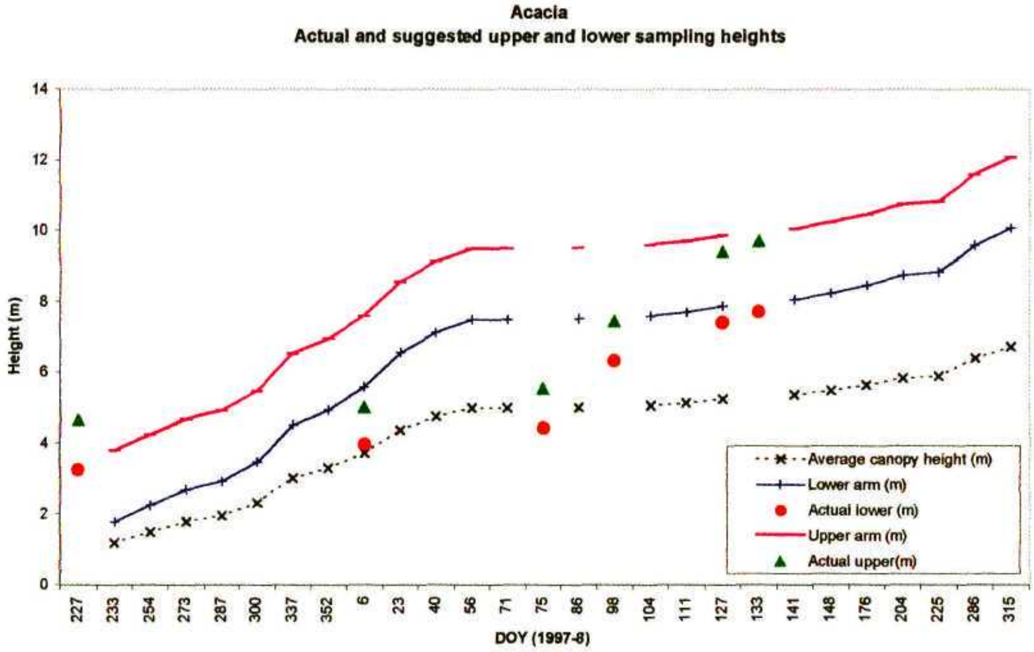

Figure 6.24 Measured (actual lower and actual upper) and suggested upper and lower sampling heights at the *Acacia* site

The measured air temperature differences during Summer 1997 (Fig. 6.25) above *Saccharum* (0.02 to 0.723 °C with an average of 0.276 °C), *Acacia* (-0.108 to 0.376 °C with an average of 0.114 °C) and *Eucalyptus* (-0.054 to 0.451 °C with an average of 0.183 °C), exceeded the air temperatures measured during Winter 1998 (Fig. 6.23) at these sites falling well within the resolution limits of the air temperature sensors.

Everson (1993) found water vapour pressure differences above grassland to be higher than above forests (*Eucalyptus smithii*). The water vapour pressure differences however, generally fell within the resolution limits of the DEW-10 hygrometer. Mean diurnal courses in the water vapour pressure differences at the *Saccharum, Acacia* and *Eucalyptus* sites during Winter 1997, are given in Fig. 6.26. The water vapour pressure differences above *Saccharum* (-0.007 to 0.065 kPa with an average of 0.02 kPa), were generally higher than above *Acacia* (-0.02 to 0.027 kPa with an average of 0.0007 kPa) and *Eucalyptus* (-0.078 to 0.024 kPa with an average of 0.0006 kPa) (Fig. 6.26). The water vapour pressure differences at both the *Acacia* and *Eucalyptus* sites fell outside the resolution (0.01 kPa) of the DEW-10 sensor and were subsequently rejected. The higher degree of turbulent mixing over forest (*Acacia* and *Eucalyptus*) as a result of the aerodynamically rough surfaces in comparison to shorter vegetation (*e.g. Saccharum*), resulted in the smaller water vapour pressure profile differences. However, as the average canopy heights increased (*Acacia* and *Eucalyptus*), the canopies closed and became more uniform. This decreased the aerodynamic roughness and increased the air temperature and water vapour pressure profile differences. Insufficient separation differences between the sampling heights and inadequate sampling heights contributed to the small water vapour pressure differences at the *Acacia* and *Eucalyptus* sites (Fig. 6.24 and Fig. 6.27). The rejected small water vapour pressure differences during Winter 1997 (Fig. 6.26) above *Acacia* and *Eucalyptus*, had little effect on the calculation of the daily evaporation totals, since they corresponded with negative air temperatures (Fig. 6.28) and small negative Bowen ratios (Fig. 6.18).

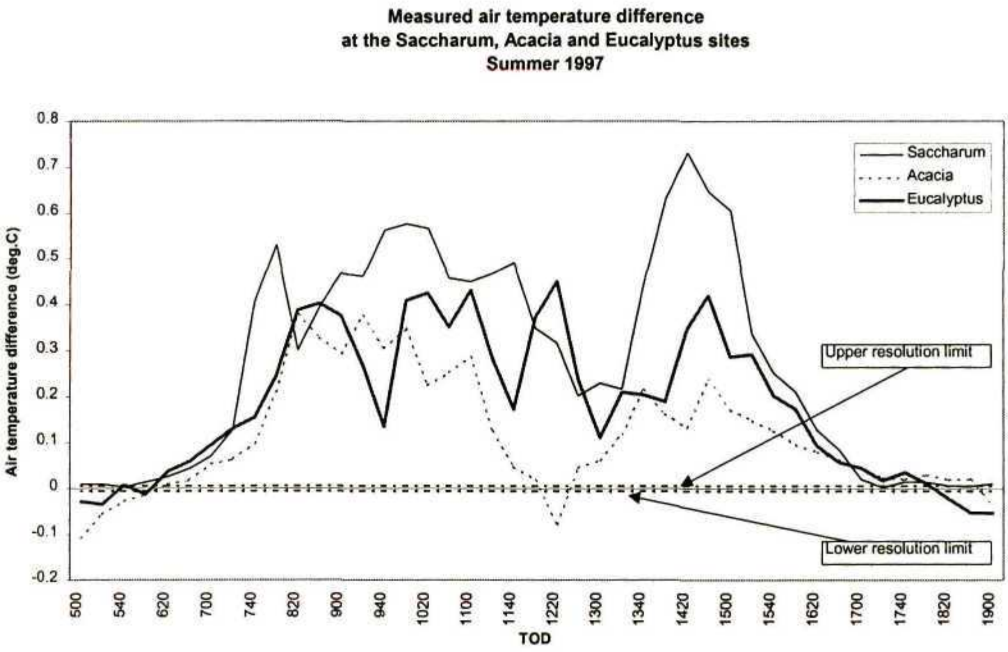

Figure 6.25 Air temperature differences at the *Saccharum, Acacia* and *Eucalyptus* sites during Summer 1997 (DOY 34)

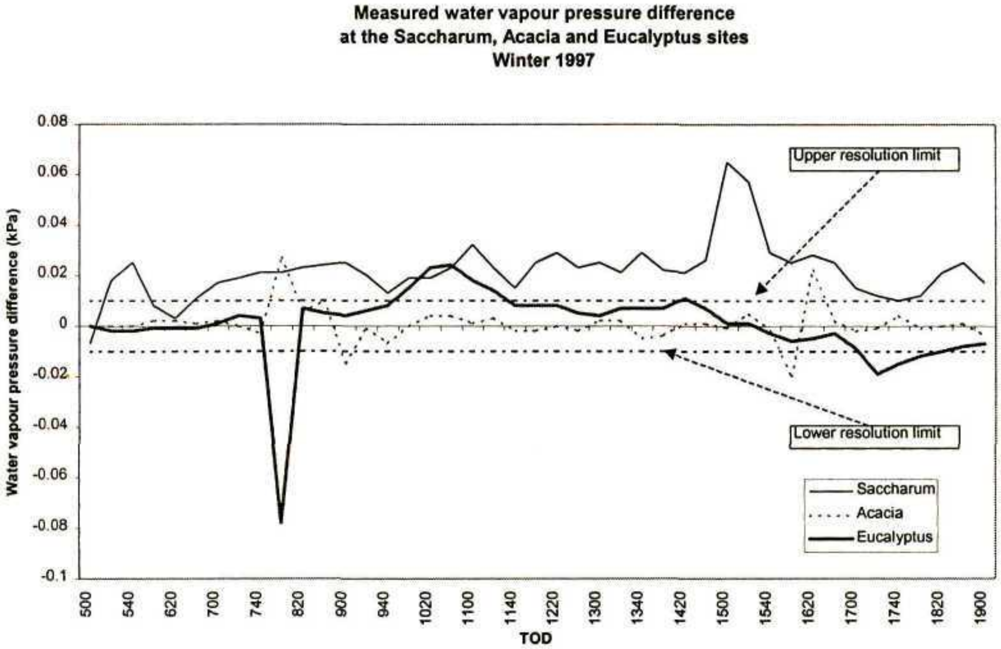

Figure 6.26 Water vapour pressure differences measured at the *Saccharum, Acacia* and *Eucalyptus* sites during Winter 1997 (DOY 229)

Typical water vapour pressure differences during Summer 1997 (Fig. 6.29) at the *Eucalyptus* site (-0.197 to 0.591 kPa with an average of 0.090 kPa), fell within the resolution limits of the DEW-10 sensor (0.01 kPa). Periodically however (08h40 and 15h40), the water vapour pressure profile differences fell outside the resolution limits of the sensor and were rejected. Small water vapour pressure profile differences were measured during Summer 1997 (-0.294 kPa to 0.053 kPa with an average of -0.020 kPa) and Summer 1998 (-0.018 kPa to 0.141 kPa with an average of 0.004 kPa) at the *Acacia* site (Fig. 6.29 and Fig. 6.30). These small differences resulted from insufficient separation differences between sampling heights, inadequate sampling heights and aerodynamically rough surfaces.

Although the air temperature and water vapour pressure profile differences measured above *Acacia* and *Eucalyptus* were significantly lower than those above *Saccharum*, they generally fell within the resolution limits of the Bowen ratio water vapour pressure and air temperature sensors.

6.1.4 Total evaporation comparison as measured by the Bowen ratio energy balance technique

As a result of discontinuous Bowen ratio evaporation data sets at the *Saccharum, Acacia* and *Eucalyptus* sites, there were few corresponding days within the respective data sets that were not excluded by the Bowen ratio energy balance rejection criteria (*Section 4.2.1.3*). The discontinuity of the evaporation data sets resulted from Bowen ratio energy balance limitations (*Section 4.2.1.2*), rejection criteria (*Section 4.2.1.3.2*), broken sensors (*Section 6.3*) and unfavourable weather conditions, while conducting the experiment. Trends within the evaporation data sets, rather than qualitative values, are therefore discussed.

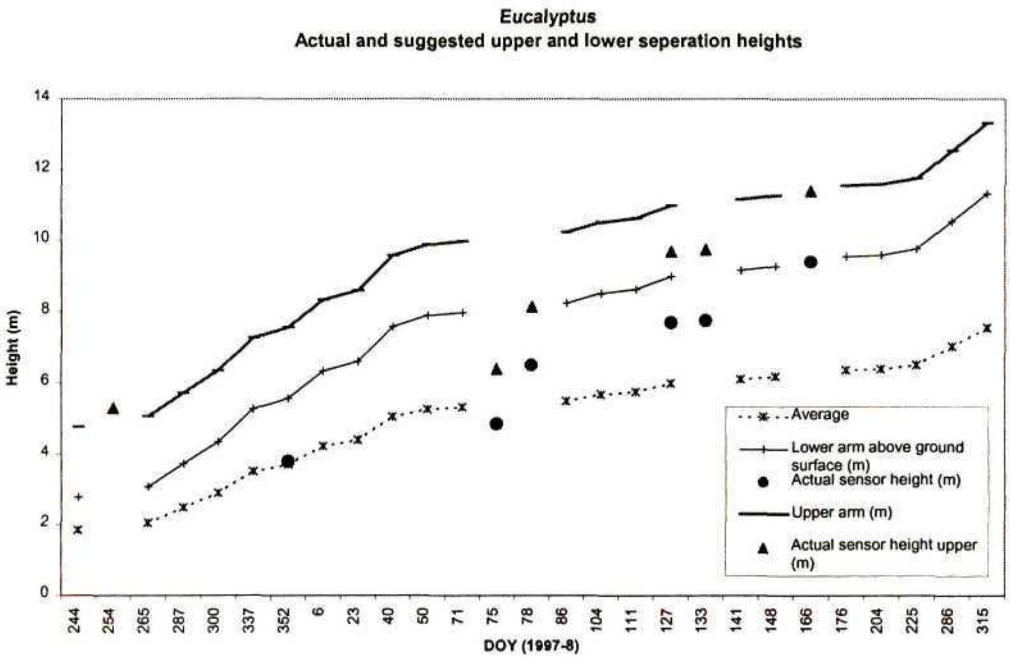

Figure 6.27 Measured and suggested upper and lower sampling heights at the *Eucalyptus* site

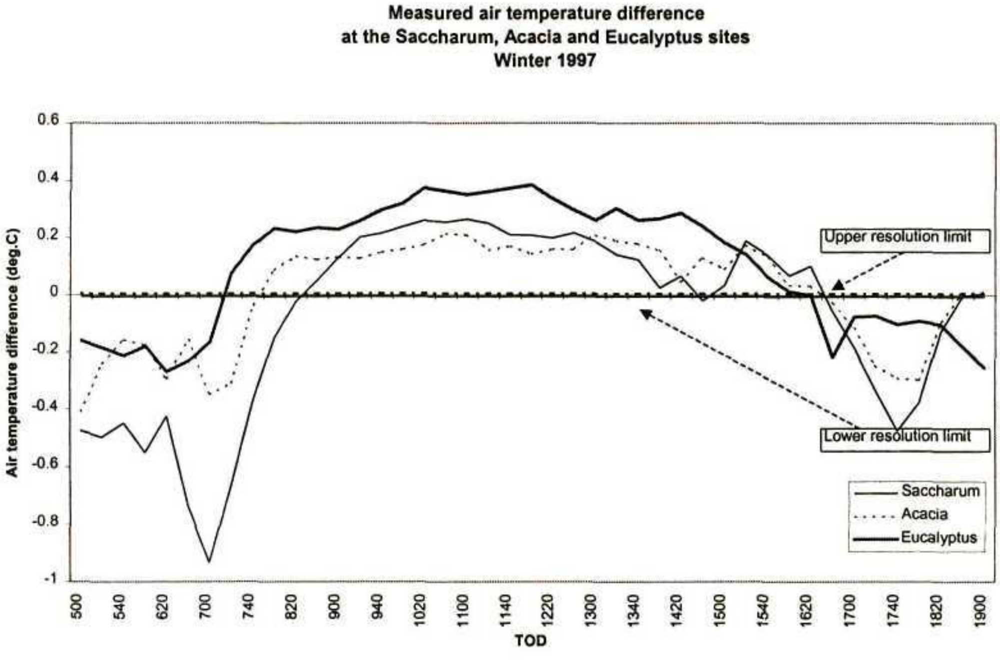

Figure 6.28 Air temperature profile differences measured at the *Saccharum, Acacia* and *Eucalyptus* sites during Winter 1997 (DOY 229)

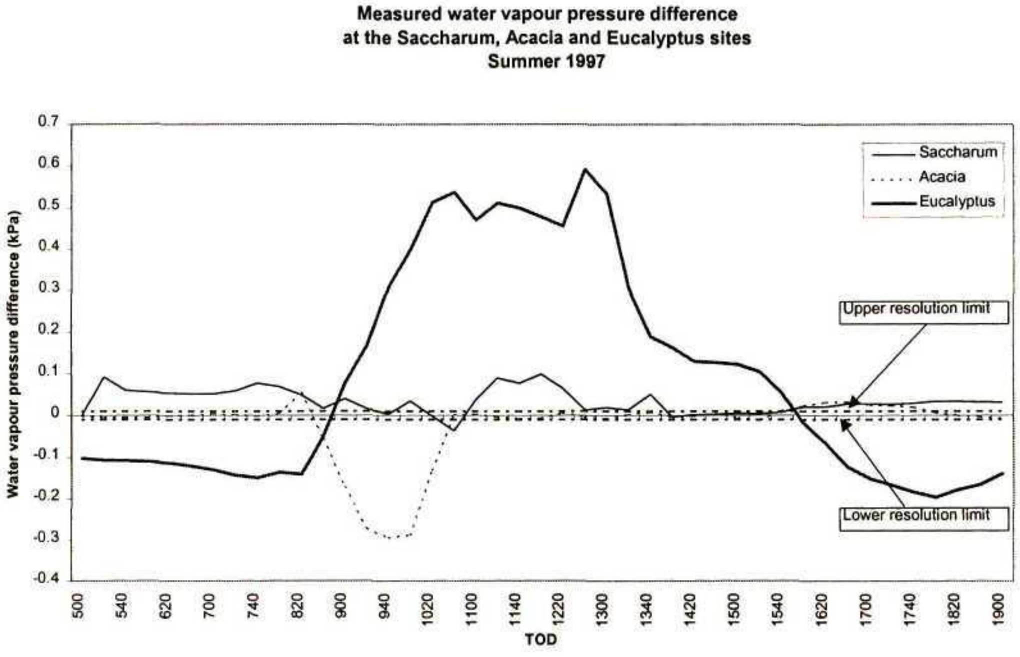

Figure 6.29 Water vapour pressure profile differences at the *Saccharum, Acacia* and *Eucalyptus* sites during Summer 1997 (DOY 34)

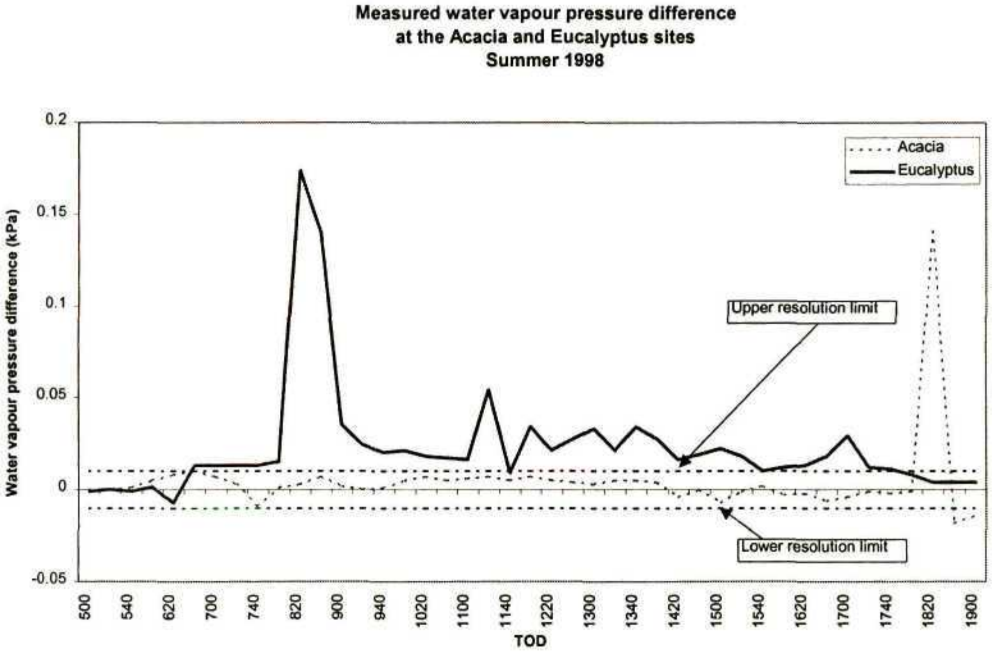

Figure 6.30 Water vapour pressure differences at the *Acacia* and *Eucalyptus* sites during Summer 1998 (DOY 291)

At the commencement of the Bowen ratio energy balance evaporation experiment (Winter 1997), the evaporation rate at the *Saccharum* site ($\approx$ 3 mm day^{-1}), exceeded the evaporation rates at both the *Acacia* and *Eucalyptus* sites by approximately 1mm day^{-1} (Fig. 6.31). Although similar amounts of available energy existed at the respective sites (Fig. 6.32), the leaf area indices at the *Saccharum* site ($\approx$ 6) exceeded the leaf area indices at both the *Acacia* ($\approx$ 1.7) and *Eucalyptus* sites ($\approx$ 1.5).

At the beginning of Summer 1997, however, the evaporation rates at both the *Acacia* and *Eucalyptus* sites increased to values approaching the *Saccharum* evaporation rate (3.5 mm day^{-1}) (DOY 300). At that time, the *Acacia* evaporation rate still exceeded the *Eucalyptus* evaporation rates. During this period (Winter 1997/Summer 1997), the leaf area indices and average canopy heights increased at both the *Acacia* and *Eucalyptus* sites (Figs 6.4 and 6.5). Increased air temperatures and solar irradiance were measured and rainfall occurred, resulting in increased evaporation rates at all three sites (Figs 6.1 to 6.3).

Towards the middle of Summer 1997 (DOY 40), the evaporation rate and the available energy (Fig. 6.33) for *Eucalyptus* exceeded that for *Acacia*. Maximum evaporation rates for *Eucalyptus* were 8 mm day^{-1}. The high evaporation rates continued for the remainder of the period studied (Winter 1998 and Summer 1998). Towards the end of Summer 1997 the *Saccharum* evaporation rate decreased slightly as a result of senescence of the sugarcane.

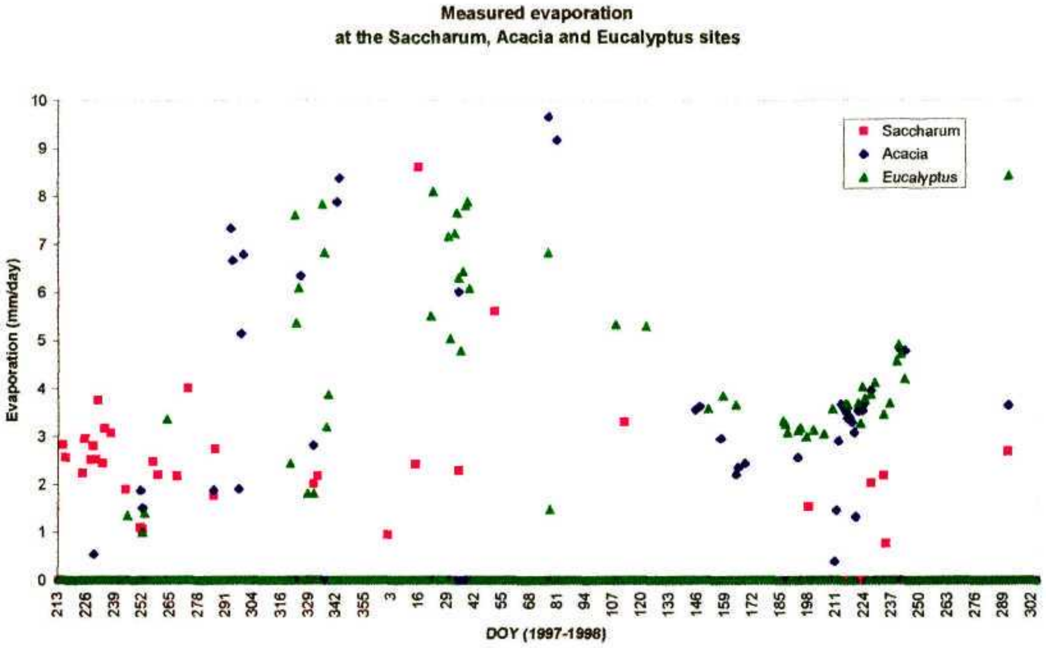

Figure 6.31 Bowen ratio total evaporation comparison at the *Saccharum, Acacia* and *Eucalyptus* sites

During Winter 1998 (DOY 180) the evaporation rates at all three sites once again decreased seasonally while the *Eucalyptus* evaporation rate exceeded both the *Saccharum* and *Acacia* evaporation rates. At the commencement of Summer 1998, the evaporation rates at both the *Acacia* and *Eucalyptus* sites started to increase with the *Eucalyptus* evaporation rate exceeding the *Acacia* evaporation rate, reaching maximum evaporation rates of approximately 6 and 5 mm day^{-1} respectively.

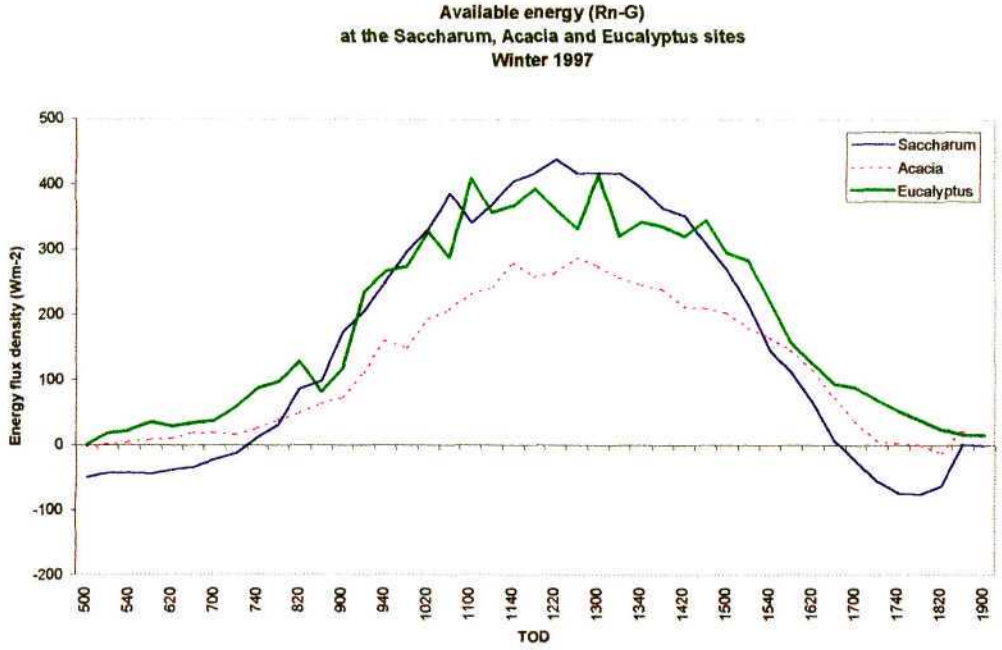

Figure 6.32 Available energy flux density (R_n - G) at the *Saccharum, Acacia* and *Eucalyptus* during Winter 1997 (DOY 229)

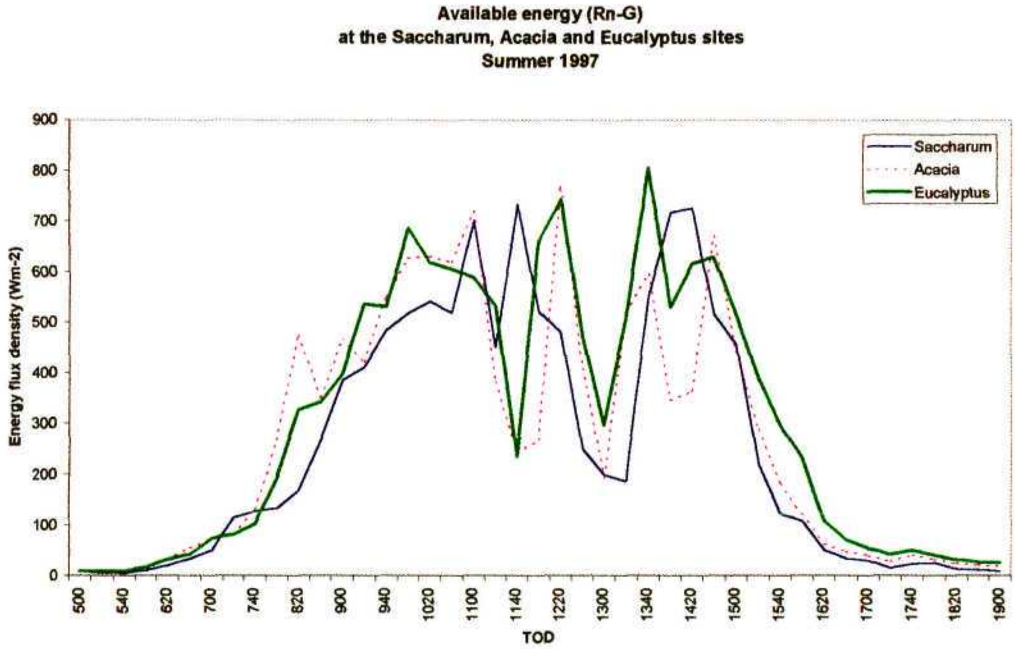

Figure 6.33 Available energy flux density (R_n - G) at the *Saccharum, Acacia* and *Eucalyptus* during Summer 1997 (DOY 34)

6.2 Total evaporation comparison as simulated by site specific Penman-Monteith equations

In order to simulate the total evaporation accurately with the site specific Penman-Monteith equation for all three sites, the components of the equation need to be calculated accurately (Appendix 1). The available energy flux density is the main contributor to the evaporation process as calculated from the simulated net irradiance (R_{ns}) and the soil heat flux density (G_s) calculated as a fraction of the simulated net irradiance.

6.2.1 *Simulation of the net irradiance*

The net irradiance required in the Penman-Monteith equation, is only available from research sites, whereas the solar irradiance is normally obtainable from automatic weather stations. The net irradiance required for this study was simulated from the solar irradiance and a site specific seasonal reflection coefficient.

The net irradiance was simulated accurately from the measured solar irradiance (R_s) and a seasonal, site-specific reflection coefficient (α_s) (Appendix 1). The relationship between the 20 minute measured (R_n) and simulated net irradiance flux densities (R_{ns}), revealed the accuracy of the simulation and the most suitable reflection coefficient to be used (Table 6.3).

Statistically significant relationships were found between the measured and simulated net irradiance during Winter 1997, with slopes (m) approaching 1 and coefficients of determination (r^2) exceeding 0.98 (Table 6.3). Reflection coefficients of approximately 0.20 (0.20, 0.22 and 0.18 of *Saccharum, Acacia* and *Eucalyptus* respectively) were used in the simulation of the net irradiance (Figs 6.34 to 6.36) during Winter 1997.

The reflection coefficients used in the simulation during Winter 1997 (Table 6.3), agreed well with reflection coefficients given in the literature (Table. 6.1) (as discussed in *Section 6.1.3.1*).

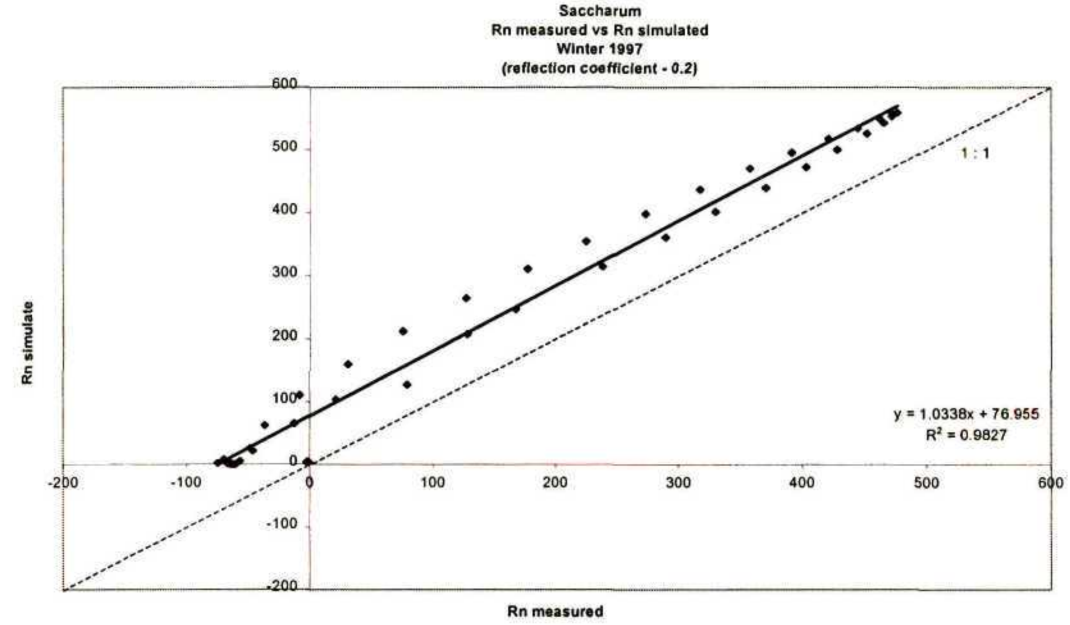

Figure 6.34 R_n measured *vs* R_{ns} simulated at the *Saccharum* site during Winter 1997 ($\alpha_s = 0.2$) (DOY 229)

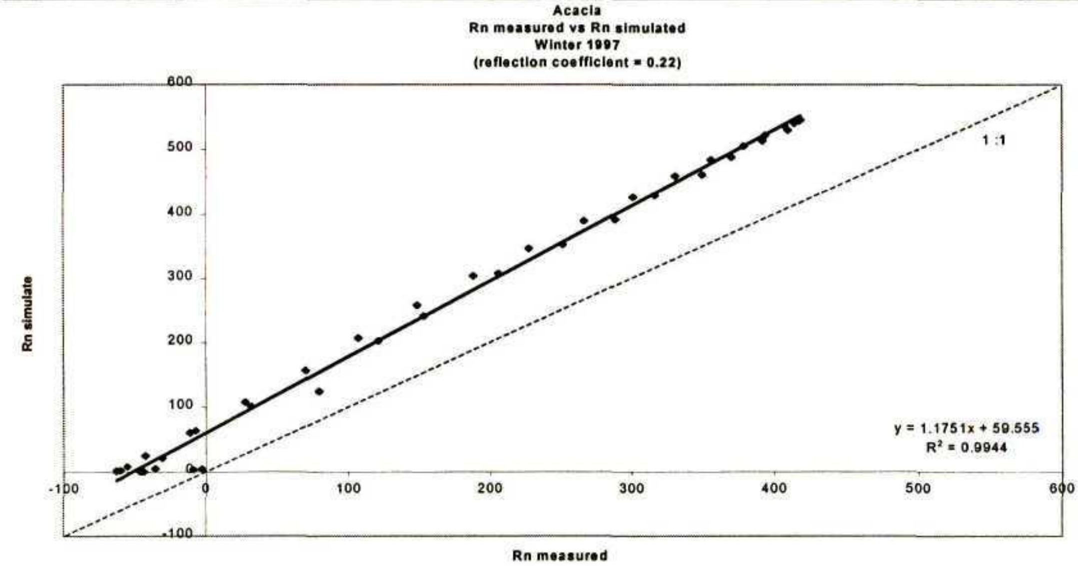

Figure 6.35 R_n measured *vs* R_{ns} simulated at the *Acacia* site during Winter 1997 (α_s=0.22) (DOY 229)

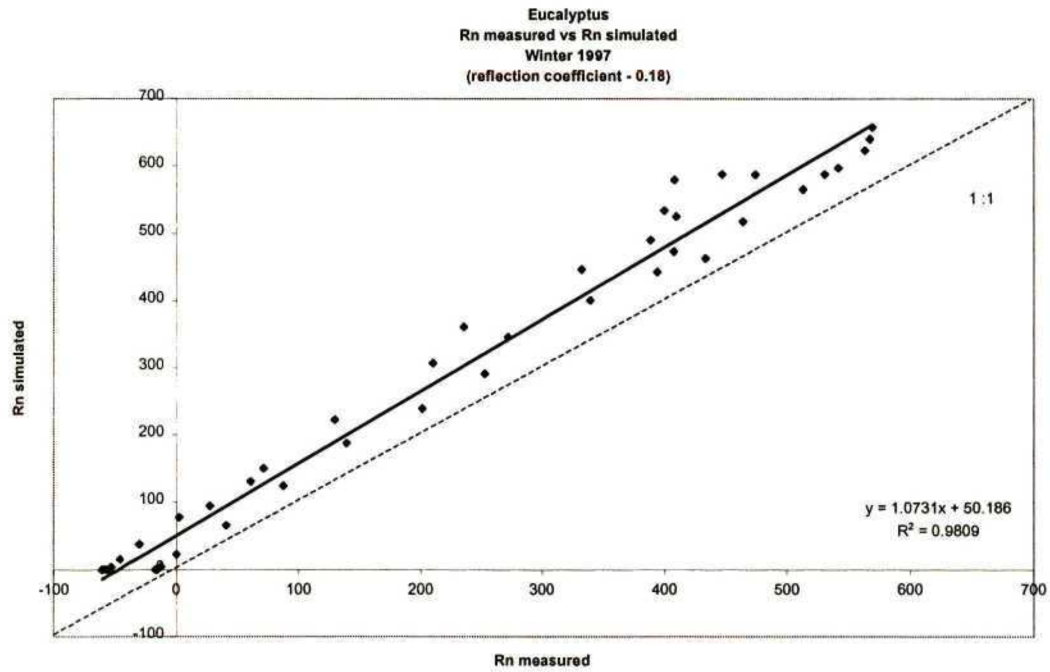

Figure 6.36 R_n measured [illegible] simulated at the *Eucalyptus* site during Winter 1997 (α_s = 0.18) (DOY 229)

Similar average canopy heights were measured during Winter 1997 at the *Saccharum*, *Acacia* and *Eucalyptus* sites (2.3 m, 1.6 m and 2 m respectively) (Fig. 6.5), partially explaining the similarity in the reflection coefficients.

During Summer 1997, Winter 1998 and Summer 1998, reflection coefficients of approximately 0.10 were used in the simulation of the net irradiance (Table 6.3). The reflection coefficient used in the simulation of the net irradiance at the *Saccharum* site (0.10) during this period, differed considerably from the average reflection coefficient given by McGlinchey and Inman-Bamber (1996) for a full-grown sugarcane canopy (Table 6.1). This reflection coefficient used at the *Saccharum* site suggested dark green (low canopy and aerodynamic resistance and well watered surfaces) fast growing canopies with high evaporation rates.

The reflection coefficients used in the simulation of the net irradiance for *Acacia* (0.1) and *Eucalyptus* (0.09 and 0.08), fell at the boundary of the range of 0.11 to 0.15 given by Rosenberg *et al.* (1983) and Monteith (1976) for coniferous forests.

Table 6.4 Statistical information (slope, m and coefficient of determination, r^2, n = 43) on the relationship between the measured (x) and simulated (y) net irradiance, using different reflection coefficients (α_s) at the *Saccharum, Acacia* and *Eucalyptus* sites, all of which is highly significant *** (99%).

	Winter 1997	Summer 1997	Winter 1998	Summer 1998
Saccharum	$\alpha_s = 0.20$ m = 1.03 $r^2 = 0.98$ ***	$\alpha_s = 0.10$ m = 0.98 $r^2 = 0.98$ ***	$\alpha_s = 0.10$ m = 0.97 $r^2 = 0.99$ ***	
Acacia	$\alpha_s = 0.22$ m = 1.18 $r^2 = 0.99$ ***	$\alpha_s = 0.10$ m =0.93 $r^2 = 0.97$ ***	$\alpha_s = 0.10$ m = 0.97 $r^2 = 0.98$ ***	$\alpha_s = 0.10$ m = 0.95 $r^2 = 0.97$ ***
Eucalyptus	$\alpha_s = 0.18$ m = 1.07 $r^2 = 0.98$ ***	$\alpha_s = 0.09$ m = 0.88 $r^2 = 0.96$ ***	$\alpha_s = 0.08$ m = 0.91 $r^2 = 0.99$ ***	$\alpha_s = 0.08$ m = 0.91 $r^2 = 0.97$ ***

The increase in the average canopy heights at the *Acacia* and *Eucalyptus* sites from Winter 1997 (1.60 m and 2 m respectively) to Summer 1997 (4.97 m and 5.26 m respectively), partially explained the decrease in the magnitude of the reflection coefficient over the same period (Table 6.4).

Statistically significant relationships between the measured and simulated net irradiance ($m \approx 1$, $r^2 > 0.96$), indicated that the net irradiance can be simulated accurately utilizing measured solar irradiance and seasonal, site specific reflection coefficients.

*** p = < 0.01

6.2.2 *Calculation of the soil heat flux density (G_s) from the simulated net irradiance (R_{ns})*

The soil heat flux density (G) reduces the energy flux density available (R_n - G) for partitioning between the sensible and latent heat flux densities, and was calculated as a fraction of the simulated net irradiance (R_{ns}). The accuracy of the calculated soil heat flux density was dependent on the accuracy to which the net irradiance was simulated and the degree to which a linear relationship between the soil heat flux density and net irradiance existed.

Simple linear relationships were found between the soil heat flux density (G) and net irradiance (R_n) for all sites and for all seasons studied. These relationships were derived from typical soil heat flux density to net irradiance ratios ($G : R_n$) (%) (Table 6.5). Typical, seasonal site specific ratios ($G : R_n$), were subsequently used to calculate the soil heat flux density as a fraction of the simulated net irradiance.

The degree to which the soil was shaded by the vegetation, determined the soil heat flux density (Monteith, 1975) and the ratio between the soil heat flux density and net irradiance ($G : R_n$). Monteith (1975) found the soil heat flux density inversely proportional to the amount of direct soil shading. During Winter 1997, the *Saccharum* leaf area index (≈ 6) (*i.e.* a dense canopy), exceeded the leaf area indices for both *Acacia* (≈ 1.7) and *Eucalyptus* (≈ 1.5). The low leaf area indices measured at the *Acacia* and *Eucalyptus* sites (*i.e.* little soil shading), resulted in large soil heat flux densities measured (Fig. 6.37) and high G to R_n ratios (Table 6.5).

Table 6.5 Statistical information (m and r^2) on the relationship between G (y) and R_n (x), all of which is highly significant *** (99 %).

G *vs* R_n		Winter 1997	Summer 1997	Winter 1998	Summer 1998
	m	0.11	0.06	0.07	-
Saccharum	r^2	0.73 ***	0.38 ***	0.45 ***	
	n	43	43	43	
Acacia	m	0.44	0.09	0.11	0.14
	r^2	0.90 ***	0.69 ***	0.93 ***	0.63 ***
	n	43	43	43	43
Eucalyptus	m	0.42	0.12	0.13	0.09
	r^2	0.72 ***	0.71 ***	0.72 ***	0.79 ***
	n	43	43	43	43
LAI					
Saccharum		6	6	7	-
Acacia		1.7	2	1.0 - 1.5	2.3
Eucalyptus		1.5	3	3	3.4

During Winter 1997, the soil heat flux density contributed significantly to the energy balance and accounted for approximately 44 and 42 % of the net irradiance at the *Acacia* and *Eucalyptus* sites respectively (m = 0.44 and m = 0.42 respectively) (Fig. 6.38 and Fig. 6.39), leaving little energy available (R_n - G) for partitioning between the sensible and latent heat flux densities (Fig. 6.40). As a result of little available energy at these sites, high Bowen ratios (Fig. 6.22) and low evaporation rates were expected. At the *Saccharum* site (Winter 1997) however, the soil heat flux density accounted for approximately 10 % of the net irradiance (m = 0.1099) (Fig. 6.41), as a result of high leaf area indices and subsequent sufficient soil shading. The soil heat flux density (G) was estimated as 10 % of the net irradiance (R_n) (Campbell, undated). Subsequent low Bowen ratios (Fig. 6.22) and high evaporation rates were expected.

*** $p = < 0.01$

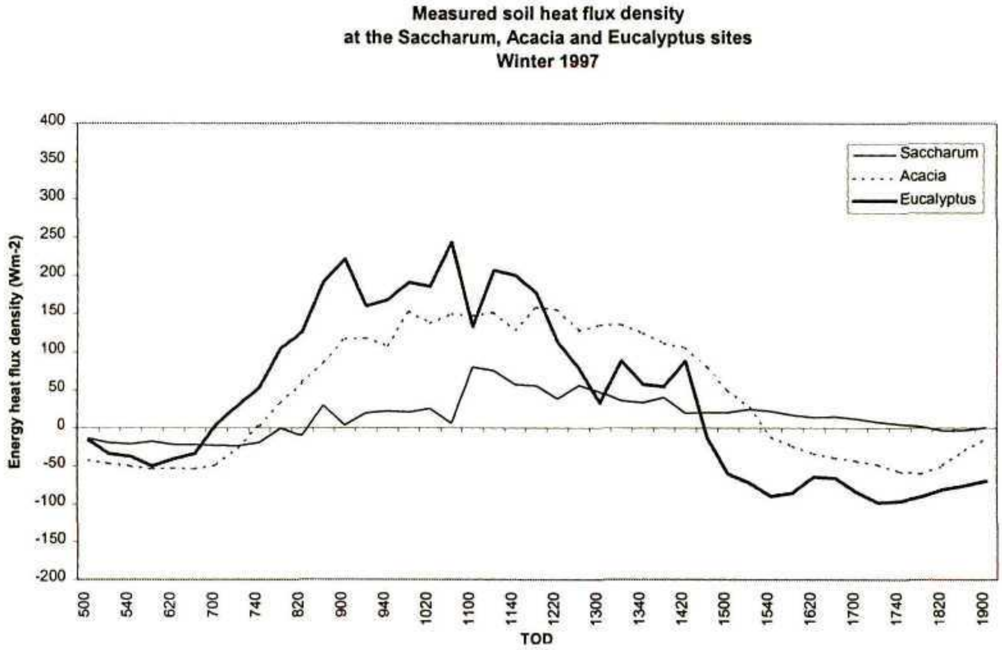

Figure 6.37 Measured soil heat flux density during Winter 1997 (DOY 229)

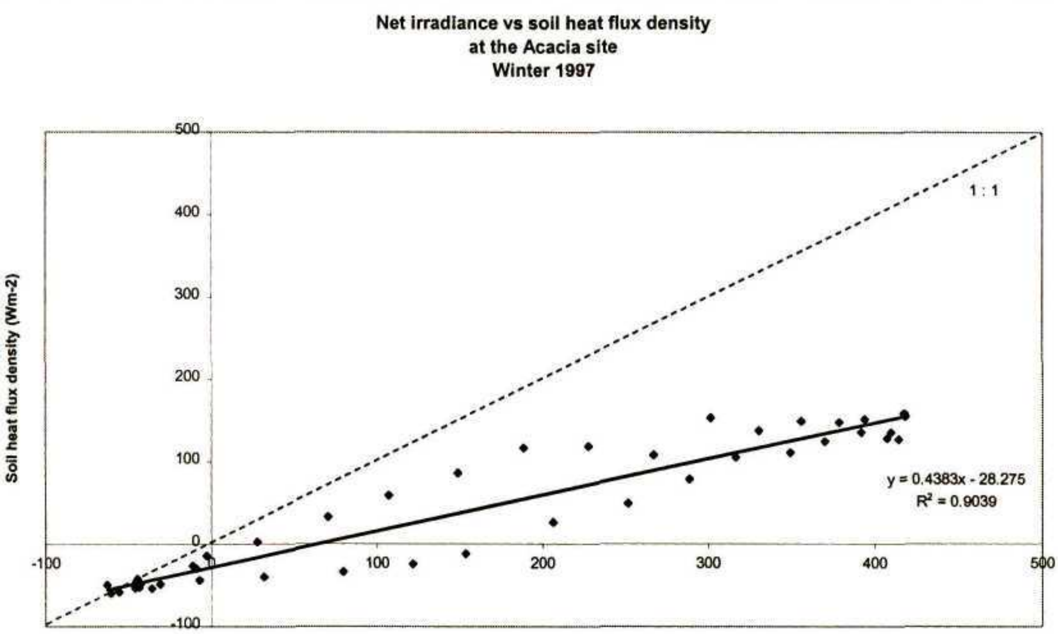

Figure 6.38 Measured net irradiance *vs* soil heat flux density at the *Acacia* site during Winter 1997 (DOY 229)

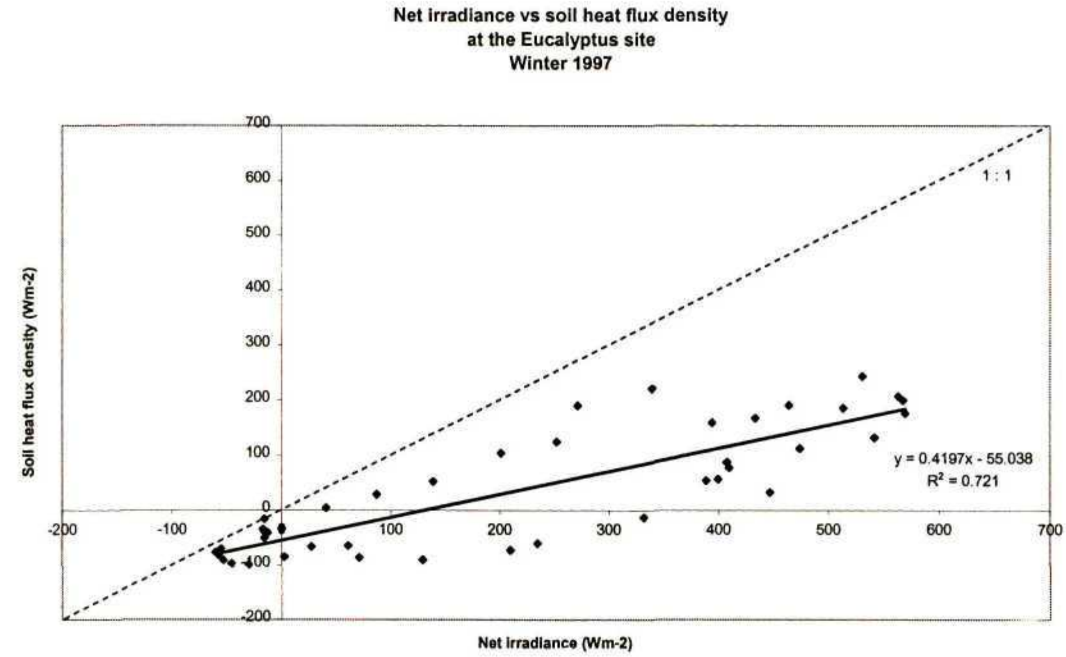

Figure 6.39 Measured net irradiance *vs* soil heat flux density at the *Eucalyptus* site during Winter 1997 (DOY 229)

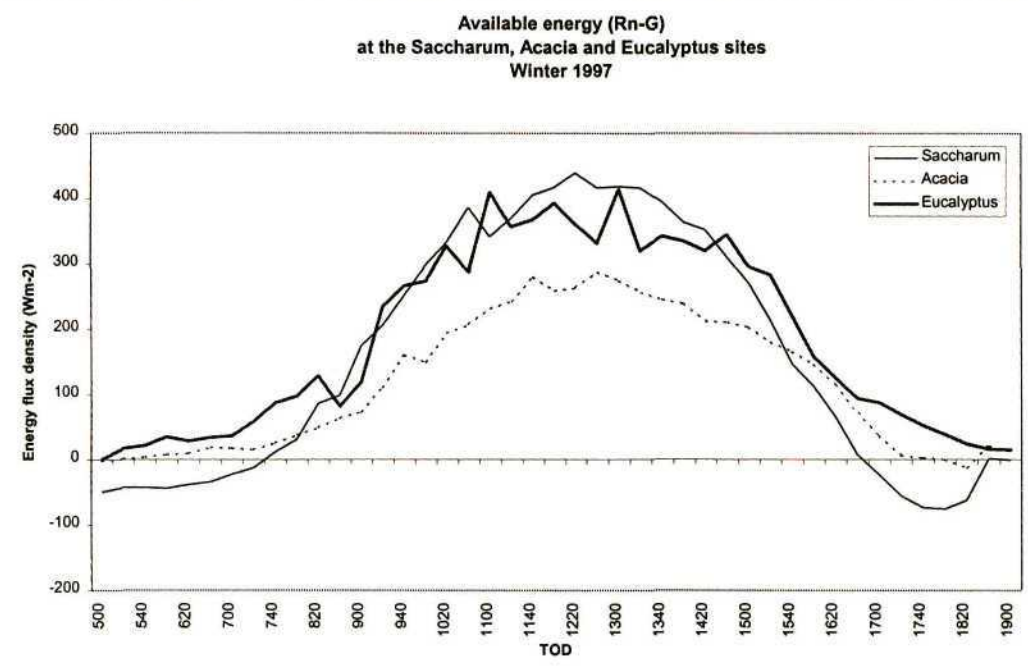

Figure 6.40 Available energy flux density during Winter 1997 (DOY 229)

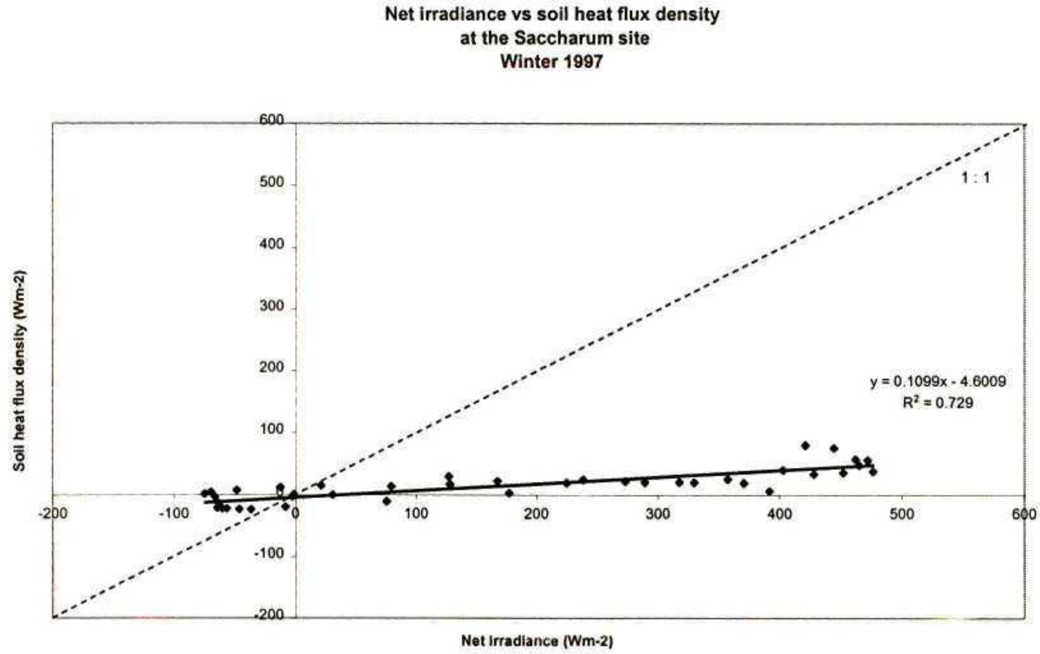

Figure 6.41 Measured net irradiance *vs* soil heat flux density at the *Saccharum* site during Winter 1997 (DOY 229)

Table 6.6 Calculation of the soil heat flux density as a fraction of the net irradiance (%)

	Winter 1997	Summer 1997	Winter 1998	Summer 1998
Saccharum	10	10	10	10
Acacia	40	[L] 10	[L] 10	[L] 10
Eucalyptus	40	[L]10	[L] 10	[L] 10

Increased average daily air temperatures (14.3 °C to 18.3 °C) (Fig. 6.2), solar radiant density (11.9 MJ m^{-2} to 14.2 MJ m^{-2}) (Fig. 6.3) and rainfall (70 mm) (Fig. 6.1) from Winter 1997 to Summer 1997, resulted in increased leaf area indices (Fig. 6.4) and average canopy heights for all sites (Fig. 6.5). As a result of increased soil shading, subsequent decreases in the soil heat flux density to net irradiance ratios (%) (0.4 to 0.1) were noticeable at the *Acacia* and *Eucalyptus* sites.

[L] For leaf area indices more than 2

During Summer 1997 (as well as Winter 1998 and Summer 1998), the soil heat flux density accounted for 10 % of the net irradiance (Table 6.6). The soil heat flux density therefore became less dependent on the net irradiance. The diurnal soil heat flux density curve followed the net irradiance curve closely where low leaf area indices were measured (*e.g. Eucalyptus* during Winter 1997), opposed to where high leaf area indices were measured (*e.g. Saccharum* during Winter 1997). As a result, the soil heat flux density became less dependent on the net irradiance and contributed to a coefficient of determination (r^2) for the relationship between the measured and calculated soil heat flux densities, much lower than for other periods studied with high leaf area indices (Table 6.6). This was clearly illustrated at the *Saccharum* site during Summer 1997 ($r^2 = 0.38$) (Fig. 6.42) (Table 6.6).

Typical R_n to G ratios (Table 6.5) were used in simple linear relationships to calculate the soil heat flux density as a fraction of the net irradiance (Table 6.6). Statistically significant relationships were found between the measured (G) and calculated (G_s) soil heat flux densities (m > 0.6, r^2 > 0.6) (Table 6.7).

Table 6.7 Statistical information on the relationship between the measured and calculated soil heat flux density (n = 43). All the relationships were high significant (99 %).

	Winter 1997	**Summer 1997**	**Winter 1998**	**Summer 1998**
Saccharum	m = 0.68 $r^2 = 0.71$***	m = 1.03 $r^2 = 0.72$ ***	m = 0.63 $r^2 = 0.46$ ***	
Acacia	m = 0.98 $r^2 = 0.92$ ***	m = 0.49 $r^2 = 0.69$ ***	m = 0.83 $r^2 = 0.90$ ***	m = 0.45 $r^2 = 0.68$ ***
Eucalyptus	m = 0.69 $r^2 = 0.62$ ***	m = 0.62 $r^2 = 0.71$ ***	m = 0.45 $r^2 = 0.72$***	m = 0.81 $r^2 = 0.82$ ***

*** p = < 0.01

During Winter 1997, the soil heat flux density at the *Acacia* site, was very dependent on the net irradiance (m = 0.44, r^2 = 0.90). A ratio of 0.40 was used in the calculation of the soil heat flux density and resulted in a statistically significant relationship between the measured and calculated soil heat flux densities (m = 0.98, r^2 = 0.92) (Fig. 6.43). Periodically (*e.g.* Winter 1997 at the *Saccharum* site), however, a much lower r^2 was found for the relationship between the measured and calculated soil heat flux densities (m = 0.63, r^2 = 0.46) (Fig. 6.44) as a result of a non-linear relationship between the soil heat flux density and net irradiance (m = 0.07, r^2 = 0.45) (Table 6.5) (Fig. 6.45) compared to the other seasons studied. The much lower r^2 resulted from a high leaf area index (≈ 7) and subsequent soil shading. As a result of the magnitude of the soil heat flux density and the contribution to the energy balance, the error introduced by the calculation of the soil heat flux density, using a simple linear relationship, was small.

Using the above relationship between the soil heat flux density and net irradiance, it was possible to determine accurate soil heat flux density (G_s) and available energy values for input into the site-specific Penman-Monteith equations.

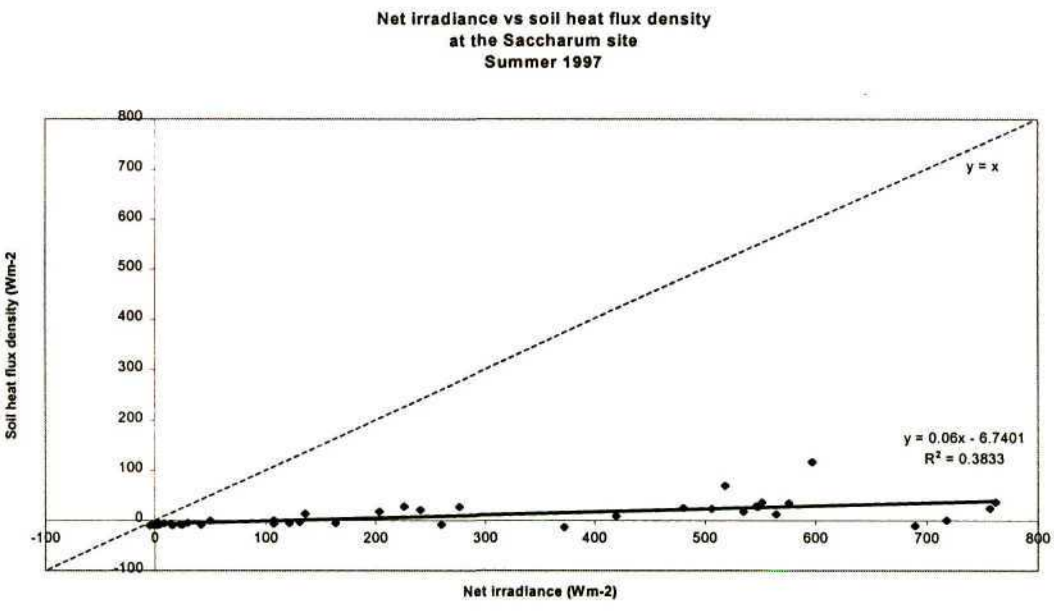

Figure 6.42 Measured net irradiance *vs* soil heat flux density at the *Saccharum* site during Summer 1997 (DOY 229)

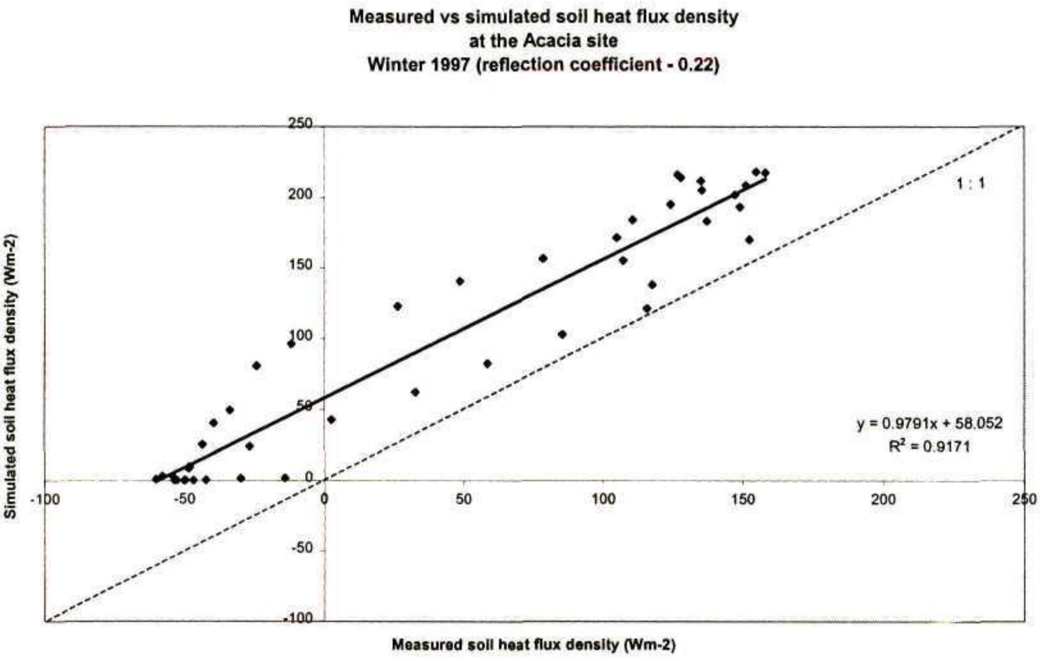

Figure 6.43 Measured *vs* simulated soil heat flux density at the *Acacia* site during Winter 1997 ($\alpha = 0.22$) (DOY 229)

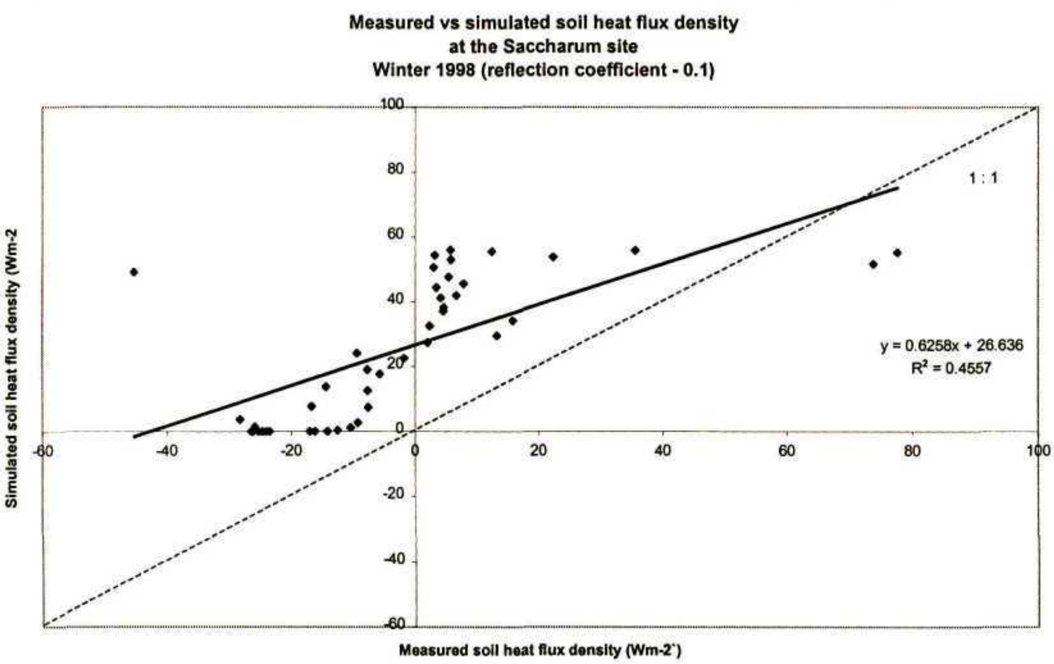

Figure 6.44 Measured *vs* simulated soil heat flux density at the *Saccharum* site during Winter 1998 ($\alpha = 0.1$) (DOY 227)

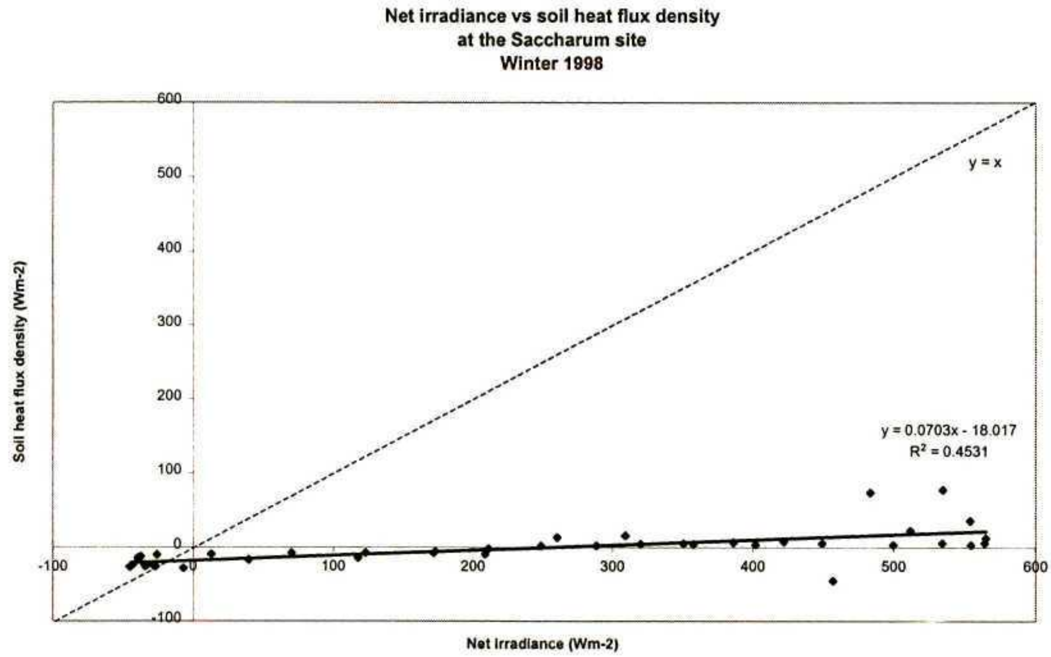

Figure 6.45 Measured net irradiance *vs* soil heat flux density at the *Saccharum* site during Winter 1998 (DOY 227)

6.2.3 *Total site specific Penman-Monteith evaporation comparison*

The Penman-Monteith equation has been successfully applied to estimate evaporation from different crops (Slabbers, 1977; McGlinchey and Inman-Bamber, 1996) and from forests (Calder, 1977; Everson, 1995). Although the Penman-Monteith equation is complex, it is extremely flexible and of wide application, particularly in modelling studies where it is necessary to predict the water balance of plant communities under different conditions (Slayan and Bernhofer, 1993). The Penman-Monteith equation requires detailed climatic data (net irradiance, air temperature, water vapour pressure and windspeed) and aerodynamic and canopy resistance data (not freely available), possibly limiting the use of this equation primarily to research applications (Rosenberg *et al.*, 1993). It is possible to estimate net irradiance from data collected from an automatic weather station. The aerodynamic resistance (r_a) is calculated from a knowledge of average canopy height and windspeed. The canopy resistance is not easily obtained and therefore site-specific studies are required to understand how it varies on a seasonal basis. The canopy resistance (r_c) can be obtained, by back calculating the canopy resistance in the Penman-Monteith equation, using the Bowen ratio evaporation estimates. The canopy resistance can also be obtained by varying the canopy resistance in the Penman-Monteith equation, to establish the best linear relationship between the Bowen ratio and Penman-Monteith evaporation estimates. The canopy resistance essentially allows for the difference between the potential and actual evaporation from canopies (Monteith, 1975).

Statistically significant linear relationships were found between the 20 minute measured (Bowen ratio) and simulated (site specific Penman-Monteith) total evaporation estimates at all three sites (Table 6.8). During Winter 1997, a canopy resistance of 80 s m^{-1} resulted in the best linear relationship between the measured and simulated evaporation ($m = 1.06$, $r^2 = 0.82$) (Table 6.8, Fig. 6.46). The Penman-Monteith equation performed well above *Acacia* during Winter 1998 ($r_c = 45$ s m^{-1}), resulting in a statistically significant relationship between the measured and simulated evaporation ($m = 0.99$, $r^2 = 0.86$) (Fig. 6.47).

The much lower r^2 found between the measured and simulated evaporation above *Acacia* during Winter 1997 (m = 0.20, r^2 = 0.01), Summer 1997 (m = 0.14, r^2 = 0.21) and Summer 1998 (m = 0.14, r^2 = 0.01) compared to Winter 1998, resulted from poor Bowen ratio data and were erroneous. The total evaporation simulated above *Eucalyptus* during Summer 1997 (r_c = 70 s m^{-1}), Winter 1998 (r_c = 35 s m^{-1}) and Summer 1998 (r_c = 65 sm^{-1}), resulted in statistically significant relationships between the measured and simulated evaporation.

Table 6.8 Statistical information of the relationship between the measured (Bowen ratio) (x) and simulated (site specific Penman-Monteith) (y) evaporation. All the relationships with the exception of *Acacia* Winter 1997, are highly significant (n = 43).

	Winter 1997	Summer 1997	Winter 1998	Summer 1998
Saccharum	m = 1.11 $r^2 = 0.82^{***}$ r_c = 80 s m^{-1}	m = 1.10 $r^2 = 0.54^{B***}$ r_c = 150 s m^{-1}	m = 1.05 $r^2 = 0.41^{B***}$ r_c = 50 s m^{-1}	
Acacia	m = 0.20 $r^2 = 0.01^{B\ NS}$ r_c = 70 s m^{-1}	m = 0.14 $r^2 = 0.21^{B***}$ r_c = 50 s m^{-1}	m = 0.99 $r^2 = 0.86^{B***}$ r_c = 45 s m^{-1}	m = -0.75 $r^2 = 0.25^{B***}$ r_c =60 s m^{-1}
Eucalyptus	m = 1.05 $r^2 = 0.49^{B***}$ r_c = 100 s m^{-1}	m = 1.08 $r^2 = 0.92^{***}$ r_c = 70 s m^{-1}	m = 0.99 $r^2 = 0.86^{***}$ r_c = 35 s m^{-1}	m = 0.99 $r^2 = 0.86^{***}$ r_c = 60 s m^{-1}

*** p = < 0.01

^{B} Bowen evaporation data rejected

^{NS} p = < 0.1

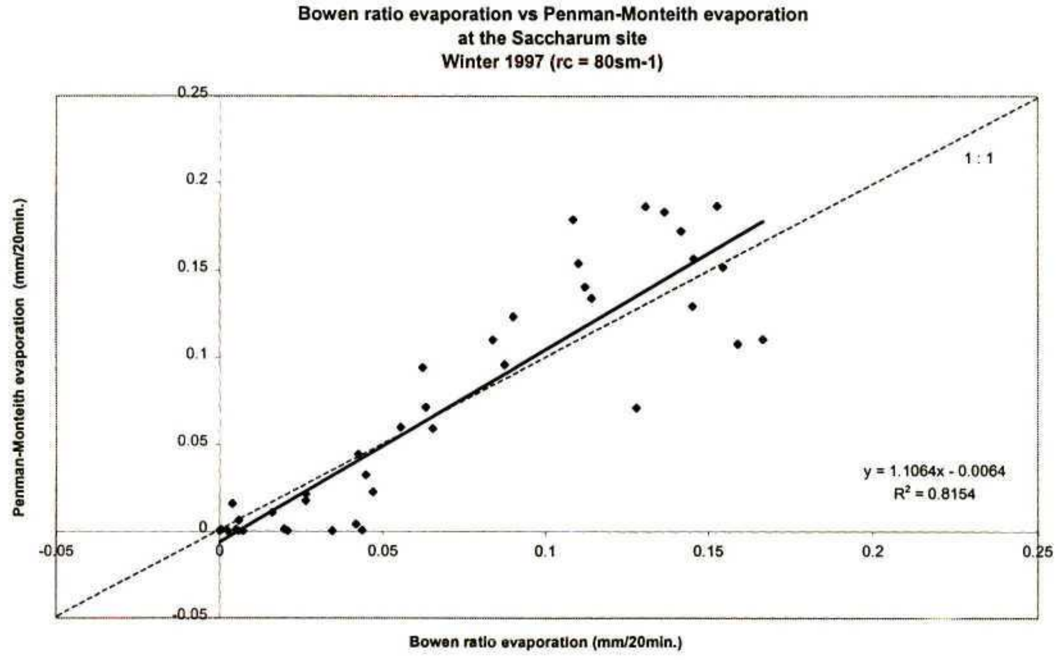

Figure 6.46 Bowen ratio *vs* Penman-Monteith evaporation at the *Saccharum* site during Winter 1997 (DOY 227)

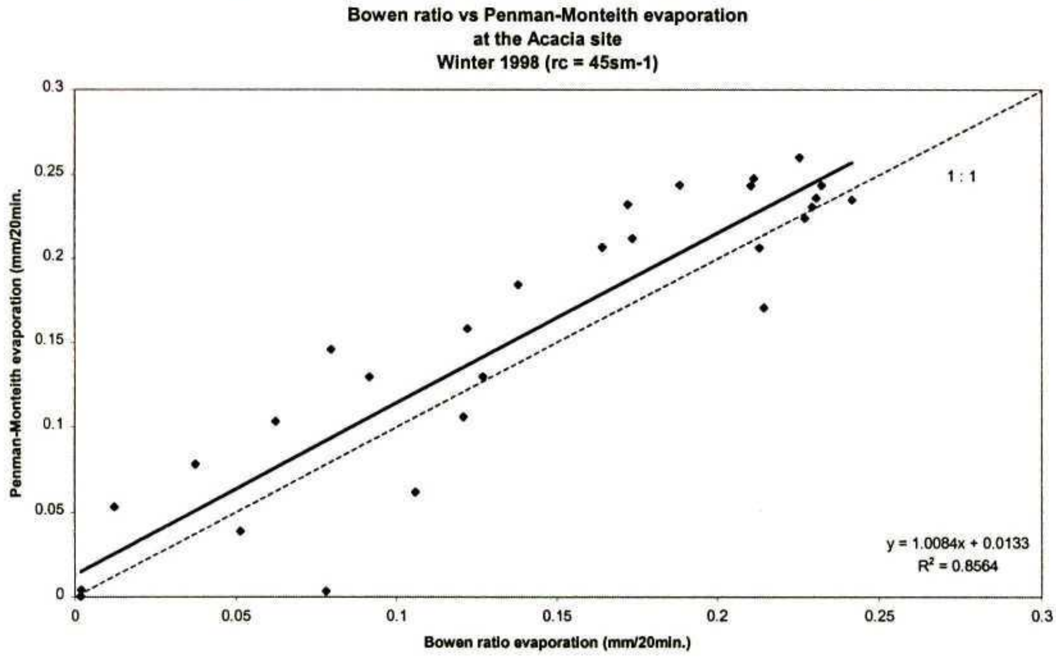

Figure 6.47 Bowen ratio *vs* Penman-Monteith evaporation at the *Acacia* site during Winter 1998 (DOY 229)

The evaporation simulated at all three sites was subsequently accumulated over 17 day periods. At the beginning of the project (Winter 1997), the accumulated evaporation from *Saccharum* (42 mm) exceeded the accumulated evaporation from *Acacia* (28 mm) by approximately 33 % (Table 6.9, Fig. 6.48) (*Eucalyptus* data unavailable). The differences in the evaporation from *Saccharum* and *Acacia* evaporation resulted from differences in the energy balance components at these sites. The differences in the simulated net irradiance at the *Saccharum, Acacia* and *Eucalyptus* sites, contributed mainly to the evaporation differences. The higher reflection coefficient used in the simulation of the net irradiance at the *Acacia* site (0.22) compared to the *Saccharum* site (0.20) resulted in a greater net irradiance at the *Saccharum* site. In addition during Winter 1997, the soil heat flux density was calculated as 40 % of the simulated net irradiance at the *Acacia* site compared to 10 % at the *Saccharum* site. The differences in the soil heat flux density resulted from the differences in the soil shading between the *Saccharum* (LAI $\approx$ 6) and *Acacia* (LAI $\approx$ 1.7) sites (Fig. 6.4) and therefore contributed significantly to the energy balance. The high soil heat flux density at the *Acacia* site, reduced the energy available for partitioning between the sensible and latent heat flux densities. Different canopy resistances (80 s m^{-1} and 70 s m^{-1} at the *Saccharum* and *Acacia* sites respectively) in addition to the available energy differences, resulted in an evaporation rate above *Saccharum* (2.5 mm day^{-1}) exceeding the evaporation rate above *Acacia* (1.6 mm day^{-1}).

During Spring 1997 (Fig. 6.49) as was the case during Winter 1997, the evaporation from *Saccharum* exceeded the evaporation from *Acacia*. The accumulated evaporation difference (6 mm) between these sites was small compared to that during Winter 1997 (14 mm). The decreased evaporation differences during Spring 1997 resulted from the increased leaf area indices at the *Acacia* site (LAI $\approx$ 1.7 to LAI > 2).

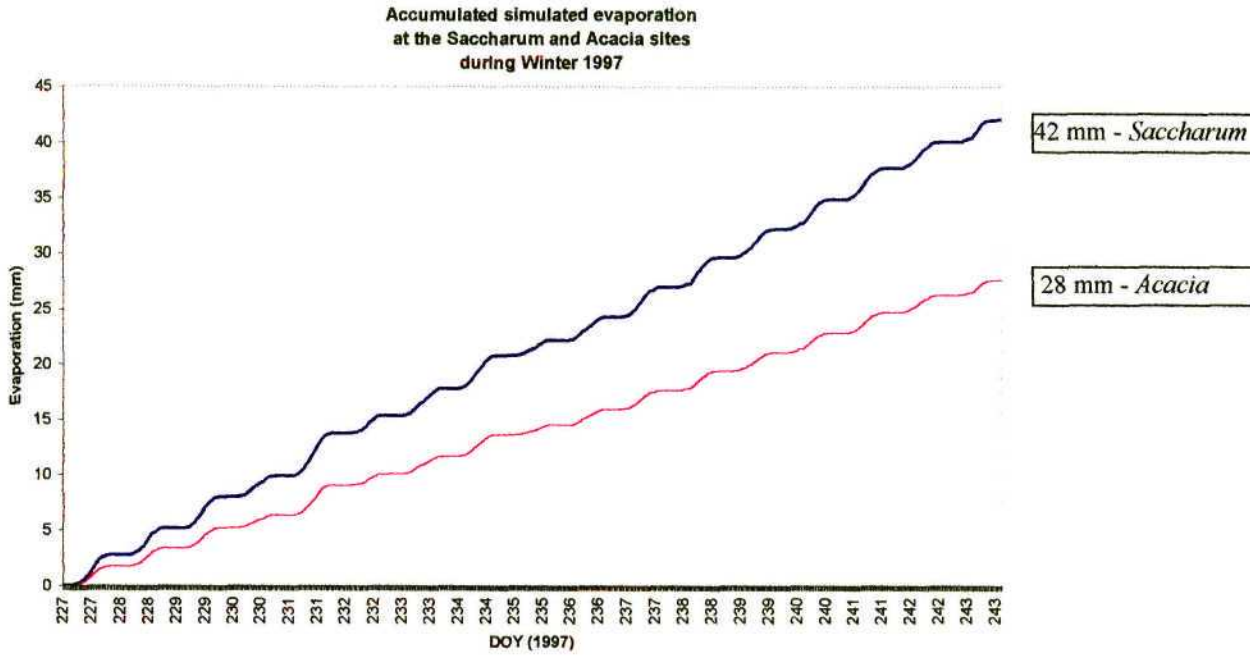

Figure 6.48 Accumulated simulated evaporation at the *Saccharum* and *Acacia* sites during Winter 1997 over a 17 day period (DOY 227 to 243)

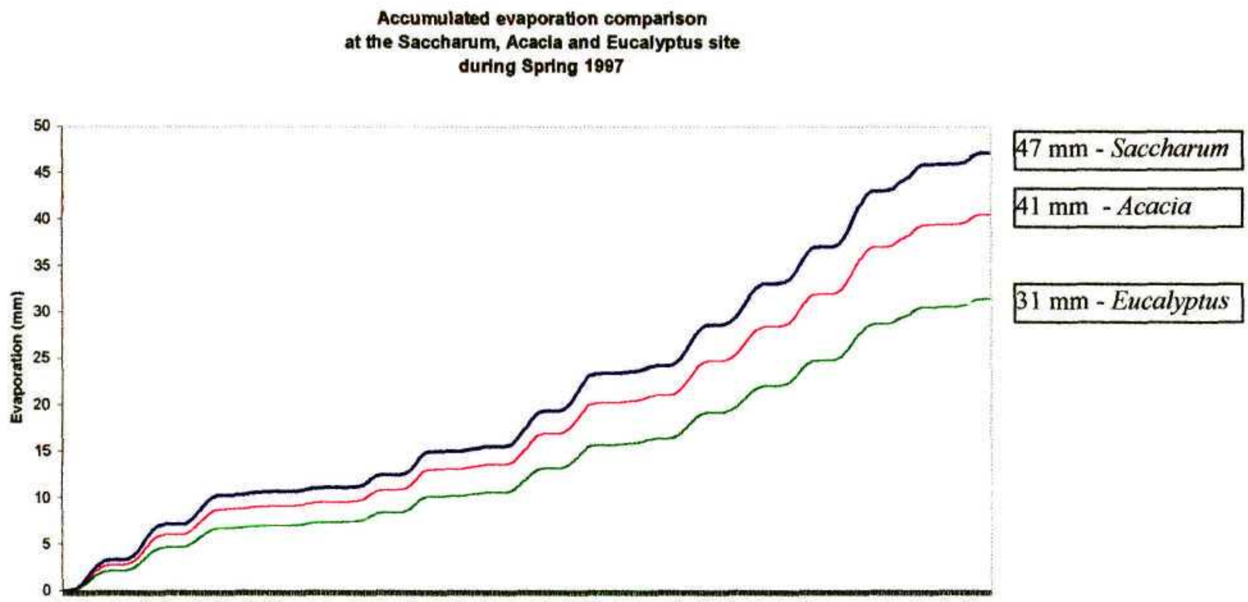

Figure 6.49 Accumulated simulated evaporation during Spring 1997 over a 17 day period (DOY 257 to 273)

The differences in the simulated net irradiance, calculated soil heat flux densities and canopy resistances between the *Saccharum, Acacia* and *Eucalyptus* sites (Table 6.8), resulted in the evaporation differences. A lower reflection coefficient was used in the evaporation simulation at the *Eucalyptus* site (0.18) compared 0.22 for the *Acacia* site. This resulted in higher net irradiance and therefore increased available energy at the *Eucalyptus* site compared to the *Acacia* site, suggesting a higher evaporation rate above *Eucalyptus*. The higher canopy resistance (100 s m^{-1}) used at the *Eucalyptus* site, however resulted in a lower evaporation rate above *Eucalyptus* (1.8 mm day^{-1}) when compared to the *Acacia* site (2.4 mm day^{-1}). In addition to the smaller contribution of the soil heat flux density (*Acacia* and *Eucalyptus*) to the energy balance ($G_s = 0.1R_{ns}$), the lower reflection coefficient resulted in an increased net irradiance and consequently an increased evaporation rate as the season progressed. Towards the end of Summer 1997, the accumulated evaporation above *Eucalyptus* (73 mm) exceeded that above *Acacia* (63 mm) and *Saccharum* (36 mm). The low *Saccharum* daily evaporation rate (2.1 mm day^{-1}) compared to the *Acacia* (3.7 mm day^{-1}) and *Eucalyptus* (4.3 mm day^{-1}) daily evaporation rate, resulted mainly from the high canopy resistance (r_c = 150 s m^{-1}) used in the simulation at the *Saccharum* site, compared to the *Acacia* (80 s m^{-1}) and *Eucalyptus* (70 s m^{-1}) sites (Fig. 6.50).

At the end of Winter 1998, the evaporation rates at all three sites increased (Table 6.9, Fig. 6.51). Accumulated evaporation totals of 96 mm, 83 mm and 63 mm were calculated at the *Saccharum, Acacia* and *Eucalyptus* sites respectively. The accumulated evaporation difference of 10 mm between *Eucalyptus* and *Acacia* during Summer 1997 increased to 13 mm during Winter 1998, as a result of increased evaporation rates (5.6 mm day^{-1} and 4.9 mm day^{-1} respectively).

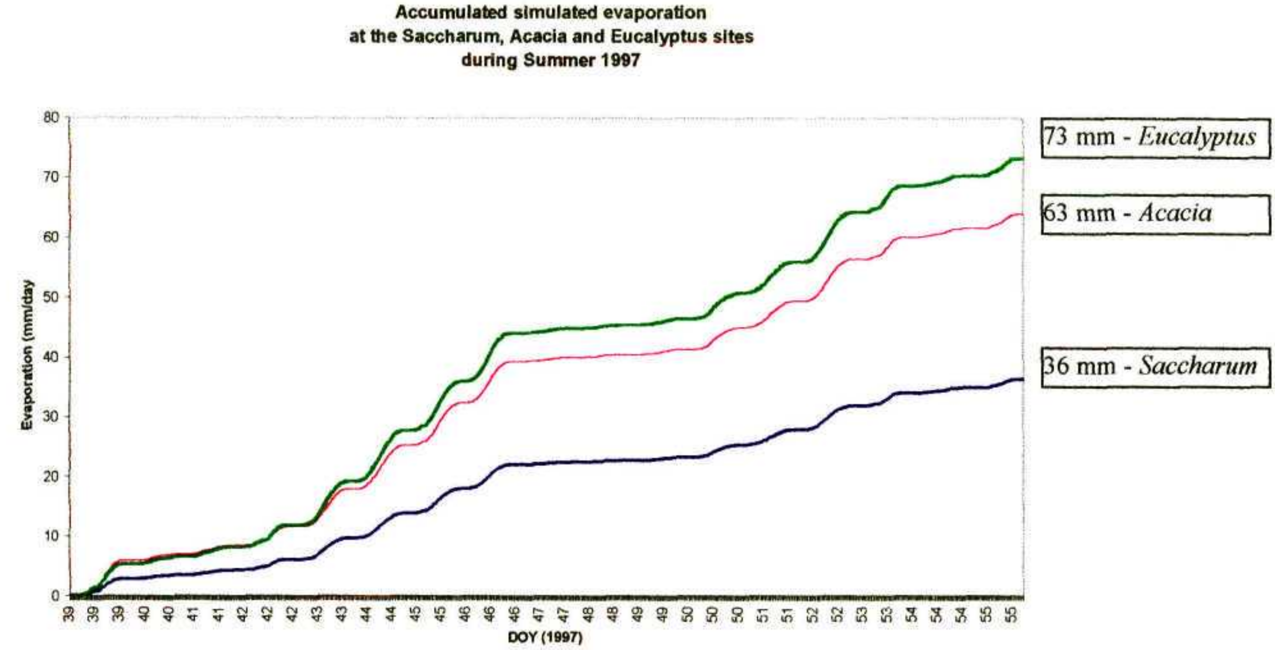

Figure 6.50 Accumulated simulated evaporation during Summer 1997 over a 17 day period (DOY 39 to 55)

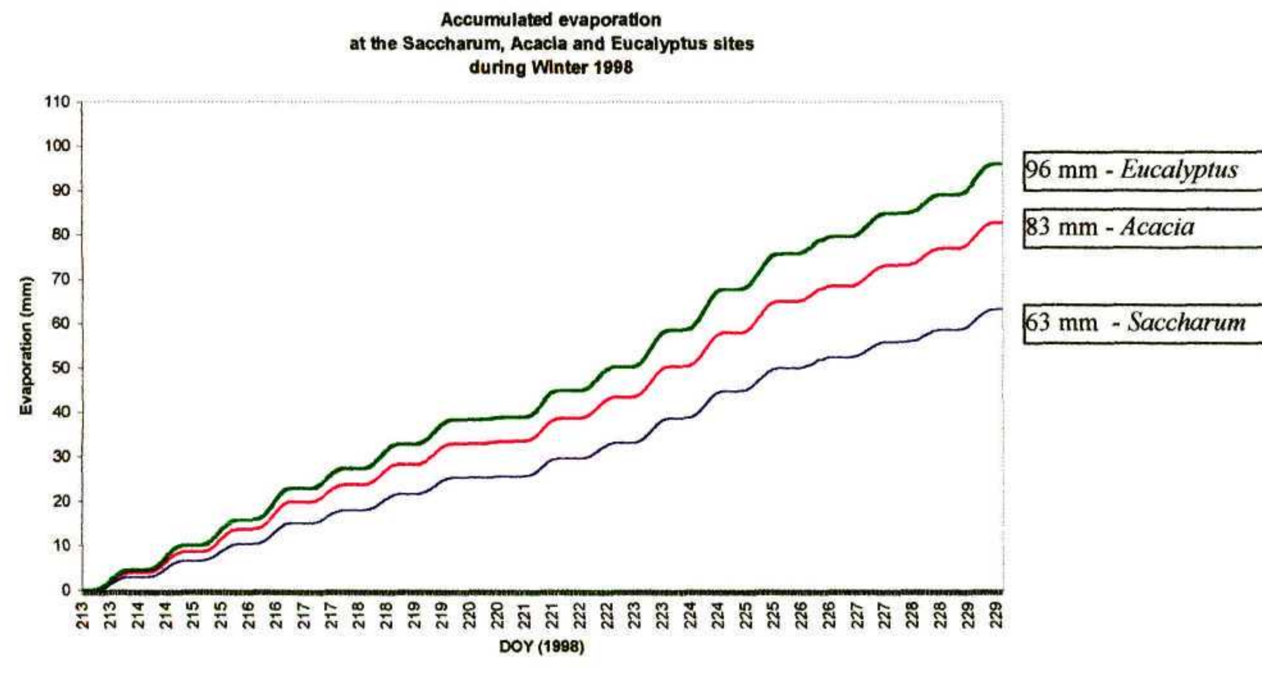

Figure 6.51 Accumulated simulated evaporation during Winter 1998 over a 17 day period (DOY 213 to 229)

Table 6.9 Information on simulated site-specific Penman-Monteith evaporation: monthly average temperature T_a, monthly total radiant density R_s, canopy resistance r_c and reflection coefficient α_s

		Winter 1997	Spring 1997	Summer 1997	Winter 1998	Summer 1998
Saccharum	T_a (°C)	14.32	15.48	19.00	14.75	17.32
	R_s (MJ m^{-2})	11.92	11.95	13.82	10.11	8.79
	ET_{tot} (mm)	42	47	36	63	-
	Et_{avg}(mm day^{-1})	2.50	2.76	2.10	3.70	-
	α_s	0.20	0.20	0.10	0.10	-
	r_c (s m^{-1})	80	80	150	50	-
Acacia	ET_{tot}	28	41	63	83	84
	Et_{avg}	1.60	2.40	3.70	4.90	4.90
	α_s	0.22	0.22	0.1	0.1	0.1
	r_c	70	70	80	45	60
Eucalyptus	ET_{tot}	-	31	73	96	91
	Et_{avg}	-	1.80	4.30	5.60	5.40
	α_s	-	0.18	0.09	0.08	0.08
	r_c	-	100	70	35	60

Towards the end of the experiment (beginning of Summer 1998), the *Acacia* and *Eucalyptus* evaporation rates were similar to those calculated during Winter 1997, with the evaporation rate above *Eucalyptus* (5.4 mm day^{-1}) still exceeding that above *Acacia* (4.9 mm day^{-1}) (Fig. 6.52). The high evaporation rates resulted from the low reflection coefficient used in the simulation of the net irradiance and the small contribution of the soil heat flux density to the energy balance ($G_s = 0.1\ R_{ns}$).

It can be concluded that the evaporation from a mature sugarcane (*Saccharum*) canopy exceeded the evaporation from young (2 year old) commercial forestry trees (*Acacia* and *Eucalyptus*) during Winter 1997. This resulted mainly from differences in the reflection coefficients and subsequently the simulated net irradiance, differences in the contribution of the soil heat flux density ($R_n : G$) to the energy balance and differences in the canopy resistances. Even though the available energy at the *Eucalyptus* site exceeded the available energy at the *Acacia* site during Spring 1997, the higher canopy resistance (100 s m^{-1}) at the *Eucalyptus* site, resulted in a higher evaporation rate above *Acacia* (2.4 mm day^{-1}) compared to *Eucalyptus* (1.8 mm day^{-1}). The mature *Saccharum* and two year old *Acacia* and *Eucalyptus* canopies were conservative water users during Winter 1997 and Spring 1997, with average evaporation rates less than 2.8 mm day^{-1}.

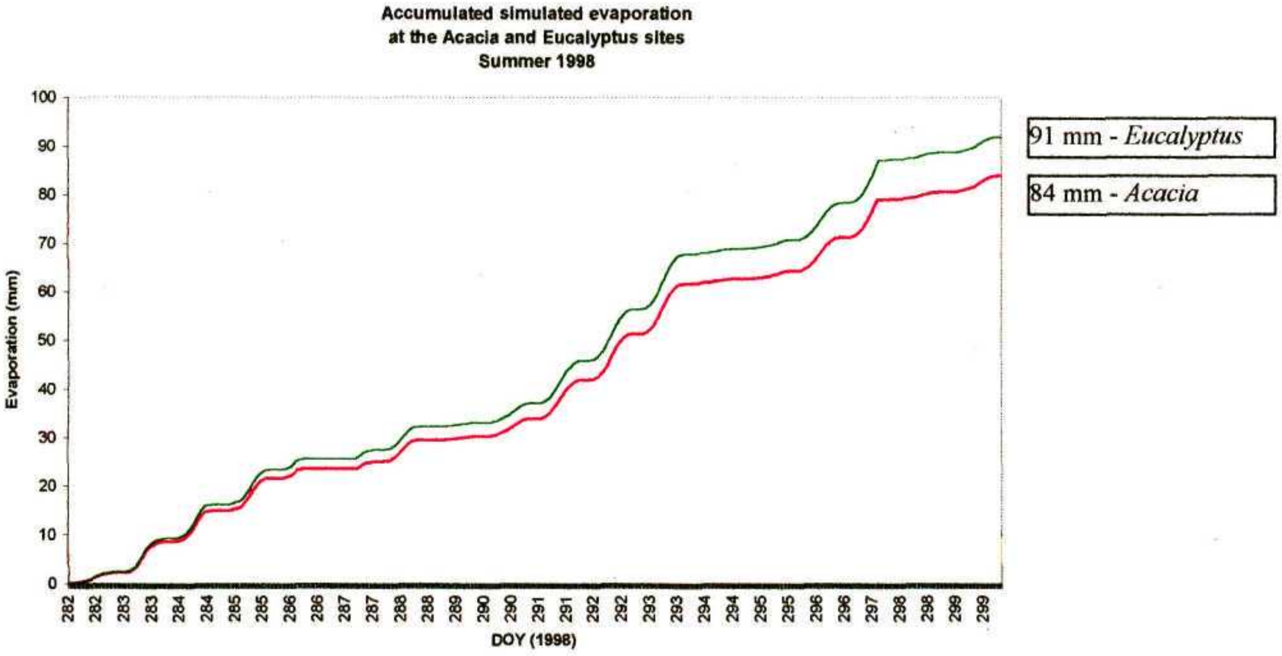

Figure 6.52 Accumulated simulated evaporation at the *Acacia* and *Eucalyptus* sites during Summer 1998 over a 17 day period (DOY 282 to 297)

Rutter (1972) found that the water use by deep-rooted trees under dry conditions, exceeded the water use by grassland and agricultural crops. Under wet conditions the forest water use exceeded grassland and agricultural water use, as a result of higher rainfall interception efficiency, lower canopy reflectivity and lower aerodynamic resistance. Denmead (1969) found evaporation from a forest (*Pinus radiata*) exceeded the evaporation from a wheat field. He noted that these differences between forest and agricultural crops, resulted partly from differences in the canopy development and partly as a result of significant differences in the reflectivities of the different communities. Everson (1995) however found no significant differences in the water use of trees (*Eucalyptus* spp.), grassland, maize and wheat in a marginal forestry area under extensive drought conditions.

The increase in the average forestry canopy (*Acacia* and *Eucalyptus*) heights from Winter 1997 to Summer 1997 resulted in lower canopy reflection coefficients at these sites and higher net irradiance. Stanhill (1970) found the reflection coefficients above tall canopies to be less than that for short vegetation. In addition to the lower reflection coefficients at both the *Acacia* (0.1) and *Eucalyptus* (0.08 to 0.09) sites, the increased soil shading at these sites (*i.e.* low *G's*) resulted in more energy available for partitioning between the sensible and latent heat flux densities and higher evaporation rates, compared to *Saccharum*.

The evaporation rate above the *Eucalyptus* trees exceeded the evaporation rate above the even-aged *Acacia* trees during Winter 1998 and Summer 1998 as a result of the slightly lower reflection coefficient at the *Eucalyptus* site. The evaporation differences between these two sites resulted mainly from the differences in the reflection coefficients and canopy resistance (Table 6.9).

6.3 Problems encountered conducting the Bowen ratio evaporation experiment

Beringer and Tapper (1996) gave evidence of the possibility of collecting long term, reliable Bowen ratio energy balance data. In their six month experiment, the Bowen ratio system was left unattended for four months. However, in the comparative evaporation experiment conducted at Sevenoaks, periodic instrument problems, left gaps in the energy balance and evaporation data sets. This was caused by broken sensors (DEW-10 hygrometers, Model 207 humidity probe, soil heat flux plates and thermocouples), leaks in the Bowen ratio water vapour pressure system and incorrect wiring (Appendix 8).

6.4 Recommendations relating to the Bowen ratio energy balance technique

The following recommendations resulted from the evaporation experiment conducted at Sevenoaks.

A measure of the water stress experienced by the *Saccharum* crop and *Acacia* and *Eucalyptus* trees, could contribute significantly to the comparative evaporation experiment. This, however, was found to be beyond the scope of this project. It is recommended that the available soil water content and/or the soil water potential be monitored at various depths in the soil profile.

Reflection coefficients used in the simulation of the net irradiance at the different sites were obtained from the literature or from the best relationships found between the measured and simulated net irradiance while changing the reflection coefficients. It is therefore recommended that the reflection coefficients be measured seasonally for comparison with the reflection coefficients input into the radiation model.

Bowen ratio energy balance data sets were often incomplete because of the remoteness of the experimental sites. It is therefore recommended that the three sites be linked to a telemetry system, to provide continual real time access to the Bowen ratio energy balance data from the different study sites.

It is also recommended that in addition to the routine maintenance activities suggested by the commercial suppliers (Anonymous, 1998), checks for cracks in the mixing bottles and hoses after six months of use, be added. These checks, ideally should be conducted in the laboratory.

Chapter 7
CONCLUSIONS

Bowen ratio energy balance measurements for this comparative evaporation study showed that the resolution of the Bowen ratio energy balance technique, was generally sufficient for detecting small air temperature and water vapour pressure profile differences for young *Acacia* and *Eucalyptus*. The exception was the Winter of 1997 where aerodynamically rough canopies partially covering the soil, existed. The study further showed that the application of the air temperature difference rejection criteria above forest and sugarcane canopies, as proposed by Ohmura (1982) was too rigorous leading to the rejection of most of the Bowen ratio energy balance data set. However, the application of the rejection criteria for when the Bowen ratio approaches -1, the actual water vapour pressure exceeds the saturated water vapour pressure and when the air temperature and water vapour pressure differences are outside general data ranges, together with experience, proved to be sufficient in the rejection of imprecise Bowen ratio energy balance data.

In the study important features of the energy balance above the *Saccharum, Acacia* and *Eucalyptus* canopies were highlighted using the Bowen ratio energy balance technique. Where low leaf area indices existed, the soil heat flux density contributed significantly to the energy balance ($G = 0.4R_n$). When comparing the evaporation from mature *Saccharum* canopies with young *Acacia* and *Eucalyptus* canopies during Winter 1997, the *Acacia* (2.4 mm day^{-1}) and *Eucalyptus* (1.8 mm day^{-1}) trees were using less water than the sugarcane (2.8 mm day^{-1}). These evaporation differences resulted from changes in the leaf area indices and canopy reflection coefficient. However, with increased average canopy height at the *Acacia* and *Eucalyptus* sites from Winter 1997 to Winter 1998, *Acacia* and *Eucalyptus* were freely transpiring water (4.9 mm day^{-1} and 5.4 mm day^{-1} respectively) at near potential rates during summer.

Physiological maturity and high canopy resistance (possible stress conditions) during Summer 1997 of the *Saccharum* canopy contributed to the lower evaporation rate above *Saccharum* during Summer 1997 (2.1 mm day^{-1}) and Winter 1998 (3.7 mm day^{-1}). No stress conditions were visible at the *Acacia* (3.7 mm day^{-1} and 4.9 mm day^{-1} respectively) and *Eucalyptus* (4.3 mm day^{-1} and 5.6 mm day^{-1} respectively) during Summer 1997 and Winter 1998 and resulted from the ability of the deep-rooted trees to reach water supplies not readily available to the *Saccharum*.

Towards the end of Winter 1998 and Summer 1998, the evaporation above the maturing *Eucalyptus* and *Acacia* canopies exceeded that above the mature *Saccharum* canopy. Differences in the energy balance components and reflection coefficients of the canopies, contributed to these evaporation differences. The comparison of evaporation between commercial forest and sugarcane canopies showed that the young trees do not use significantly more water than mature sugarcane. The two-year-old *Eucalyptus* trees however, used slightly more water than *Acacia* trees as a result of the higher available energy brought about by the lower reflection coefficient of *Eucalyptus*.

Close agreement was found between the measured (Bowen ratio) and simulated (site specific Penman-Monteith) evaporation rates ($m \approx 1$, $r^2 > 0.8$). The site specific Penman-Monteith equations require detailed climatic data (net irradiance, soil heat flux density, air temperature, water vapour pressure and windspeed) available from automatic weather stations, as well as physiological data (canopy resistance). The net irradiance was simulated accurately ($m \approx 1$, $r^2 > 0.96$) using the measured solar irradiance and different reflection coefficients, whereas the soil heat flux density was calculated as a fraction of the simulated net irradiance using a simple linear relationship ($m \approx 0.7$, $r^2 > 0.7$). This study demonstrated the effectiveness of using the Penman-Monteith equation to predict evaporation, provided that the correct radiation (*i.e.* reflection coefficient) and resistances (canopy and aerodynamic) are used.

REFERENCES

Allen RG Jensen ME Wright JL and Burnman RD (1989) Operational estimates of reference evapotranspiration *Agron J* 81 650-662.

Angus DE and Watts PJ (1984) Evapotranspiration - how good is the Bowen ratio method? *Agric Water Manage* 8 133-150.

Anonymous (1991) Instruction manual CSI Bowen ratio Revision 4/91 Campbell Scientific, Inc.

Anonymous (1998) Instruction manual CSI Bowen ratio Revision 1/98 Campbell Scientific, Inc.

Barr AG King KM Gillespie TJ Den Hartog GD and Neumann HH (1994) A comparison of Bowen ratio and eddy correlation sensible and latent heat flux measurements above deciduous forest *Bound Layer Meteorol* 71 21-40.

Beringer J and Tapper N (1996) Evapotranspiration measurements using the Campbell Scientific Bowen ratio system *Conf Proc 2nd Austr Conf Agric Meteorol, Oct 1-4* 264-296.

Black TA and McNaughton KG (1971) Psychrometric apparatus for Bowen ratio determination over forests *Bound Layer Meteorol* 2 246-254.

Blad BL and Rosenberg NJ (1974) Lysimetric calibration of the Bowen ratio-energy balance method for evapotranspiration estimation in the Central Great Plains *J Appl Meteorol* 13 227-236.

Bowen IS (1926) The ratio of heat losses by conduction and by evaporation from any water surface *Phys Rev* 27 779-787.

Brutsaert W (1982) Evaporation into the Atmosphere Reidel, Dordrecht, 299 pp (Cited by Pieri and Fuchs, 1990).

Brutsaert W and Stricker H (1979) An advection-aridity approach to estimate actual regional evapotranspiration *Water Resour Research* 15 443-450.

Businger JA (1986) Evaluation of the accuracy with which dry deposition can be measured with current meteorological techniques *J Clim Appl Meteorol* 25 1100-1124.

Calder IR (1977) A model of transpiration and interception loss from spruce forest in Plynlimon, Central Wales *J Hydrol* 33 247-265.

Campbell AP (1973) The effect of stability on evaporation rates measured by the energy balance method *Agric Meteorol* 11 261-267.

Campbell GS (undated) On-line measurement of potential evapotranspiration with the Campbell Scientific automated weather station, *Application note by Campbell Scientific Inc.*, Department of Crop and Soil Sciences, Washington State University.

Cellier P and Olioso A (1993) A simple system for automated long-term Bowen ratio measurement *Agric Forest Meteorol* 66 81-92.

Denmead OT (1969) Comparative micrometeorology of a wheat field and a forest of *Pinus radiata Agric Meteorol* 6 357-371.

Denmead OT and McIllroy IC (1970) Measurements of non-potential evaporation from wheat *Agric Meteorol* 7 285-302.

Doorenbos J and Pruit WO (1977) Irrigation water requirements *FAO Irrig and Drainage Paper 24, United Nations, New York* (Cited by Allen *et al.*, 1989).

Everson CS (1993) Comparative estimates of evaporation from a *Eucalyptus* plantation and grassland *Sixth South African National hydrological symposium Volume 1*, Lorentz SA Kienzle SW and Dent MC (Eds.) Pietermaritzburg, 8-10 September 1993.

Everson CS (1995) Measurement of transpiration using Bowen ratio technology from plantation canopy surfaces, grassland, wheat and maize in the Natal midlands *CSIR Report no. FOR-DEA-924* 28 pp.

Fritschen LJ (1966) Evapotranspiration rates of field crops determined by the Bowen ratio method *Agron J* 58 339-342.

Fuchs M and Tanner CB (1970) Error analysis of Bowen ratios measured by differential psychrometery *Agric Meteorol* 7 329-334.

Garratt JR (1978) Flux profile relations above tall vegetation *Q J R Meteorol Soc* 104 199-211 (Cited by Heilman and Brittin, 1989).

Hanks RJ Allen LH and Gardner RH (1971) Advection and evapotranspiration in wide-row sorghum in the Central Great Plains *Agron J* 63 520-527.

Heilman JL and Brittin CL (1989) Fetch requirements for Bowen ratio measurements of latent and sensible heat fluxes *Agric Forest Meteorol* 44 261-273.

Huschke RE (1959) (Editor) Glossary of Meteorology, American Meteorological Society, Boston, Massachusetts 638 pp.

Ibanez M Perez PJ Caselles V and Castellvi F (1998) A simple method for estimating the latent heat flux over grass from radiative Bowen ratio *J Appl Meteorol* 37 387-392.

Jensen ME Burman RD and Allen RG (Editors) (1989) Evapotranspiration and irrigation water requirements American Society of Civil Engineers, New York 332 pp.

Lukunga G (1998) Bowen ratio and surface temperature techniques for measuring evaporation from cabbages Unpublished MSc Agric thesis University of Natal 166 pp.

Massman WJ (1992) A surface energy balance method for partitioning evapotranspiration data into plant and soil components *Water Resour Res* 28 1723-1732.

Malek E (1993) Comparison of the Bowen ratio-energy balance and stability corrected aerodynamic methods for measurement of evapotranspiration *Theo Appl Climatol* 48 167-178.

Malek E and Bingham GE (1993) Comparison of the Bowen ratio-energy balance and the water balance methods for the measurement of evapotranspiration *J Hydrol* 146 205-220.

McGlinchey MG and Inman-Bamber NG (1996) Predicting sugarcane water use with the Penman-Monteith equation *Evaporation and Irrigation Scheduling Proceedings of the International conference* Camp CR Sadler EJ and Yoder RE (Eds.) 592-598.

Metelerkamp BR (1993) The use of the Bowen ratio energy balance method for the determination of total evaporation over a grassed surface Unpublished MSc Agric thesis University of Natal 153 pp.

Monteith JL (1963) Gas Exchange in Plant Communities *Environmental Control in Plant Growth Academic Press* Evans LJ (Ed.) New York 95-112 (Cited by Rosenberg *et al., 1983*).

Monteith JL (1964) Evaporation and Environment. The State and Movement of Water in Living Organisms *19 the Symp Soc Exp Biol*, Academic Press, New York, 205-234 (Cited by Rosenberg *et al., 1983*).

Monteith JL (1975) Vegetation and the Atmosphere *Volume I Principles Academic Press, London* 278 pp.

Monteith JL (1976) Vegetation and the Atmosphere *Volume II Case Studies Academic Press, London* 439 pp.

Monteith JL and Unsworth MH (1990) Principles of Environmental Physics 2nd ed. London Edward Arnold 291 pp.

Munro DS and Oke TR (1975) Aerodynamic boundary layer adjustment over a crop in neutral stability *Bound Layer Meteorol* 9 53-61.

Nie D Flitcroft ID and Kanemasu ET (1992) Performance of Bowen ratio systems on a slope *Agric Forest Meteorol* 59 165-181.

Ohmura A (1982) Objective criteria for rejecting data for Bowen ratio flux calculation *J Appl Meteorol* 21 595-598.

Oke TR (1978) Boundary Layer Climates 2nd ed. London Methuen, 435 pp.

Ortega-Farias SO (1996) Daytime variation of sensible heat flux estimatedby the bulk aerodynamic method over a grass canopy *Agric Forest Meteorol* 81 131-143.

Penman HL (1948) Natural evaporation from open water, bare soil and grass *Proc R Soc London Ser A* 193 120-145 (Cited by Rosenberg *et al.*, 1993).

Pieri P and Fuchs M (1990) Comparison of Bowen ratio and aerodynamic estimates of evapotranspiration *Agric Forest Meteorol* 49 243-256.

Priestley CHB and Taylor RJ (1972) On the assessment of surface heat flux and evaporation using large-scale parameters *Mon Weather Rev* 100 81-92 (Cited by Rosenberg *et al.*, 1983).

Revheim KJA and Jordan RB (1976) Precision of evaporation measurements using the Bowen ratio *Bound Layer Meteorol* 10 97-111.

Rosenberg NJ Blad BL and Verma SB (1983) MICROCLIMATE The Biological Environment 2nd ed. New York Wiley 495 pp.

Rutter AJ (1972) Evaporation from forests Research papers in Forest Meteorology, Cambrian News (Aberystwyth) Ltd, Aberystwyth 75-90.

Savage MJ Graham ADN and Lightbody KE (1993) Use the stem steady state real energy balance technique for the *in situ* measurement of transpiration in *Eucalyptus grandis*: Theory and errors *J S Afr Soc Hort Sci* 3 46-51.

Savage MJ McInnes KJ and Heilman JL (1996) The "footprints" of eddy correlation sensible heat flux density, and other micrometeorological measurements *SA J Scien* 92 137-142.

Savage MJ Everson CS and Metelerkamp BR (1997) Evaporation measurement above vegetated surfaces using micro-meteorological techniques *WRC Report no 349/1/97* 227 pp.

Sinclair TR Allen LH and Lemon ER (1975) An analysis of errors in the calculation of energy flux densities above vegetation by a Bowen ratio profile method *Bound Layer Meteorol* 8 129-139.

Slabbers PJ (1977) Surface roughness of crops and potential evapotranspiration *J Hydrol* 34 181-191 (Cited by Rosenberg *et al.*, 1993).

Slayan L and Bernhofer CH (1993) Using the Penman-Monteith approach to extrapolate soyabean evapotranspiration *Theor Appl Climatol* 46 241-246.

Spittlehouse DL and Black TA (1980a) Determination of forest evapotranspiration using Bowen ratio and eddy correlation measurements *J Appl Meteorolo* 18 647-653.

Spittlehouse DL and Black TA (1980) Determination of forest evapotranspiration using Bowen ratio and eddy correlation measurements *J Appl Meteoro* 18 647-653.

Stanhill G (1970) *Solar energy* 13 59-66 (Cited by Monteith, 1976).

Stannard DI (1997) A theoretically based determination of Bowen ratio fetch requirements *Bound Layer Meteorol* 83 375-406.

Stull RB (1988) An Introduction to Boundary Layer Meteorology Dordrecht Kluwer, 666pp.

Tanner CB (1960) Energy balance approach to evapotranspiration from plants and soils *J Soil Water Conserv* 12 221-227 (Cited by Malek, 1993).

Thom AS (1975) Momentum, Mass and Heat Exchange in Plant Communities *Vegetation and the Atmosphere Vol. 1 Principles Acad Press* Monteith JL (Ed.) London 57-109.

Unland HE Arain AM Harlow C Houser PR Garatuza-Payan J Scott P Sen OL and Shuttleworth WJ (1998) Evaporation from a riparian system in a semi-arid environment *Hygrol Process* 12 527-542.

Van Dam JC Huygen J Wesseling JG Feddes RA Kabat P Van Walsum PEV Groenendijk P and Van Diepen CA (1997) Simulation of water flow, solute transport and plant growth in the soil-water-atmosphere-plant environment Theory of SWAP version 2.0 *Report 71, Technical report 45, Department of Water Resources, Wageningen Agricultural University.*

Van Zyl WH and De Jager JM (1992) Errors in micro-meteorological estimates of reference crop evaporation due to advection *Water SA* 18 255-264.

Wicke W and Bernhofer CH (1996) Energy balance comparison of the Hartheim forest and adjacent grassland site during the HartXExperiment *Theo Appl Climatol* 53 49-58.

Wright JL (1981) Crop coefficients for estimates of daily crop evapotranspiration *Irrigation scheduling for water and energy conservation in the 80s Proc Irrig Scheduling Conf Chicago IL 14-15 Dec ASAE St Joseph MI* 18-26 (Cited by Allen *et al.*, 1989).

Wright JL (1982) New evapotranspiration crop coefficients *J Irrig Drain Div Am Soc Civ Eng* 108 57-74 (Cited by Allen *et al.*, 1989).

Yeh GT and Brutseart WH (1971) A solution for simultaneous turbulent heat and vapour transfer between a water surface and the atmosphere *Bound Layer Meteorol* 2 64-82.

APPENDIX 1 Calculation of the Penman-Monteith reference evaporation

The Penman-Monteith reference evaporation (Campbell, undated) is given by

$$ET_o = \Delta(R_n - G)/[\lambda(\Delta + \gamma^*)] + \gamma^* M_w (e_s - e_a)/[R\theta r_v (\Delta + \gamma^*)] \qquad 1$$

with ET_o as the potential evaporation rate (mm/s), R_n the net irradiance (kW m^2), G the soil heat flux density (kW m^{-2}), M_w the molecular mass of water (0.018 kg mol^{-1}), R the gas constant (8.31 x 10^{-3} kJ mol^{-1} K^{-1}), θ the Kelvin temperature (293 K), $(e_s - e_a)$ the vapour pressure deficit of the air (kPa), λ the latent heat of vaporization of water (2450 kJ kg^{-1}), r_v the combined resistance for vapour (s m^{-1}), Δ the slope of the saturation water vapour pressure function (Pa °C^{-1}) and γ^* the apparent psychrometer constant (Pa °C^{-1}).

The net irradiance, R_n, is the sum of the net solar irradiance and the net long-wave irradiance and is approximated as

$$R_n = \alpha_s R_s + L_{ni} \qquad 2$$

where α_s is the absorptivity of the crop, R_s is the measured solar irradiance measured by the datalogger and L_{ni} is the atmospheric radiant emittance minus the crop emittance at air temperature. Under clear skies, L_{ni} (kW m^{-2}) is given by

$$L_{nic} = 0.0003\, T_a - 0.107 \qquad 3$$

with T_a as the air temperature (°C). Under cloudy skies L_{ni} approaches zero. Cloudiness is estimated from the ratio of measured to potential solar irradiance during daylight hours (R_s/R_o). A cloudiness function, $f(R_s/R_o)$ is computed

$$f(R_s/R_o) = 1\text{-}1/[1 + 0.034 \exp(7.9\, R_s/R_o)] \qquad 4$$

The net isothermal long-wave irradiance (L_{ni}) is then calculated as

$$L_{ni} = f(R_s/R_o)\, L_{nic} \qquad 5$$

The cloudiness function (*Eq. 4*) requires the computation of the potential solar irradiance on a horizontal surface outside the earth's atmosphere, R_o

$$R_o = 1.36 \sin \varphi \qquad 6$$

where *1.36* (kW m^{-2}) is the solar constant, and φ the elevation angle of the sun

$$\sin \varphi = \sin d \sin l + \cos d \cos l \cos [15(t-t_o)] \qquad 7$$

where d is the solar declination angle, l the latitude at the site, t the local time and t_o the time of solar noon. *Sin d* is approximated using the polynomial

$$\sin d = -0.37726 - 0.10564\, j + 1.2458\, j^2 - 0.75478\, j^3 + 0.13627\, j^4 - 0.00572\, j^5 \qquad 8$$

where j is the day of the year (DOY) divided by 100 (DOY/100) and d is the declination. The cosine of d is computed from the trigonometric identity

$$\cos d = (1 - \sin^2 d)^{0.5} \qquad 9$$

The time t is the datalogger local time less half the time increment from the last ET_o computation. The time of solar noon, t_o, is given by

$$t_o = 12.5 - L_c - t_e \qquad 10$$

with L_c the longitude correction and t_e the "equation of time". The longitude correction is calculated by determining the difference between the longitude of the site and the longitude of the standard meridian. The longitude correction is given as

$$L_c = (L_s - L)/15 \qquad 11$$

The "equation of time" is an additional correction to the time of solar noon that depends on the day of year. Two equations is used to calculate t_e - one for the first half of the year (for DOY < 180, where j = DOY/100)

$$t_e = -0.04056 - 0.74503\, j + 0.08823\, j^2 + 2.0515\, j^3 - 1.8111\, j^4 + 0.42832\, j^5 \qquad 12$$

and one for the second half of the year (for DOY > 180, where j = (DOY-180)/100)

$$t_e = -0.05039 - 0.33954\, j + 0.04084\, j^2 + 1.8928\, j^3 - 1.7619\, j^4 + 0.4224\, j^5 \qquad 13$$

Evaporation occurs mainly during daytime hours when the net irradiance is the main driving force of the evaporation and positive. The soil heat flux density can be estimated as a fraction of the net irradiance. For a complete canopy cover, G is assumed to be approximately 10 % of the net irradiance (*Eq. 14*)

$$G = 0.1\, R_n \qquad 14$$

During the night $R_s = 0$ and G assumed to be 50 % of the net irradiance (*Eq. 15*)

$$G = 0.5\, R_n \qquad 15$$

The slope of the saturation vapour pressure function ($Pa\ °C^{-1}$) depends on air temperature, yielding

$$\Delta = 45.3 + 2.97\ T_a + 0.0549\ T_a^2 + 0.00223\ T_a^3 \qquad 16$$

with T_a the average air temperature (°C).

The apparent psychrometer constant γ^* is calculated as

$$\gamma^* = \gamma (r_v/r_a) \qquad 17$$

where γ *is* the thermodynamic psychrometer constant, r_v the combined aerodynamic and canopy resistance to water vapour and r_a the convective resistance for heat transfer. The vapour resistance is computed as

$$r_v = r_a + r_c \qquad 18$$

where the canopy resistance is 70 s m^{-1} for a reference crop.

The aerodynamic resistance (r_a) is given by

$$r_a = ln[z_u - d/z_{om}]\ ln[z_t - d/z_{oh}]/k^2\ u_z \qquad 19$$

with k the Von Karman constant (0.41), z_u the height of the anemometer above the soil surface and z_t the height of the temperature and humidity sensor above the soil surface. For clipped grass the zeroplane displacement (d), roughness length for momentum transfer (z_{om}) and heat and water vapour transfer (z_{oh}) are

$$d = 0.67\,h \tag{20}$$

$$z_{om} = 0.12\,h \tag{21}$$

$$z_{oh} = 0.1\,z_{om} \tag{22}$$

where h is the average canopy height.

Ignoring the psychrometer constant's weak temperature dependence and taking the pressure dependence into account, the ratio between the atmospheric pressure and sea level pressure (P/P_o) is

$$P/P_o = exp(-A/8500) \tag{23}$$

where A is the altitude (m).

The Kelvin temperature is set as 293 K, yielding a constant value of $M_w/R\theta$.

The saturated (e_s) and actual (e_a) water vapour pressures are computed from the air temperature and relative humidity measurements (Campbell, undated; Monteith and Unsworth, 1990).

APPENDIX 2 Net radiometer and Bowen ratio arm installation heights

In order to overcome heterogeneity caused by the horizontal distribution of foliage, the measurements must be made sufficiently high above the surface layer (Brutseart, 1982). The average sampling heights above *Saccharum, Acacia* and *Eucalyptus* changed during 1997 and 1998 as a result of changes in the average canopy heights. Garratt (1978) suggested that the lower arm be installed three to five times the roughness length above the soil surface. The lower arm was subsequently installed low enough so as not to sense the bulk crop surface environment and the upper arm was installed low enough not to sense a different environment upwind.

Crop	YEAR	DOY	Height of net radiometers (m)	Height of upper arm above the soil surface (m)	Height of lower arm above the soil surface (m)	Distance between the arms (m)
Saccharum	1997	213	0.70	4.50	3.40	1.10
	1998	75	3.51	4.53	3.39	1.14
		133	4.90	6.55	4.55	2.00
		148	-	6.52	4.52	2.00
Acacia	1997	227	2.59	4.65	3.25	1.40
	1998	6	2.85	5.00	3.95	1.05
		75	2.84	5.53	4.42	1.11
		127	6.40	9.40	7.40	2.00
		133	-	9.70	7.70	2.00
Eucalyptus	1998	75	3.55	6.39	4.85	1.54
		78	6.45	8.14	6.65	1.49
		127	6.40	9.70	7.70	2.00
		133	-	9.75	7.75	2.00
		166	9.47	11.40	9.40	2.00

APPENDIX 3 An overview on additional sensors utilised

Additional to the Bowen ratio energy balance system, all three sites were equipped with time domain reflectometry (CS615) probes, used to measure real time volumetric soil water content. A complete automatic weather station (solarimeter, air temperature and humidity sensor, windspeed and direction sensor, rain gauge) was installed at the *Saccharum* site.

Sensor/Instrument	Model	Measurement
Solarimeter	Kipp & Zonen	Solar irradiance
Model 207 temperature and humidity sensor	Model 207 temperature and humidity sensor	Air temperature (°C) and relative humidity (%)
Three cup anemometer	MCS 177 Wind speed sensor	Average wind speed (m s^{-1})
Windvane	MCS 176 Wind direction sensor	Sample wind direction (°)
Raingauge	Lamprecht tipping bucket (0.1mm)	Total rainfall (mm)
TDR probe	CS 615	Soil water content (%)

APPENDIX 4 Programme for a Bowen ratio system and automatic weather station

```
Programme for Bowen ratio system
and Automatic weather station
(Wind speed, wind direction,
rainfall, solar irradiance, CS207?
probe) and CS615 TDR probe

;{21X}
*Table 1 Program
 01: 1.0000   Execution Interval
(seconds)

1: Internal Temperature (P17)
 1: 1      Loc [ Tint    ]

2: Thermocouple Temp (SE) (P13)
 1: 1      Reps
 2: 1      5 mV Slow Range
 3: 8      SE Channel
 4: 2      Type E (Chromel-
Constantan)
 5: 1      Ref Temp Loc [ Tint    ]
 6: 3      Loc [ T1      ]
 7: 1      Mult
 8: 0      Offset

3: Thermocouple Temp (DIFF)
(P14)
 1: 1      Reps
 2: 1      5 mV Slow Range
 3: 4      DIFF Channel
 4: 2      Type E (Chromel-
Constantan)
 5: 3      Ref Temp Loc [ T1      ]
 6: 2      Loc [ T2      ]
 7: 1      Mult
 8: 0      Offset

4: Volts (SE) (P1)
 1: 1      Reps
 2: 4      500 mV Slow Range
 3: 12     SE Channel
 4: 6      Loc [ Rs      ]
 5: 78.431  Mult
 6: 0      Offset

5: Temp 107 Probe (P11)
 1: 1      Reps
 2: 15     SE Channel
 3: 2      Excite all reps w/Exchan 2
 4: 12     Loc [ T207    ]
 5: 1      Mult
 6: 0      Offset

6: Saturation Vapor Pressure (P56)
 1: 12     Temperature Loc [ T207
]
 2: 13     Loc [ es      ]

7: R.H. 207 Probe (P12)
 1: 1      Reps
 2: 16     SE Channel
 3: 2      Excite all reps w/Exchan 2
 4: 12     Temperature Loc [ T207
]
 5: 14     Loc [ RHfrac   ]
 6: 1      Mult
 7: 0      Offset

8: Z=X*F (P37)
 1: 14     X Loc [ RHfrac   ]
 2: .01    F
 3: 14     Z Loc [ RHfrac   ]

9: Z=X*Y (P36)
 1: 13     X Loc [ es       ]
 2: 14     Y Loc [ RHfrac   ]
 3: 13     Z Loc [ es       ]

10: Full Bridge (P6)
 1: 1      Reps
 2: 1      5 mV Slow Range
 3: 2      DIFF Channel
 4: 1      Excite all reps w/Exchan 1
 5: 5000   mV Excitation
 6: 8      Loc [ Td      ]
 7: .001   Mult
 8: .00498  Offset

11: Z=X-Y (P35)
 1: 3      X Loc [ T1      ]
 2: 2      Y Loc [ T2      ]
 3: 4      Z Loc [ Tdiff   ]

12: BR Transform Rf[X/(1-X)]
(P59)
 1: 1      Reps
 2: 8      Loc [ Td      ]
 3: 200    Mult (Rf)

13: Temperature RTD (P16)
 1: 1      Reps
 2: 8      R/R0 Loc [ Td      ]
 3: 8      Loc [ Td      ]
 4: 1      Mult
 5: 0      Offset

14: Saturation Vapor Pressure (P56)
 1: 8      Temperature Loc [ Td      ]
 2: 9      Loc [ VP      ]

15: Z=F (P30)
 1: 1      F
 2: 32     Z Loc [ StationID ]

16: If Flag/Port (P91)
 1: 15     Do if Flag 5 is High
 2: 0      Go to end of Program
Table

17: If time is (P92)
 1: 0      Minutes into a
 2: 20     Minute Interval
 3: 10     Set Output Flag High

18: If Flag/Port (P91)
 1: 14     Do if Flag 4 is High
 2: 30     Then Do

19: Do (P86)
 1: 10     Set Output Flag High

20: Do (P86)
 1: 15     Set Flag 5 High

21: End (P95)

22: Real Time (P77)
 1: 1220   Year,Day,Hour/Minute
(midnight = 2400)

23: Sample (P70)
 1: 1      Reps
 2: 32     Loc [ StationID ]

24: Average (P71)
 1: 2      Reps
 2: 3      Loc [ T1      ]

25: If Flag/Port (P91)
 1: 12     Do if Flag 2 is High
 2: 30     Then Do

26: Do (P86)
 1: 19     Set Intermed. Proc.
Disable Flag High (Flag 9)

27: Else (P94)

28: If Flag/Port (P91)
 1: 11     Do if Flag 1 is High
 2: 19     Set Intermed. Proc.
Disable Flag High (Flag 9)

29: End (P95)

30: Average (P71)
 1: 2      Reps
 2: 8      Loc [ Td      ]

31: Do (P86)
 1: 29     Set Intermed. Proc.
Disable Flag Low (Flag 9)

32: If Flag/Port (P91)
 1: 22     Do if Flag 2 is Low
 2: 30     Then Do

33: Do (P86)
 1: 19     Set Intermed. Proc.
Disable Flag High (Flag 9)

34: Else (P94)

35: If Flag/Port (P91)
 1: 11     Do if Flag 1 is High
```

2: 19 Set Intermed. Proc. Disable Flag High (Flag 9)

36: End (P95)

37: Average (P71)
1: 2 Reps
2: 8 Loc [Td]

38: Average (P71)
1: 2 Reps
2: 12 Loc [T207]

39: Average (P71)
1: 1 Reps
2: 6 Loc [Rs]

*Table 2 Program
01: 10.0000 Execution Interval (seconds)

1: Time (P18)
1: 0 Tenths of seconds into current minute (maximum 600)
2: 400 Mod/By
3: 11 Loc [Secinmin]

2: IF (X<=>F) (P89)
1: 11 X Loc [Secinmin]
2: 4 <
3: 100 F
4: 21 Set Flag 1 Low

3: If Flag/Port (P91)
1: 15 Do if Flag 5 is High
2: 30 Then Do

4: If Flag/Port (P91)
1: 24 Do if Flag 4 is Low
2: 1 Call Subroutine 1

5: End (P95)

6: If time is (P92)
1: 0 Minutes into a
2: 2 Minute Interval
3: 30 Then Do

7: Do (P86)
1: 11 Set Flag 1 High

8: If time is (P92)
1: 0 Minutes into a
2: 4 Minute Interval
3: 30 Then Do

9: Set Port (P20)
1: 1 Set High
2: 2 Port Number

10: Do (P86)
1: 12 Set Flag 2 High

11: Else (P94)

12: Set Port (P20)
1: 1 Set High
2: 1 Port Number

13: Do (P86)
1: 22 Set Flag 2 Low

14: End (P95)

15: Excitation with Delay (P22)
1: 1 Ex Channel
2: 0 Delay w/Ex (units = 0.01 sec)
3: 2 Delay After Ex (units = 0.01 sec)
4: 0 mV Excitation

16: Set Port (P20)
1: 0 Set Low
2: 1 Port Number

17: Set Port (P20)
1: 0 Set Low
2: 2 Port Number

18: End (P95)

19: Batt Voltage (P10)
1: 10 Loc [BattV]

20: Volt (Diff) (P2)
1: 1 Reps
2: 4 500 mV Slow Range
3: 1 DIFF Channel
4: 15 Loc [Rn]
5: 13.9 Mult
6: 0 Offset

21: Volts (SE) (P1)
1: 2 Reps
2: 2 15 mV Slow Range
3: 9 SE Channel
4: 16 Loc [HFP1]
5: 37.45 Mult
6: 0 Offset

22: Thermocouple Temp (DIFF) (P14)
1: 1 Reps
2: 1 5 mV Slow Range
3: 3 DIFF Channel
4: 2 Type E (Chromel-Constantan)
5: 1 Ref Temp Loc [Tint]
6: 20 Loc [Ts]
7: 1 Mult
8: 0 Offset

23: Pulse (P3)
1: 1 Reps
2: 3 Pulse Input Channel
3: 2 Switch Closure, All Counts
4: 26 Loc [Rain]
5: .1 Mult
6: 0 Offset

24: Z=F (P30)
1: 5000 F
2: 27 Z Loc [Analogout]

25: Analog Out (P21)
1: 1 CAO Channel
2: 27 mV Loc [Analogout]

26: Pulse (P3)
1: 1 Reps
2: 2 Pulse Input Channel
3: 20 High Frequency, Output Hz
4: 28 Loc [Windspeed]
5: 1.175 Mult
6: -.6 Offset

27: Excite Delay Volt (SE) (P4)
1: 1 Reps
2: 5 5000 mV Slow Range
3: 13 SE Channel
4: 3 Excite all reps w/Exchan 3
5: 10 Delay (units 0.01 sec)
6: 2000 mV Excitation
7: 7 Loc [Winddir]
8: .18 Mult
9: 0 Offset

28: If time is (P92)
1: 15 Minutes into a
2: 20 Minute Interval
3: 18 Set Flag 8 High

29: If Flag/Port (P91)
1: 18 Do if Flag 8 is High
2: 30 Then Do

30: Z=X+Y (P33)
1: 20 X Loc [Ts]
2: 21 Y Loc [Tstotal]
3: 21 Z Loc [Tstotal]

31: Z=Z+1 (P32)
1: 22 Z Loc [Nosamples]

32: End (P95)

33: If time is (P92)
1: 0 Minutes into a
2: 20 Minute Interval
3: 30 Then Do

34: Z=X/Y (P38)
1: 21 X Loc [Tstotal]
2: 22 Y Loc [Nosamples]
3: 24 Z Loc [Tsaverage]

35: Z=X-Y (P35)
1: 24 X Loc [Tsaverage]
2: 23 Y Loc [Tsprevave]
3: 25 Z Loc [Tsdiff]

36: Z=X (P31)
1: 24 X Loc [Tsaverage]
2: 23 Z Loc [Tsprevave]

37: Z=F (P30)
1: 0 F
2: 21 Z Loc [Tstotal]

38: Z=F (P30)
1: 0 F
2: 22 Z Loc [Nosamples]

39: Do (P86)
1: 28 Set Flag 8 Low

40: Do (P86)
1: 10 Set Output Flag High

41: End (P95)

42: Real Time (P77)
1: 1220 Year,Day,Hour/Minute (midnight = 2400)

43: Average (P71)
1: 3 Reps
2: 15 Loc [Rn]

44: Sample (P70)
1: 2 Reps
2: 24 Loc [Tsaverage]

45: Totalize (P72)
1: 1 Reps
2: 26 Loc [Rain]

46: Average (P71)
1: 1 Reps
2: 28 Loc [Windspeed]

47: Sample (P70)
1: 1 Reps
2: 7 Loc [Winddir]

48: Average (P71)
1: 1 Reps
2: 18 Loc [TDRraw]

49: Serial Out (P96)
1: 30 SM192/SM716/CSM1

50: Do (P86)
1: 2 Call Subroutine 2

51: Do (P86)
1: 3 Call Subroutine 3

*Table 3 Subroutines

1: Beginning of Subroutine (P85)
1: 1 Subroutine 1

2: Do (P86)
1: 25 Set Flag 5 Low

3: Do (P86)
1: 10 Set Output Flag High

4: Real Time (P77)
1: 220 Day,Hour/Minute (midnight = 2400)

5: End (P95)

6: Beginning of Subroutine (P85)
1: 2 Subroutine 2

7: Z=F (P30)
1: 300 F
2: 29 Z Loc [Pumpon]

8: Z=F (P30)
1: 1140 F
2: 30 Z Loc [Pumpoff]

9: Time (P18)
1: 1 Minutes into current day (maximum 1440)
2: 0 Mod/By
3: 31 Loc [Mininday]

10: IF (X<=>Y) (P88)
1: 29 X Loc [Pumpon]
2: 1 =
3: 31 Y Loc [Mininday]
4: 16 Set Flag 6 High

11: Set Port (P20)
1: 16 Set According to Flag 6
2: 3 Port Number

12: Do (P86)
1: 26 Set Flag 6 Low

13: IF (X<=>Y) (P88)
1: 30 X Loc [Pumpoff]
2: 1 =
3: 31 Y Loc [Mininday]
4: 17 Set Flag 7 High

14: Set Port (P20)
1: 17 Set According to Flag 7
2: 4 Port Number

15: Do (P86)
1: 27 Set Flag 7 Low

16: IF (X<=>F) (P89)
1: 10 X Loc [BattV]
2: 4 <
3: 11.5 F
4: 30 Then Do

17: If Flag/Port (P91)
1: 23 Do if Flag 3 is Low
2: 30 Then Do

18: Set Port (P20)
1: 1 Set High
2: 4 Port Number

19: Excitation with Delay (P22)
1: 4 Ex Channel
2: 0 Delay w/Ex (units = 0.01 sec)
3: 1 Delay After Ex (units = 0.01 sec)
4: 0 mV Excitation

20: Set Port (P20)
1: 0 Set Low
2: 4 Port Number

21: Do (P86)
1: 13 Set Flag 3 High

22: Do (P86)
1: 10 Set Output Flag High

23: Real Time (P77)
1: 220 Day,Hour/Minute (midnight = 2400)

24: Sample (P70)
1: 1 Reps
2: 10 Loc [BattV]

25: End (P95)

26: Else (P94)

27: If Flag/Port (P91)
1: 13 Do if Flag 3 is High
2: 30 Then Do

28: IF (X<=>F) (P89)
1: 10 X Loc [BattV]
2: 3 >=
3: 12 F
4: 30 Then Do

29: Set Port (P20)
1: 1 Set High
2: 3 Port Number

30: Excitation with Delay (P22)
1: 4 Ex Channel
2: 0 Delay w/Ex (units = 0.01 sec)
3: 1 Delay After Ex (units = 0.01 sec)
4: 0 mV Excitation

31: Set Port (P20)
1: 0 Set Low
2: 3 Port Number

32: Do (P86)
1: 23 Set Flag 3 Low

33: Do (P86)
1: 10 Set Output Flag High

34: Real Time (P77)
1: 220 Day,Hour/Minute (midnight = 2400)

35: Sample (P70)
1: 1 Reps
2: 10 Loc [BattV]

36: End (P95)

37: End (P95)

38: End (P95)

39: End (P95)

40: Beginning of Subroutine (P85)
1: 3 Subroutine 3

41: Set Port (P20)
1: 1 Set High
2: 5 Port Number

42: Beginning of Loop (P87)
1: 1 Delay
2: 2 Loop Count

43: End (P95)

44: Pulse (P3)
1: 1 Reps
2: 4 Pulse Input Channel
3: 21 Low Level AC, Output Hz

```
4: 18      Loc [ TDRraw   ]
5: .001    Mult
6: 0       Offset

45: Set Port (P20)
1: 0       Set Low
2: 5       Port Number

46: End (P95)

End Program


-Input Locations-
1 Tint      1 2 1
2 T2        1 1 1
3 T1        1 3 1
4 Tdiff     1 2 1
5 ________ 0 0 0
6 Rs        1 1 1
7 Winddir   1 1 1
8 Td        1 5 3
9 VP        1 2 1
10 BattV    1 4 1
11 Secinmin 1 1 1
12 T207     1 3 1
13 es       1 3 2
14 RHfrac   1 2 2
15 Rn       1 1 1
16 HFP1     5 1 1
17 HFP2     17 1 1
18 TDRraw   1 1 1
19 ________ 0 0 0
20 Ts       1 1 1
21 Tstotal  1 2 2
22 Nosamples 1 2 2
23 Tsprevave 1 1 1
24 Tsaverage 1 3 1
25 Tsdiff   1 2 1
26 Rain     1 1 1
27 Analogout 1 1 1
28 Windspeed 1 1 1
29 Pumpon   1 1 1
30 Pumpoff  1 1 1
31 Mininday 1 2 3
32 StationID 1 1 1
33 ________ 0 0 0
34 ______ 0 0 0
35 ________ 0 0 0
36 ________ 0 0 0
37 ________ 0 0 0
38 ________ 0 0 0
39 ________ 0 0 0
40 ________ 0 0 0
41 ________ 0 0 0
-Program Security-
0
0000
0000

Final Storage Label File for:
SGBTDR98.CSI
Date: 3/11/1998
Time: 08:09:08

117 Output_Table 20.00 Min
1 117 L

119 Output_Table 20.00 Min
1 119 L
2 Year_RTM L
3 Day_RTM L
4 Hour_Minute_RTM L
5 StationID L
6 T1_AVG L
7 Tdiff_AVG L
8 Td_AVG L
9 VP_AVG L
10 Td_AVG L
11 VP_AVG L
12 T207_AVG L
13 es_AVG L
14 Rs_AVG L

303 Output_Table 10.00 Sec
1 303 L
2 Day_RTM L
3 Hour_Minute_RTM L

240 Output_Table 10.00 Sec
1 240 L
2 Year_RTM L
3 Day_RTM L
4 Hour_Minute_RTM L
5 Rn_AVG L
6 HFP1_AVG L
7 HFP2_AVG L
8 Tsaverage L
9 Tsdiff L
10 Rain_TOT L
11 Windspeed_AVG L
12 Winddir L
13 TDRraw_AVG L

322 Output_Table 10.00 Sec
1 322 L
2 Day_RTM L
3 Hour_Minute_RTM L
4 BattV L

333 Output_Table 10.00 Sec
1 333 L
2 Day_RTM L
3 Hour_Minute_RTM L
4 BattV L


Estimated Total Final Storage
Locations used per day 208368.0
```

APPENDIX 5 Programme for a Bowen ratio system

Programme for Bowen ratio system with a CS615 TDR probe

```
;{21X}
*Table 1 Program
 01: 1.0000   Execution Interval
(seconds)

1: Internal Temperature (P17)
 1: 1      Loc [ Tint     ]

2: Thermocouple Temp (SE) (P13)
 1: 1      Reps
 2: 1      5 mV Slow Range
 3: 8      SE Channel
 4: 2      Type E (Chromel-
Constantan)
 5: 1      Ref Temp Loc [ Tint     ]
 6: 3      Loc [ T1      ]
 7: 1      Mult
 8: 0      Offset

3: Thermocouple Temp (DIFF)
(P14)
 1: 1      Reps
 2: 1      5 mV Slow Range
 3: 4      DIFF Channel
 4: 2      Type E (Chromel-
Constantan)
 5: 3      Ref Temp Loc [ T1      ]
 6: 2      Loc [ T2      ]
 7: 1      Mult
 8: 0      Offset

4: Full Bridge (P6)
 1: 1      Reps
 2: 1      5 mV Slow Range
 3: 2      DIFF Channel
 4: 1      Excite all reps w/Exchan 1
 5: 5000   mV Excitation
 6: 8      Loc [ Td      ]
 7: .001   Mult
 8: .00498 Offset

5: Z=X-Y (P35)
 1: 3      X Loc [ T1      ]
 2: 2      Y Loc [ T2      ]
 3: 4      Z Loc [ Tdiff   ]

6: BR Transform Rf[X/(1-X)] (P59)
 1: 1      Reps
 2: 8      Loc [ Td      ]
 3: 200    Mult (Rf)

7: Temperature RTD (P16)
 1: 1      Reps
 2: 8      R/R0 Loc [ Td      ]
 3: 8      Loc [ Td      ]
 4: 1      Mult
 5: 0      Offset

8: Saturation Vapor Pressure (P56)
 1: 8      Temperature Loc [ Td      ]
 2: 9      Loc [ VP      ]

9: Z=F (P30)
 1: 3      F
 2: 32     Z Loc [ StationID ]

10: If Flag/Port (P91)
 1: 15     Do if Flag 5 is High
 2: 0      Go to end of Program
Table

11: If time is (P92)
 1: 0      Minutes into a
 2: 20     Minute Interval
 3: 10     Set Output Flag High

12: If Flag/Port (P91)
 1: 14     Do if Flag 4 is High
 2: 30     Then Do

13: Do (P86)
 1: 10     Set Output Flag High

14: Do (P86)
 1: 15     Set Flag 5 High

15: End (P95)

16: Real Time (P77)
 1: 1220   Year,Day,Hour/Minute
(midnight = 2400)

17: Sample (P70)
 1: 1      Reps
 2: 32     Loc [ StationID ]

18: Sample (P70)
 1: 1      Reps
 2: 1      Loc [ Tint     ]

19: Average (P71)
 1: 2      Reps
 2: 3      Loc [ T1      ]

20: If Flag/Port (P91)
 1: 12     Do if Flag 2 is High
 2: 30     Then Do

21: Do (P86)
 1: 19     Set Intermed. Proc.
Disable Flag High (Flag 9)

22: Else (P94)

23: If Flag/Port (P91)
 1: 11     Do if Flag 1 is High
 2: 19     Set Intermed. Proc.
Disable Flag High (Flag 9)

24: End (P95)

25: Average (P71)
 1: 2      Reps
 2: 8      Loc [ Td      ]

26: Do (P86)
 1: 29     Set Intermed. Proc.
Disable Flag Low (Flag 9)

27: If Flag/Port (P91)
 1: 22     Do if Flag 2 is Low
 2: 30     Then Do

28: Do (P86)
 1: 19     Set Intermed. Proc.
Disable Flag High (Flag 9)

29: Else (P94)

30: If Flag/Port (P91)
 1: 11     Do if Flag 1 is High
 2: 19     Set Intermed. Proc.
Disable Flag High (Flag 9)

31: End (P95)

32: Average (P71)
 1: 2      Reps
 2: 8      Loc [ Td      ]

*Table 2 Program
 01: 20.0000  Execution Interval
(seconds)

1: Time (P18)
 1: 0      Tenths of seconds into
current minute (maximum 600)
 2: 400    Mod/By
 3: 11     Loc [ Secinmin  ]

2: IF (X<=>F) (P89)
 1: 11     X Loc [ Secinmin  ]
 2: 4      <
 3: 100    F
 4: 21     Set Flag 1 Low

3: If Flag/Port (P91)
 1: 15     Do if Flag 5 is High
 2: 30     Then Do

4: If Flag/Port (P91)
 1: 24     Do if Flag 4 is Low
 2: 1      Call Subroutine 1

5: End (P95)

6: If time is (P92)
 1: 0      Minutes into a
 2: 2      Minute Interval
 3: 30     Then Do

7: Do (P86)
 1: 11     Set Flag 1 High

8: If time is (P92)
 1: 0      Minutes into a
 2: 4      Minute Interval
 3: 30     Then Do

9: Set Port (P20)
```

```
 1: 1      Set High
 2: 2      Port Number

10: Do (P86)
 1: 12     Set Flag 2 High

11: Else (P94)

12: Set Port (P20)
 1: 1      Set High
 2: 1      Port Number

13: Do (P86)
 1: 22     Set Flag 2 Low

14: End (P95)

15: Excitation with Delay (P22)
 1: 1      Ex Channel
 2: 0      Delay w/Ex (units = 0.01
sec)
 3: 2      Delay After Ex (units =
0.01 sec)
 4: 0      mV Excitation

16: Set Port (P20)
 1: 0      Set Low
 2: 1      Port Number

17: Set Port (P20)
 1: 0      Set Low
 2: 2      Port Number

18: End (P95)

19: Batt Voltage (P10)
 1: 10     Loc [ BatV     ]

20: Volt (Diff) (P2)
 1: 1      Reps
 2: 4      500 mV Slow Range
 3: 1      DIFF Channel
 4: 15     Loc [ Rnet     ]
 5: 13.9   Mult
 6: 0      Offset

21: Volts (SE) (P1)
 1: 2      Reps
 2: 2      15 mV Slow Range
 3: 9      SE Channel
 4: 16     Loc [ HFP1     ]
 5: 1      Mult
 6: 0      Offset

22: Thermocouple Temp (DIFF)
(P14)
 1: 1      Reps
 2: 1      5 mV Slow Range
 3: 3      DIFF Channel
 4: 2      Type E (Chromel-
Constantan)
 5: 1      Ref Temp Loc [ Tint     ]
 6: 20     Loc [ Tsoil    ]
 7: 1      Mult
 8: 0      Offset

23: Z=F (P30)
 1: 5000   F
 2: 27     Z Loc [ Analogout ]

24: Analog Out (P21)
 1: 1      CAO Channel
 2: 27     mV Loc [ Analogout ]

25: Z=X*F (P37)
 1: 16     X Loc [ HFP1     ]
 2: 35.9   F
 3: 16     Z Loc [ HFP1     ]

26: Z=X*F (P37)
 1: 17     X Loc [ HFP2     ]
 2: 35.3   F
 3: 17     Z Loc [ HFP2     ]

27: If time is (P92)
 1: 15     Minutes into a
 2: 20     Minute Interval
 3: 18     Set Flag 8 High

28: If Flag/Port (P91)
 1: 18     Do if Flag 8 is High
 2: 30     Then Do

29: Z=X+Y (P33)
 1: 20     X Loc [ Tsoil    ]
 2: 21     Y Loc [ Tstotal  ]
 3: 21     Z Loc [ Tstotal  ]

30: Z=Z+1 (P32)
 1: 22     Z Loc [ Nosamples ]

31: End (P95)

32: If time is (P92)
 1: 0      Minutes into a
 2: 20     Minute Interval
 3: 30     Then Do

33: Z=X/Y (P38)
 1: 21     X Loc [ Tstotal  ]
 2: 22     Y Loc [ Nosamples ]
 3: 24     Z Loc [ Tsaverage ]

34: Z=X-Y (P35)
 1: 24     X Loc [ Tsaverage ]
 2: 23     Y Loc [ Tsprevave ]
 3: 25     Z Loc [ ________ ]

35: Z=X (P31)
 1: 24     X Loc [ Tsaverage ]
 2: 23     Z Loc [ Tsprevave ]

36: Z=F (P30)
 1: 0      F
 2: 21     Z Loc [ Tstotal  ]

37: Z=F (P30)
 1: 0      F
 2: 22     Z Loc [ Nosamples ]

38: Do (P86)
 1: 28     Set Flag 8 Low

39: Do (P86)
 1: 10     Set Output Flag High

40: End (P95)

41: Real Time (P77)
 1: 1220   Year,Day,Hour/Minute
(midnight = 2400)

42: Average (P71)
 1: 3      Reps
 2: 15     Loc [ Rnet     ]

43: Sample (P70)
 1: 2      Reps
 2: 24     Loc [ Tsaverage ]

44: Average (P71)
 1: 1      Reps
 2: 18     Loc [ TDRraw   ]

45: Serial Out (P96)
 1: 30     SM192/SM716/CSM1

46: Do (P86)
 1: 2      Call Subroutine 2

47: Do (P86)
 1: 3      Call Subroutine 3
```

***Table 3 Subroutines**

```
1: Beginning of Subroutine (P85)
 1: 1      Subroutine 1

2: Do (P86)
 1: 25     Set Flag 5 Low

3: Do (P86)
 1: 10     Set Output Flag High

4: Real Time (P77)
 1: 220    Day,Hour/Minute
(midnight = 2400)

5: End (P95)

6: Beginning of Subroutine (P85)
 1: 2      Subroutine 2

7: Z=F (P30)
 1: 300    F
 2: 29     Z Loc [ Pumpon   ]

8: Z=F (P30)
 1: 1140   F
 2: 30     Z Loc [ Pumpoff  ]

9: Time (P18)
 1: 1      Minutes into current day
(maximum 1440)
 2: 0      Mod/By
 3: 31     Loc [ Mininday ]

10: IF (X<=>Y) (P88)
 1: 29     X Loc [ Pumpon   ]
 2: 1      =
 3: 31     Y Loc [ Mininday ]
 4: 16     Set Flag 6 High

11: Set Port (P20)
 1: 16     Set According to Flag 6
 2: 3      Port Number

12: Do (P86)
 1: 26     Set Flag 6 Low
```

```
13: Set Port (P20)
 1: 17      Set According to Flag 7
 2: 4       Port Number

14: Do (P86)
 1: 27      Set Flag 7 Low

15: IF (X<=>F) (P89)
 1: 10      X Loc [ BatV     ]
 2: 4       <
 3: 11.5    F
 4: 30      Then Do

16: If Flag/Port (P91)
 1: 23      Do if Flag 3 is Low
 2: 30      Then Do

17: Set Port (P20)
 1: 1       Set High
 2: 4       Port Number

18: Excitation with Delay (P22)
 1: 4       Ex Channel
 2: 0       Delay w/Ex (units = 0.01
sec)
 3: 1       Delay After Ex (units =
0.01 sec)
 4: 0       mV Excitation

19: Set Port (P20)
 1: 0       Set Low
 2: 4       Port Number

20: Do (P86)
 1: 13      Set Flag 3 High

21: Do (P86)
 1: 10      Set Output Flag High

22: Real Time (P77)
 1: 110     Day,Hour/Minute
(midnight = 0000)

23: Sample (P70)
 1: 1       Reps
 2: 10      Loc [ BatV     ]

24: End (P95)

25: Else (P94)

26: If Flag/Port (P91)
 1: 13      Do if Flag 3 is High
 2: 30      Then Do

27: IF (X<=>F) (P89)
 1: 10      X Loc [ BatV     ]
 2: 3       >=
 3: 12      F
 4: 30      Then Do

28: Set Port (P20)
 1: 1       Set High
 2: 3       Port Number

29: Excitation with Delay (P22)
 1: 4       Ex Channel
 2: 0       Delay w/Ex (units = 0.01
sec)
 3: 1       Delay After Ex (units =
0.01 sec)
 4: 0       mV Excitation

30: Set Port (P20)
 1: 0       Set Low
 2: 3       Port Number

31: Do (P86)
 1: 23      Set Flag 3 Low

32: Do (P86)
 1: 10      Set Output Flag High

33: Real Time (P77)
 1: 220     Day,Hour/Minute
(midnight = 2400)

34: Sample (P70)
 1: 1       Reps
 2: 10      Loc [ BatV     ]

35: End (P95)

36: End (P95)

37: End (P95)

38: End (P95)

39: Beginning of Subroutine (P85)
 1: 3       Subroutine 3

40: Set Port (P20)
 1: 1       Set High
 2: 5       Port Number

41: Beginning of Loop (P87)
 1: 1       Delay
 2: 2       Loop Count

42: End (P95)

43: Pulse (P3)
 1: 1       Reps
 2: 4       Pulse Input Channel
 3: 21      Low Level AC, Output Hz
 4: 18      Loc [ TDRraw     ]
 5: .001    Mult
 6: 0       Offset

44: Set Port (P20)
 1: 0       Set Low
 2: 5       Port Number

45: End (P95)

End Program
```

-Input Locations-

```
1 Tint       1 3 1
2 T2         1 1 1
3 T1         1 3 1
4 Tdiff      1 2 1
5 ________ 0 0 0
6 ________ 0 0 0
7 ________ 0 0 0
8 Td         1 5 3
9 VP         1 2 1
10 BatV      1 4 1
11 Secinmin  1 1 1
12 ________ 0 0 0
13 ________ 0 0 0
14 ________ 0 0 0
15 Rnet      1 1 1
16 HFP1      5 2 2
17 HFP2      17 2 2
18 TDRraw    1 1 1
19 ________ 0 0 0
20 Tsoil     1 1 1
21 Tstotal   1 2 2
22 Nosamples 1 2 2
23 Tsprevave 1 1 1
24 Tsaverage 1 3 1
25 ________ 1 2 1
26 ________ 0 0 0
27 Analogout 1 1 1
28 ________ 0 0 0
29 Pumpon    1 1 1
30 Pumpoff   1 0 1
31 Mininday  1 1 2
32 StationID 1 1 1
33 ________ 0 0 0
34 ________ 0 0 0
35 ________ 0 0 0
-Program Security-
0000
0000
0000
```

Final Storage Label File for:
EUCS.CSI
Date: 5/22/1998
Time: 11:18:11

```
111 Output_Table  20.00 Min
1 111 L

113 Output_Table  20.00 Min
1 113 L
2 Year_RTM  L
3 Day_RTM  L
4 Hour_Minute_RTM  L
5 StationID  L
6 Tint  L
7 T1_AVG  L
8 Tdiff_AVG  L
9 Td_AVG  L
10 VP_AVG  L
11 Td_AVG  L
12 VP_AVG  L

303 Output_Table  20.00 Sec
1 303 L
2 Day_RTM  L
3 Hour_Minute_RTM  L

239 Output_Table  20.00 Sec
1 239 L
2 Year_RTM  L
3 Day_RTM  L
4 Hour_Minute_RTM  L
5 Rnet_AVG  L
6 HFP1_AVG  L
7 HFP2_AVG  L
8 Tsaverage  L
9 ________ L

321 Output_Table  20.00 Sec
```

1 321 L
2 Day_RTM L
3 Hour_Minute_RTM L
4 BatV L

332 Output_Table 20.00 Sec
1 332 L
2 Day_RTM L
3 Hour_Minute_RTM L
4 BatV L

Estimated Total Final Storage
Locations used per day 87264.0

APPENDIX 6 CR21X datalogger/sensor wiring connections

The following wiring connections for all Bowen ratio energy balance system and automatic weather station sensors to a 21 datalogger, were used:

CR21X Input	Connection	Colour
ANALOG		
1 H	R NET +	RED
L	R NET -	BLACK
GND		
2 H	COOLED MIRROR PRT	GREEN
L	COOLED MIRROR PRT	WHITE
GND	COOLED MIRROR PRT	BLACK
3 H	SOIL TEMP TC - CHROMEL	PURPLE
L	SOIL TEMP TC - CONSTANTAN	RED
GND	RAIN GAUGE	WHITE
4 H	UPPER 0.006 TC - CHROMEL	PURPLE
L	LOWER 0.006 TC - CHROMEL	PURPLE
GND	AIR TEMP TC' s - CONSTANTAN	RED
5 H	SOIL HEAT FLUX PLATE #1 HIGH	BLACK
L	SOIL HEAT FLUX PLATE #2 HIGH	BLACK
GND	HEAT FLUX PLATE GROUNS	WHITE
6 H	SOLARIMETER	BROWN
L	CS615	ORANGE
GND	SOLARIMETER	BLACK
7 H	WIND DIRECTION	WHITE
L		
GND	WINDSPEED, WIND DIRECTION	BLACK, BLACK
8 H	MODEL 207 PROBE	RED
L	MODEL 207 PROBE	WHITE
GND	MODEL 207 PROBE	PURPLE

EXCITATION		
1	COOLED MIRROR EXCITATION	RED
2	MODEL 207 PROBE	BLACK
3	WIND DIRECTION	BROWN
4		
CAO		
1	WINDSPEED	BROWN
2		
3		
4		
PULSE		
1		
2	WINDSPEED	WHITE
3	RAIN GAUGE	WHITE WITH STRIPES
4	CS615	GREEN
GND	CS615	BLACK/CLEAR
CONTROL PORTS	**023 RELAY DRIVER CABLE**	
1	PULSE FROM LOWER AIR INTAKE	GREEN
2	PULSE FOR UPPER AIR INTAKE	WHITE
3	PULSE TO TURN ON POWER TO MIRROR AND PUMP (FLAG 6)	BLACK
4	PULSE TO TURN OFF POWER TO MIRROR AND PUMP (FLAG 7)	RED
GND	GROUND WIRE	CLEAR
+12V	CS615	RED

APPENDIX 7 Component power requirements

The 20 W solar panels and 70 A h batteries installed at the *Saccharum, Acacia* and *Eucalyptus* sites, provided 300 to 350 mA, which fell well within the component (DEW-10 cooled mirror, Bowen ratio energy balance system pump, 21X datalogger and CS615 time domain reflectometry sensor) power requirements.

Component	Current at 12 VDC
DEW10 cooled mirror	150 to 500 mA
Pump	60 mA
21X	< 5 mA
CS615	< 2 mA

APPENDIX 8 Problems encountered conducting the Bowen ratio evaporation experiment

Periodical instrumentation problems caused by broken sensors (DEW-10 hygrometers, Model 207 humidity probe, soil heat flux plates and thermocouples), leaks in the Bowen ratio water vapour pressure system and incorrect wiring, left gaps in the energy balance and evaporation data sets.

8.1 *Influence of a damaged DEW-10 hygrometer on the water vapour pressure measurements*

Broken DEW-10 sensor platinum resistance thermometers (PRT) eventually required replacing at all three sites (approximately 6 years old). Faulty DEW-10 PRT's resulted in sensors unable to detect the thickness of the water film formed on the DEW-10 hygrometer mirror. This often resulted in ice forming on the cooled mirror. Broken DEW-10 sensors further resulted in small measured water vapour pressures ($\approx$ 0.5 kPa) (Fig. 1) and water vapour pressure profile differences (< 0.01 kPa) (Fig. 2). The water vapour pressure and water vapour pressure profile difference curves did not follow a smooth diurnal pattern during these periods. After the replacement of the new DEW-10 sensors (DOY 86), the water vapour pressure (2 kPa) and water vapour pressure differences (0.04 kPa) increased significantly. As a result of the replacement of the broken sensor, clear diurnal patterns in both the water vapour pressure and water vapour pressure profile differences were noted.

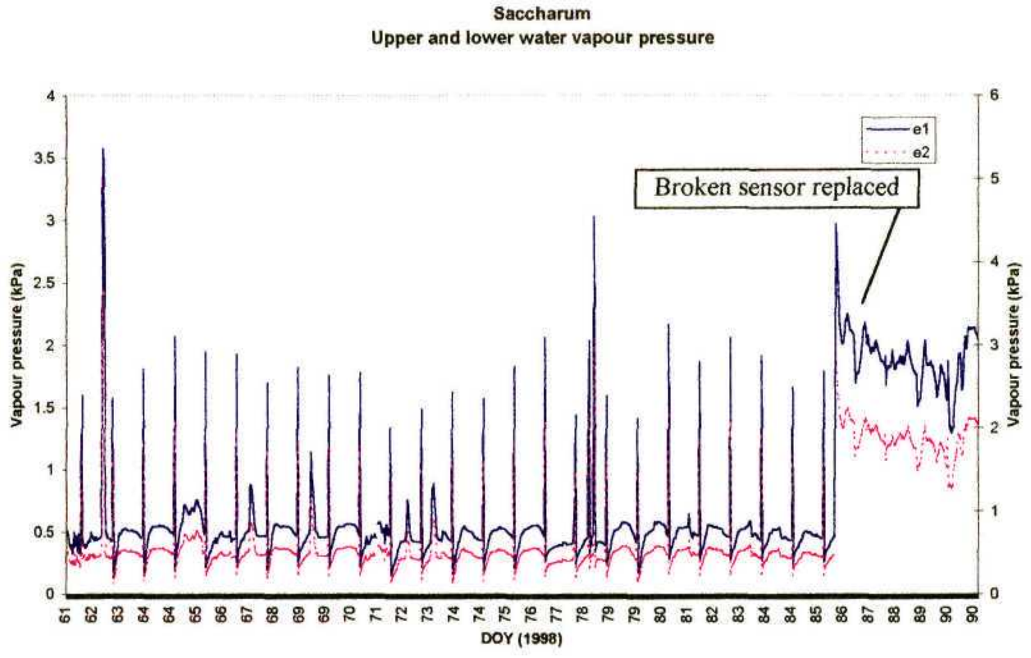

Figure 1 Water vapour pressure (e_1 and e_2) before and after broken DEW-10 sensor had been replaced (DOY 86)

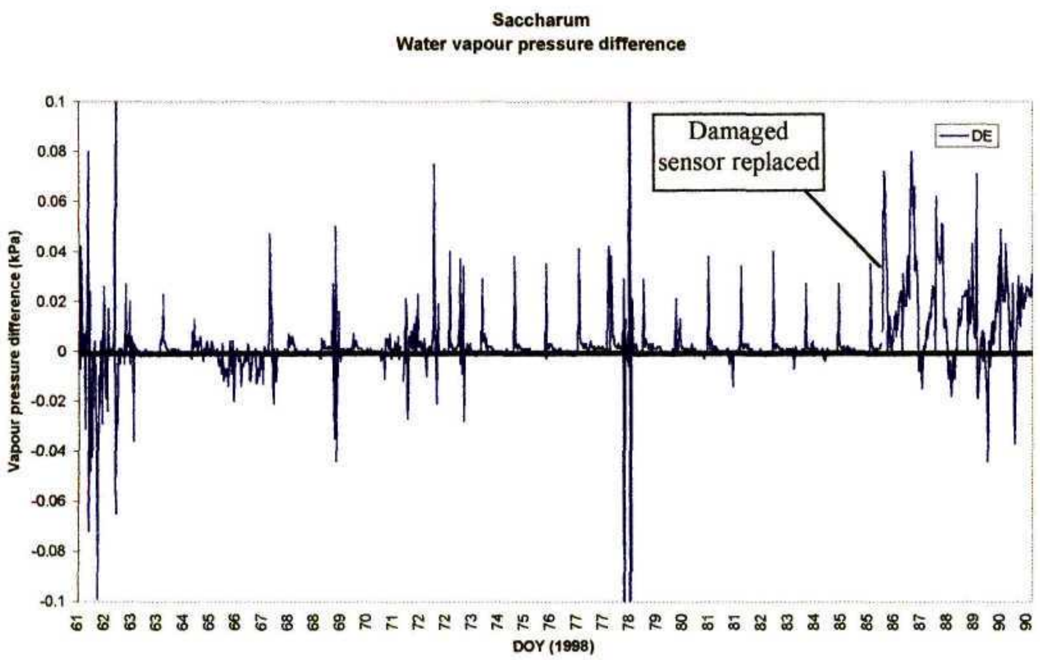

Figure 2 Water vapour pressure profile differences before and after broken DEW-10 sensor had been replaced (DOY 86)

8.2 *Influence of a broken Model 207 humidity probe on the water vapour pressure*

The water vapour pressure chip (PCRC-11) (Model 207 humidity probe) was replaced after very low water vapour pressures (e207) (0.5 kPa) (compared to the Bowen ratio water vapour pressures) (e_1) (2 kPa) were measured. The removal of the chip revealed the degradation of the carbon on the chip. After the replacement of the PRCR-11 chip (DOY 301), water vapour pressures measured by the Model 207 (≈ 2 kPa) humidity probe, compared well with the Bowen ratio water vapour pressures (≈ 2 kPa) measured (Fig. 3).

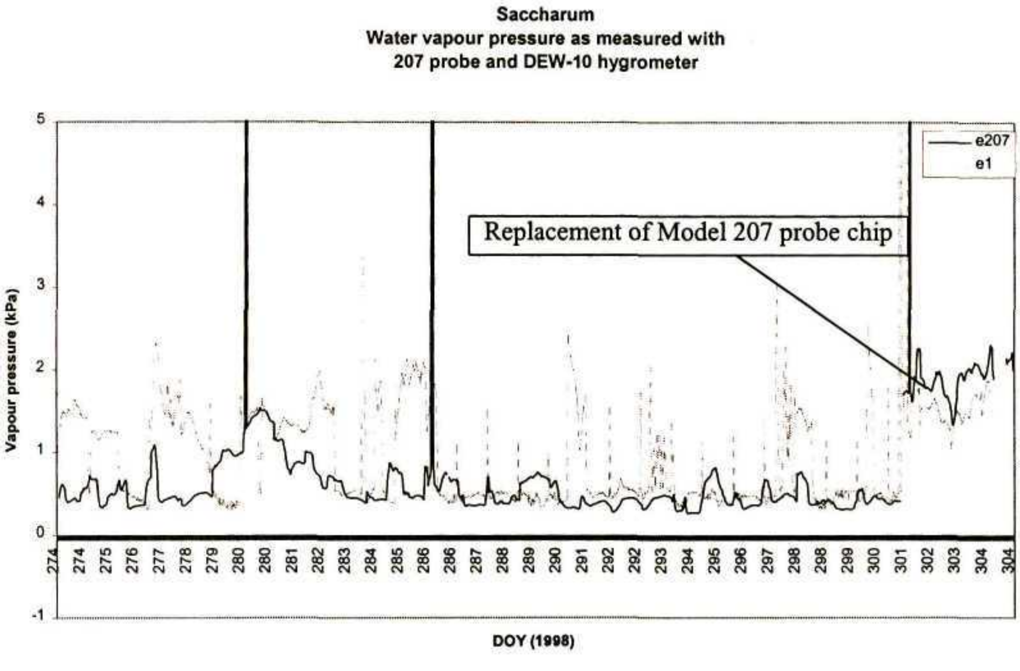

Figure 3 Water vapour pressure before and after replacement (DOY 301) of Model 207 humidity probe water vapour pressure chip

8.3 *Influence of a damaged soil heat flux plate on the calculation of the soil heat flux density*

A damaged soil heat flux plate measured a large, unrealistic diurnal variation in the soil heat flux density (Damaged HFP) (Fig. 4). The faulty soil heat flux plate produced useless data for the calculation of the soil heat flux density at the soil surface (G) and the completion of the energy balance *(Eq. 4.1)*. The 21X datalogger output -6999 data values when the measured voltage was out of the range programmed.

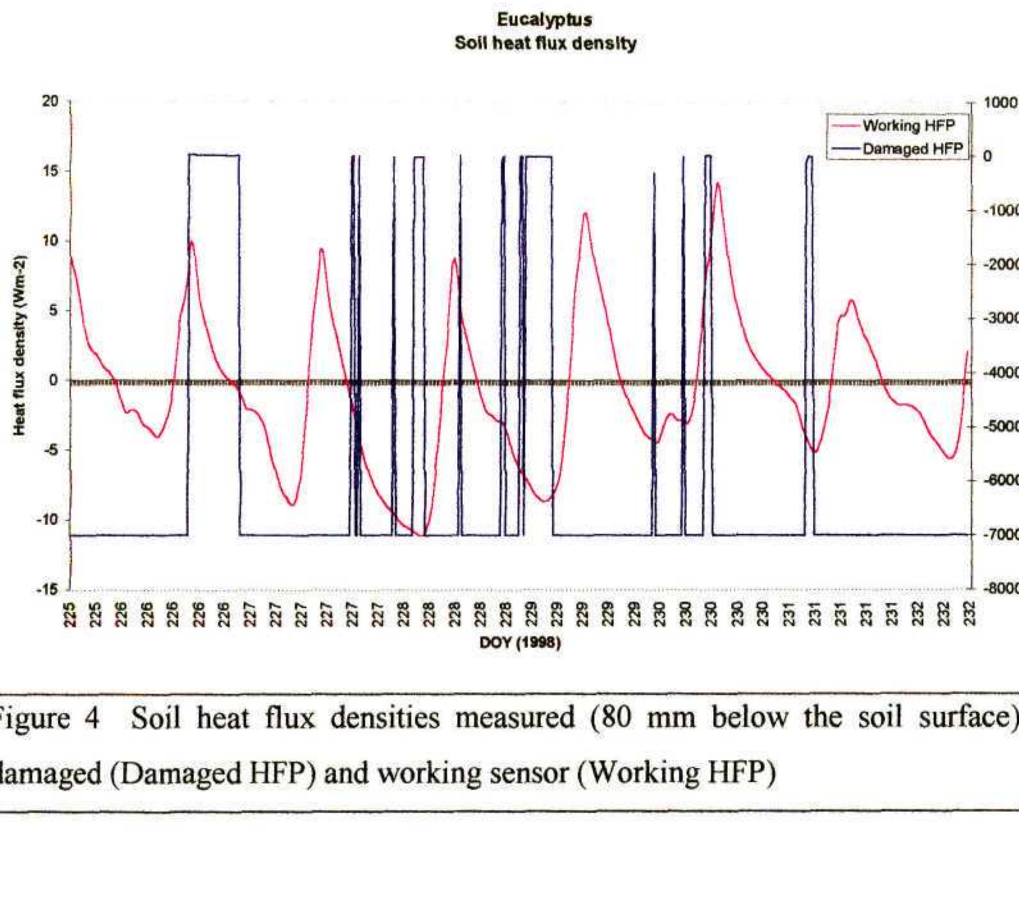

Figure 4 Soil heat flux densities measured (80 mm below the soil surface) with a damaged (Damaged HFP) and working sensor (Working HFP)

8.4 *Influence of a leak on the Bowen ratio water vapour pressure system*

A leak in the Bowen ratio water vapour pressure system (DOY 128 to 148) as a result of cracks in the tubing and/or cracks in the mixing bottle corners (Fig. 5.8), resulted in small water vapour pressure differences measured (< 0.05 kPa). After the leaks were sealed (DOY 148), larger water vapour pressure differences (> 0.2 kPa) were measured (Fig. 5).

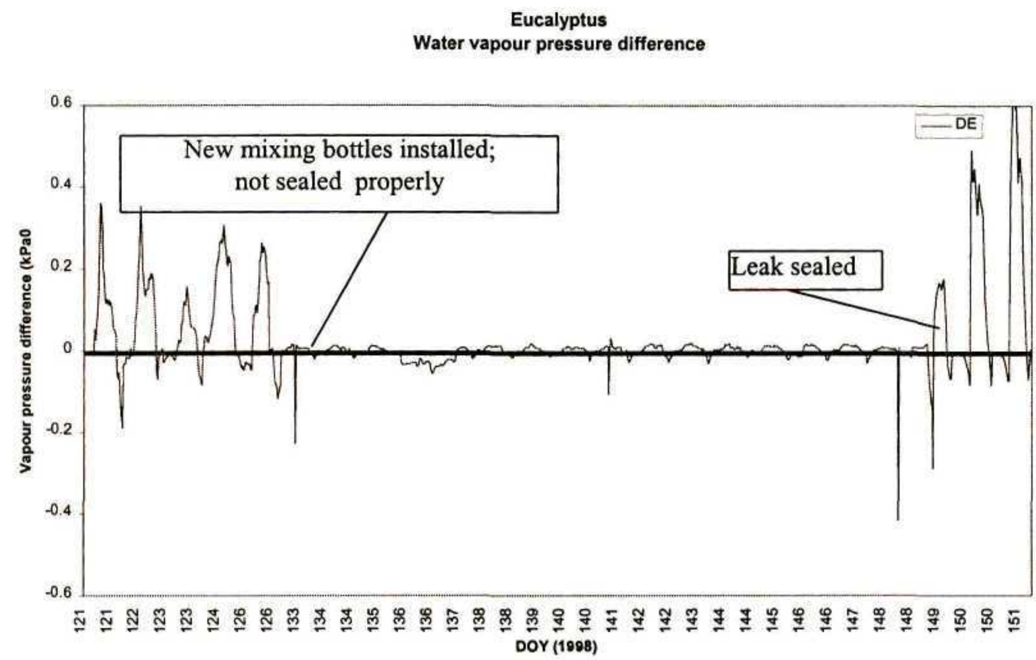

Figure 5 Influence of a leak in the Bowen ratio system on the water vapour pressure profile differences (before and after)

8.5 *Influence of an incorrect type of air temperature sensor extension wire on the air temperature profile differences*

The use of an incorrect thermocouple type (copper-constantan) to extend the air temperature sensor wire, resulted in very high air temperature differences (>2 °C) (Fig.6). The high air temperature differences were a result of the different reference temperatures. After the incorrect wire was replaced with chromel-constantan wire, the air temperature differences decreased significantly to realistic air temperature differences (≈ 0.04 °C) (DOY 128).

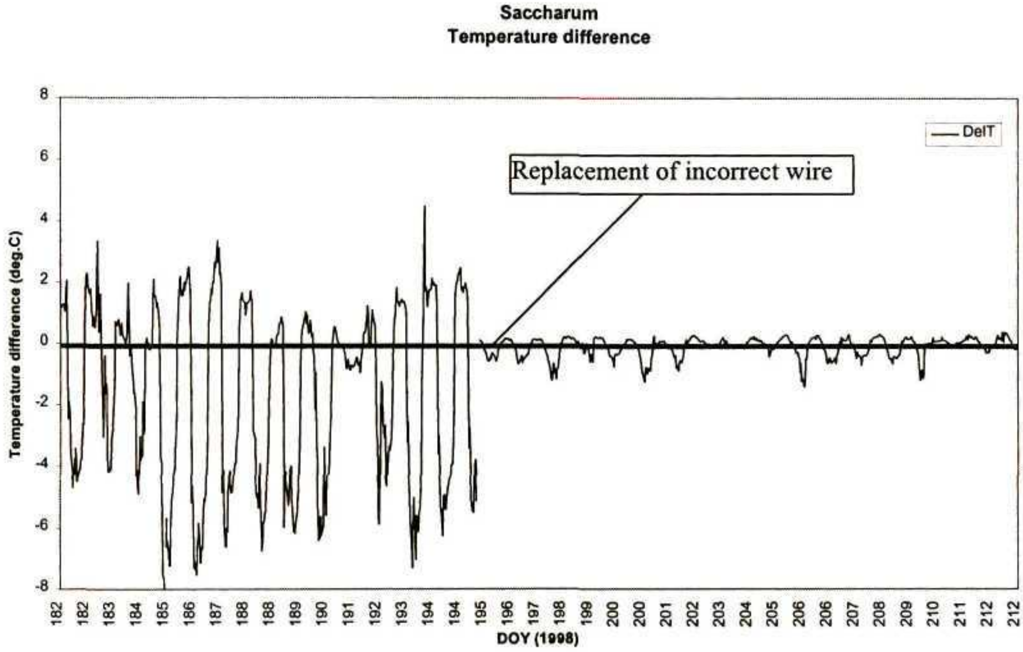

Figure 6 The influence of the use of the incorrect wire on the air temperature difference (before and after replacement with chromel-constantan wire)